The Role of the UL25 Protein of Herpes Simplex Virus 1 During Assembly, Cell Entry and Nuclear Import of the Viral Genome

Von der Naturwissenschaftlichen Fakultät
der Gottfried Wilhelm Leibniz Universität Hannover
zur Erlangung des Grades einer

Doktorin der Naturwissenschaften

Dr. rer. nat.

genehmigte Dissertation
von

Dipl.-Biochem. Kathrin Rode

geboren am 3. März 1979 in Hameln

Dezember 2007

Referentin:	**Prof. Dr. rer. nat. Beate Sodeik**
	Institut für Virologie, Medizinische Hochschule Hannover
Korreferent:	**Prof. Dr. med. Ingo Just**
	Institut für Toxikologie, Medizinische Hochschule Hannover

Tag der Promotion: 19. Dezember 2007

Meinen Eltern

Als Pythagoras seinen bekannten Lehrsatz entdeckte,
brachte er den Göttern hundert Ochsen dar.
Seitdem zittern die Ochsen, so oft eine neue Wahrheit ans Licht kommt.

Carl Ludwig Börne (1786 – 1837)

Danksagung

An dieser Stelle möchte ich allen Menschen danken, die dazu beigetragen haben, dass ich diese Arbeit fertig stellen wollte und konnte. Es war nicht immer einfach, aber man wächst ja bekanntlich mit seinen Aufgaben!

Meiner Mentorin Prof. Dr. Beate Sodeik möchte ich besonders danken; zum einem für die Vergabe dieses spannendenden Projekts, zum anderen für Ihre herausragende Betreuung. Lob und Tadel, sowie Ansporn und Diskussionbereitschaft haben mir in meiner Entwicklung von einer Praktikantin bis zu einer Wissenschaftlerin sehr geholfen.

Ich danke meinem Betreuer Prof. Dr. Ingo Just für die Übernahme des Korefferates dieser Arbeit, Prof. Dr. Peter Valentin-Weigand und Dr. Hans Bakker für die Betreuung während meiner Zeit im DFG-Graduiertenkolleg 745.

Ich danke allen Kolleginnen und Kollegen des Instituts für Virologie für interessante Diskussionen, lustige Pausengespräche und vor allem für die Bereitstellung und Vermittlung von Fachwissen und Reagenzien.

Darüberhinaus danke ich auch den Kolleginnen und Kollegen des Instituts für Zellbiologie für die Zusammenarbeit bei der Elektronenmikroskopie, sowie den unlimitierten Zugang zu Mikroskopen. Ich danke besonders Dr. Rudi Bauerfeind für seine Hilfsbereitschaft bezüglich der Konfokalen Laser Mikroskopie.

Dr. Matthias Ballmaier und Christina Reimer sei gedankt für die Hilfe beim FACS Sortieren in der FACS Einrichtung der MHH.

Ich möchte mich ganz herzlich bedanken für die großzügige Bereitstellung von Viren, Plasmiden und Antikörpern bei: G. Cohen & R. Eisenberg (University of Pennsylvania, Philadelphia, USA), A.C. Minson (University of Cambridge, UK), E. Cantin (Department of Neurology, City of Hope National Medical Center, Duarte, California, USA), D. J. Tenney (Bristol-Myers Squibb Pharmaceutical Research Institute, Wallingford, Connecticut, USA), W. Newcomb & J. Brown (University of Virginia, Charlottesville, VA, USA), R. Everett (MRC Virology Unit, Glasgow, UK), J. Krijnse-Locker, (Universität Heidelberg, Germany), F. Kreppel (Universität Ulm), T.F. Schulz (Institut für Virologie, Medizinische Hochschule Hannover) und J.H. Subak-Sharpe (MRC Virology Unit, Glagow, UK)

Allen Kolleginnen und Kollegen der AG Sodeik sei gedankt für die tolle Arbeitsatmosphäre. Ich danke ganz besonders Ute Prank, der Hüterin der Zellkultur, nicht nur für die besondere Pflege unserer Hamster, Affen und Langschnauzen-kaninchenkänguruhs (bzw. das, was davon übrig geblieben ist), sondern auch für tolle Gespräche und leckeren Kuchen. Mojgan Fathollahy möchte ich besonders für ihre Hilfe in molekularbiologischen Angelegenheiten danken. Ohne Anne Binz wäre die Arbeit an dem Elektronenmikroskopie-Projekt nur halb so schön und erfolgreich gewesen, daher danke ich ihr besonders für ihre Unterstützung. Ich bedanke mich ganz herzlich bei den fleißigen Korrekturlesern Dr. Tanja Bosse, Dr. Katinka Döhner, Jessica Janus, Dr. Claus-Henning Nagel, Kerstin Radtke und Julia Schipke.
Besonders zu erwähnen sind Dr. Katinka Döhner, die immer eine besonders gute Ansprechpartnerin gewesen ist, wenn ich Probleme mit UL25 und anderen Dingen hatte; Julia Schipke und ich sind nicht nur über unsere Proteine verlinkt, sondern auch über das Israel-Projekt; Dr. Claus-Henning Nagel, mein Bürotischnachbar, ist immer offen für Fragen gewesen, sowie Dr. Kristina Theusner für die tolle Word-Vorlage.

Ein besonderer Dank geht an die Mitglieder des DFG-Graduiertenkollegs 745-2. Ein ganz spezieller Dank geht an den Tossens-Fan Club, besonders an Marcus Fulde, Tobias Schweinitzer, Stefan Kulick, Nadine Müther, Sarah Sengstake, Silke Hartmann und Falk Büttner.

Der sportliche Ausgleich wäre nur halb so schön ohne den Unterricht von Beate Jaskolowski und den Mitstreitern der Samstagsgruppe, die immer für nette Gras- und Grillabende und ausgedehnte Kakaostunden im Kabuff bei eisiger Kälte zu haben waren. Mein Dank gilt nicht nur Menschen, sondern auch Tieren. Ich danke meiner Lieblingsstute Frieda dafür, dass ich mich auch mal außerhalb des Labors verausgaben durfte.

Meinen Freunden Sebastian Seth, David Schwarzer, Nancy Bartholomes, Anja Struckmeyer und Anna Karaböczek sei gedankt für tolle Gespräche und das Beistehen in guten wie in schweren Zeiten.

Meiner lieben Oma Brigitte Köberle sei gedankt für die stetige Unterwanderung des Rode-Brötchenimperiums durch das „illegale" Beschaffen von leckeren Gersterbrötchen. Danke für alles.

Guido Rudolph danke ich für die schöne Zeit außerhalb des Labors. Ohne Dich hätte ich das alles nicht geschafft.

Ohne die immerwährende Unterstützung und Liebe meiner Eltern Jürgen und Sigrid Rode wäre ich nicht die geworden, die ich heute bin. Ich bin Euch unendlich dankbar.

Zusammenfassung

Das humanpathogene Herpes-Simplex-Virus Typ 1 (HSV1) infiziert epitheliale Zellen der Mundschleimhaut sowie der umgebenen Haut und etabliert in den Neuronen eine latente Infektion. Reaktivierungen von latenten Infektionen können erneute Entzündungen hervorrufen. Das Kapsidprotein UL25 stabilisiert das Kapsid, nachdem das virale Genom in das Kapsid eingeschleust worden ist, entweder durch Versiegelung des UL6-Portals oder durch das Verstärken des gesamten Kapsids. Darüber hinaus könnte das an die Kapside gebundende UL25 als Signal zum Verlassen des Zellkerns dienen. Für diese Doktorarbeit untersuchte ich das Kapsidprotein UL25 während der frühen Phase des viralen Lebenszyklus.

In dieser Arbeit konnte ich zeigen, dass UL25 auf den Kapsiden verbleibt, bis der Kernporenkomplex erreicht wurde. Darüberhinaus war UL25 auch mit reifen Kapsiden im Zellkern und während der Virusreifung in der Zelle assoziiert. Um eine mögliche Funktion von UL25 während des Viruseintritts in die Zelle zu untersuchen, wurde UL25 vor der HSV1 Infektion überexprimiert. Ich versprach mir von diesen Experimenten, dass UL25 im Überschuß essentielle Interaktionen zwischen Wirtsproteinen und UL25 kompetitiv hemmen könnte, welche für den Viruseintritt von Bedeutung sind. Ich konnte zeigen, dass die Expression von frühen HSV1-Proteinen durch Überexpression von UL25 signifikant reduziert wurde aber der Kapsidtransport entlang von Mikrotubuli aber nicht beeinträchtigt war. Diese Daten zeigten, dass während des Viruseintritts ein Schritt zwischen dem Erreichen der Kernpore und der frühen viralen Proteinsynthese durch überschüssiges UL25 blockiert wurde, weil dieses möglicherweise die Destabilisierung des Kapsids während der Genomfreisetzung an der Kernpore durch kapsid-assoziiertes UL25 kompetitiv hemmte.

Das Kapsid benötigt das Protein Importin β, um die Kernpore zu erreichen und dort die Genomfreisetzung zu ermöglichen. Überschüssiges UL25 könnte eine Funktion von UL25 als potenziellen Importin β Rezeptor unterbinden. Allerdings wurde keine Fehllokalisierung von Importin β oder den Kernporen in UL25 überexprimierenden Zellen beobachtet. Elektronenmikroskopische Analysen zeigten, dass die Menge an Kapsiden, die ihr Genom an der Kernpore freigesetzt haben, durch UL25-Überexpression nicht reduziert wurde. Darüberhinaus wurde gezeigt, dass UL25 unabhängig von Promotoren die Transkription leicht reduzierte. Eine generelle Inhibierung des Zellstoffwechsels könnte diese Repression der Transkription erklären. Die frühe Genexpression von Adenovirus oder Vaccinia-Virus ist in Gegenwart von UL25 nicht beeinträchtigt, daher ist die Reduzierung der HSV1 Genexpression kein genereller, sondern ein herpesspezifischer Effekt und nicht das Resultat einer generellen Inhibierung von Transkription oder Proteinsynthese.

Die subzelluläre Lokalisation der viralen DNA wurde in infizierten, UL25 überexprimierenden Zellen durch Fluoreszenz gekoppelte *In Situ* Hybridisierung analysiert. Erste Ergebnisse zeigten, dass weniger Genome in den Zellkernen akkumulierten. Somit könnte die Translokation des viralen Genoms durch die Kernpore verhindert worden sein. Überraschenderweise wurde auch die späte Vaccinia Virus Genexpression reduziert, was darauf hinweist, dass die späte Vaccinia Virus Genexpression ähnliche zelluläre Faktoren benötigt, die HSV1-UL25 bindet. Alternativ könnte die stark positiv geladene Proteinoberfläche von UL25 mit zytosolischer, viraler DNA wechselwirken und somit die Translokation von HSV1-DNA in den Zellkern oder die späte Genexpression von Vaccinia-Virus inhibieren.

UL25 ist nicht nur essentiell für die DNA-Verpackung und Kaspidreifung, sondern spielt auch während der späten Phase des Viruseintritts in die Zelle eine Rolle. Die Translokation des viralen Genoms aus dem Kapsid durch die Kernpore könnte durch überschüssiges UL25 unterbunden worden sein und somit eine Erklärung für die Inhibierung der frühen HSV1-Genexpression darstellen. Darüber hinaus könnte eine spezifische Inhibierung dieses Prozesses einen neuen Angriffspunkt zur Entwicklung neuer Medikamenten gegen Herpesviren darstellen.

Schlagworte: Herpes-Simplex-Virus, Virusreifung, Zelleintritt, Fluoreszenzmikroskopie

Abstract

Herpes simplex virus type 1 (HSV1) is a human pathogen, which infects the oral mucosa and establishes a life-long latency in neurons. Primary infection and reactivation cause several diseases. HSV1-UL25, a minor capsid-associated protein, is supposed to either seal the portal or to stabilize the capsid after genome packaging. Both scenarios are consistent with a lack of efficient DNA packaging in HSV1-ΔUL25 deletion mutants. In addition, UL25 may provide the nuclear egress signal for capsid envelopment at the inner nuclear membrane. For this thesis, I analyzed the role of HSV1-UL25 during the early phase of the HSV1 viral life cycle.

My data show that HSV1-UL25 remained attached to viral capsids during assembly, egress, as well as during cell entry and cytoplasmic transport to the nucleus. To reveal potential functions of HSV1-UL25 during cell entry, I overexpressed UL25 prior to HSV1 infection. I was hoping that the ectopically expressed UL25 would compete for essential interactions between host proteins and the incoming capsid-associated UL25 which may be required during HSV1 cell entry. Along this hypothesis, overexpression of UL25 significantly reduced the expression of immediate early HSV1 genes but had no effect on cytoplasmic transport of incoming capsids to the nucleus. Thus, excess UL25 inhibited a step between capsid arrival at the nucleus and immediate early protein synthesis, possibly by interfering with the role of capsid-associated UL25, and thus preventing capsid destabilization and genome uncoating at the nuclear pore.

The host nuclear import factor importin β targets the incoming HSV1 capsids to the nuclear pore, and binding of the capsid to the nuclear pore may provide the trigger for genome uncoating. Since UL25 may constitute a viral importin β receptor, overexpressed UL25 may sequester importin β and prevent its proper function. However, the subcellular localization of importins or the nuclear pore complex was not affected by excess UL25. Moreover, electron microscopy analysis of UL25-expressing, HSV1-infected cells revealed that UL25 did not reduce the number of empty capsids localized at the nuclear pores. Thus, uncoating took place in UL25 overexpressing cells, but possibly the released viral genomes were not functional. Luciferase reporter assays showed a minor, promoter-independent reduction of transcription but these experiments could only be executed after long transfection times, when the cell metabolism might have been further modified than in the other experiments. Moreover, after similar transfection times as for HSV1, both vaccinia virus and adenovirus early gene expression were not reduced. Thus, there was no general inhibition of transcription or translation in HSV1-UL25 overexpressing cells.

Analysis of the subcellular localization of the incoming HSV1 genomes by fluorescence *in situ* hybridization revealed that fewer genomes had accumulated in the nuclei of UL25 overexpressing cells. Interestingly, UL25 impaired also late vaccinia virus gene expression, suggesting that early HSV1 and late vaccinia virus gene expression may require similar host factors which are targeted by HSV1-UL25. Alternatively, UL25 may bind with its highly positively charged surface to cytosolic viral DNA, and thus prevent proper nuclear import in the case of HSV1, or proper late gene expression in the case of vaccinia virus.

In summary, my data suggest that overexpressed UL25 did not affect genome uncoating *per se* but rather prevented proper nuclear import of incoming HSV1 genomes, providing a first explanation how UL25 inhibited HSV1 gene expression. This experimental setup provides the first tool to specifically prevent nuclear import of HSV1 genomes, and further molecular characterization of this essential step in the life cycle of all herpesviruses might in the long run aid in the development of drug targeting this reaction.

Keywords: herpes simplex virus, virus assembly, cell entry, fluorescence microscopy

Table of Contents

Danksagung ..... **IV**

Zusammenfassung ..... **V**

Abstract ..... **VI**

1 Introduction **9**

1.1 Herpesvirales 9

1.2 Herpes Simplex Virus Type 1 Pathology 10

1.3 Life Cycle of Herpesvirus 11

1.4 The HSV1-UL25 Protein 22

1.5 Aim of the Study 27

2 Material and Methods **28**

2.1 Chemicals 28

2.2 Antibodies 28

2.3 Molecular Biological Techniques 30

2.4 Eucaryotic Cell Culture 33

2.5 Virological Techniques 34

2.6 Protein Analysis 36

2.7 In Situ Hybridization of Viral Genomes 37

2.8 Microscopy 39

3 Results **42**

3.1 The Subcellular Localization of UL25 During the HSV1 Life Cycle 42

3.1.1 UL25 Associated with Capsids During Capsid Assembly and Egress 42

3.1.2 HSV1-UL25 Remained Capsid-Associated until Arrival at the Nuclear Pore 48

3.2 Transiently Overexpressed UL25 During Virus Infection 50

3.2.1 Immediate Early HSV1 Gene Expression was Reduced 50

3.2.2 Subcellular Localization of Importin β 51

3.2.3 The Nuclear Pore Network 53

3.2.4 Nuclear Import of the Major Transcriptional Activator VP16 54

3.2.5 Transactivation of Cellular and Herpesviral Promoters 55

3.2.6 Late but Not Early Protein Synthesis of Vaccinia Virus was Slightly Impaired 60

3.2.7 Adenovirus Mediated Transgene Expression was not Influenced 60

3.2.8 Uncoating of HSV1 Genomes 62

3.2.9 Subcellular Localization of Incoming Viral Genomes 65

4 Discussion **73**

4.1 Mature Capsids Contained UL25 During Assembly, Egress and Entry 74

4.2 Reduction of HSV1 Gene Expression by Excess UL25 76

4.3 No Effect on Importin β and Nuclear Pores 76

4.4 Transcription in the Presence of Overexpressed UL25 77

4.5 Vaccinia Virus Late, but not Early Gene Expression was Impaired by Excess UL25 78

4.6 UL25 did not Reduce Adenovirus Mediated Gene Expression 79

4.7 HSV1 Genome Uncoating in the Presence of Excess UL25 79

4.8 Less Genomes Accumulated in the Nucleoplasm in the Presence of UL25 80

5 Outlook **83**

5.1 Further Analysis of UL25 During the Viral Life Cycle of HSV1 83

5.2 Perspectives 84

6 References **85**

7 Appendix **95**

List of Abbreviations

ATCC	American Type Culture Collection
ATP	adenosine triphosphate
bp	base pairs
BP	bandpass filter within microscope filter set
CCL	certified cell line
DIC	Differential Interference Contrast
DNA	deoxyribonucleic acid
EtOH	ethanol
FCS	foetal calf serum
FT	beam splitter within microscope filter set
GFP	green fluorescent protein
GST	gluthation S-transferase
gX	glycoprotein X
HAc	acetic acid
HHV	human herpesvirus
HSV1	herpes simplex virus type 1
HveC	herpesvirus entry protein C
HVEM	herpesvirus entry mediator
kb	kilo base pairs
LP	longpass emission filter within microscope filter set
MEM	Minimal Essential Medium
MOI	multiplicity of infection
MTOC	microtubule organising centre
MW_{app}	apparent molecular weight
NE	nuclear envelope
NPC	nuclear pore complex
ORF	open reading frame
PBS	phosphate buffered saline
PFA	paraformaldehyde
PFU	plaque forming units
pi	post infection
rpm	rotations per minute
RT	room temperature
SDS-PAGE	sodium dodecyl-polyacrylamide gelelectrophoresis
SP	shortpass filter with microscope filter set
UL	unique long region on the herpesvirus genome
UL25	protein encoded by the HSV1 ORF UL25
US	unique short region on the herpesvirus genome
VP	virus protein

1 Introduction

1.1 Herpesvirales

The order *Herpesvirales* is composed of enveloped double-stranded DNA viruses divided into three families characterized by their host cell range. The *Herpesviridae* replicate in mammalian, avian and reptilian host cells (McGeoch and Gatherer 2005). The *Alloherpesviridae* include piscine and amphibian herpesviruses, and the *Malacoherpesviridae* the oyster infecting invertebrate herpesvirus (Davison et al. 2005; Farley et al. 1972; McGeoch et al. 2006). The *Herpesviridae* are divided into three subfamilies, α-, β-, and γ-*herpesvirinae*, and each subfamily in turn is divided into different genera (Table 1).

Table 1: Classification of human herpesviruses (Cleator and Klapper 2004)

Common name	Official Nomenclature	Subfamily	Genus
Herpes simplex virus type 1 (HSV1)	Human herpesvirus 1 (HHV-1)	α-*herpesvirinae*	Simplexvirus
Herpes simplex virus type 2 (HSV2)	Human herpesvirus 2 (HHV-2)	α-*herpesvirinae*	Simplexvirus
Varicella zoster virus (VZV)	Human herpesvirus 3 (HHV-3)	α-*herpesvirinae*	Varicellovirus
Epstein-Barr virus (EBV)	Human herpesvirus 4 (HHV-4)	γ-*herpesvirinae*	Lymphocryptovirus
Human cytomegalovirus (HCMV)	Human herpesvirus 5 (HHV-5)	β-*herpesvirinae*	Cytomegalovirus
HHV-6A	Human herpesvirus 6A (HHV-6A)	β-*herpesvirinae*	Roseolovirus
HHV-6B	Human herpesvirus 6B (HHV-6B)	β-*herpesvirinae*	Roseolovirus
HHV-7	Human herpesvirus 7 (HHV-7)	β-*herpesvirinae*	-
Kaposi's sarcoma-associated herpesvirus (KSHV)	Human herpesvirus 8 (HHV-8)	γ-*herpesvirinae*	Rhadinovirus

Members of the herpesviruses have a genome size of 100 to 230 kb with up to more than 200 potential open reading frames (Cleator and Klapper 2004; Roizman and Knipe 2001). In addition to structural proteins, they encode a large set of enzymes for nucleic acid metabolism and protein processing. Upon entering their host, virus transcription, replication and capsid assembly of progeny virions take place in the nucleus. Newly synthesized virions can then spread to the neighboring cells. All herpesviruses establish a life-long latent infection in specific cell types, from which they can be reactivated. The subsequent virus assembly leads to the production of progeny virus that are released via exocytosis or cell to cell spread.

Nine members of the *Herpesviridae* are known to infect humans (Table 1). Herpes simplex virus type 1 (HSV1), also called Human Herpesvirus 1 (HHV-1), belongs to the neurotropic α-herpesvirinae subfamily and the genus simplexvirus. The α-*herpesvirinae* are characterized by a variable host cell range, a short life cycle, rapid spread in cell culture and efficient lysis of infected cells. HSV1 establishes latent infections primarily in sensory neurons (Roizman and Knipe 2001).

The human α-herpesviruses HSV1 and HSV2 cause the well-known *herpes labialis* and *herpes genitalis*, and the varicella-zoster virus chickenpox and shingles. Human cytomegalovirus (HCMV), human herpesviruses 6A and 6B as well as human herpesvirus 7 are the human β-herpesviruses. HCMV is the most common virus and a severe threat in immunocompromised patients, where it causes pneumonia, retinitis or hepatitis. Moreover, when acquired via a congenital route, neurological disorders of the newborn can occur. The human γ-herpesviruses Epstein-Barr virus (EBV) and Kaposi's sarcoma-associated herpesvirus (KSHV) are associated with the induction of malignant neoplasia in immunocompromised patients, like patients with AIDS. A primary infection with EBV causing infectious mononucleosis is prominent as "kissing disease" or "Pfeiffer's syndrome". Kaposi sarcomas are caused by KSHV in HIV infected, immunocompromised patients (Doerr 2002).

1.2 Herpes Simplex Virus Type 1 Pathology

Primary HSV1 infections are usually acquired during childhood when a susceptible person comes into close contact with an individual who is actively shedding the virus. HSV1 infects epithelial cells and keratinocytes of the oral and perioral skin and mucosa (Figure 1).

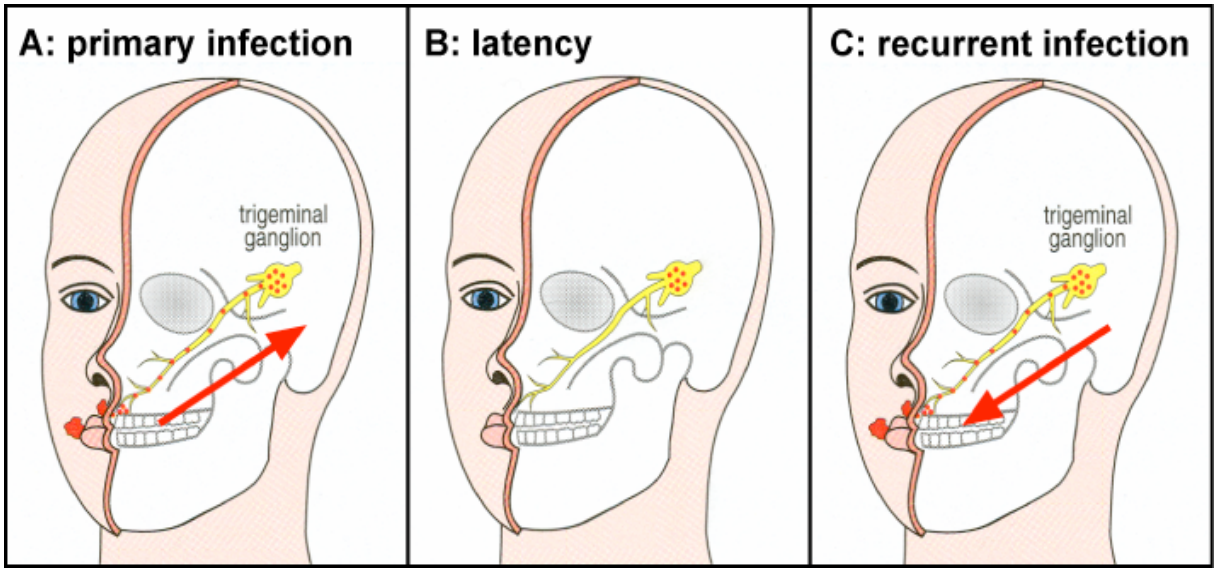

Figure 1: HSV1 infection. HSV1 infects keratinocytes and epithelial cells of the oral and perioral region (A; primary infection). Progeny viruses then enter neurons innervating that area and are transported retrogradely to cranial ganglia, for example the trigeminal ganglion (A; red arrow), where a latent infection is established (B; latency). Upon stress factors like UV light or a compromised immune system, latent viruses become reactivated and newly synthesized viruses are transported anterogradely from the trigeminal ganglion to the synapse (C; recurrent infection, red arrow). After release from the sensory nerve endings they reinfect the epithelium causing cold sores (Scheme derived and modified from Caroll 2001).

The primary infection is unremarkable in most cases but may cause a *herpes gingivostomatitis* (Cleator and Klapper 2004). The virus replicates and progeny virus infects sensory neurons innervating that area. Viral particles are transported towards the cell body of cranial ganglia, such as the trigeminus ganglion (Vrabec and Alford 2004) and then the viral genome is released into the nucleus where it circularizes (Roizman and Knipe 2001). HSV1 either initiates an acute or a latent infection, a state in which the viral genome exists as an episome, and virus replication appears to be suppressed by the host's immune system (Decman et al. 2005; Khanna et al. 2004). Reactivation of latent genomes can be triggered by several stress causing factors such as UV light or a compromised immune system and results in the activation of the lytic cycle. Progeny virions are produced and transported back to the initial site of infection where epithelial cells and keratinocytes become infected again. This leads to the secretion of infectious virions and lesion formation, known as *herpes labialis* or cold sores. In rare cases, progeny viruses travel further to neurons of the central nervous system, which results in a life-threatening *herpes encephalitis*. HSV1 can also spread to the eye and cause *keratokonjunctovitis herpetika*, a scarring and clouding of the cornea that ultimately lead to blindness (Jerome and Ashley 2003).

Herpesvirus infections cannot be cured because medication that will attack the virus episome, that lies dormant in the nerve cells, will also damage the nerve cells. However, there is treatment available for acute outbreaks that involve the use of anti-viral drugs such as acyclovir and its derivatives valacyclovir, famciclovir and penciclovir (De Clercq 2007; Spruance et al. 1990). All these nucleoside drugs in this class depend on the activity of the viral thymidine kinase UL23. Nucleoside drugs are phosphorylated by UL23 and subsequently by cellular kinases. The resulting inhibition of the viral DNA polymerase UL30 is due to chain termination. Foscarnet is a phosphonic acid derivate and not dependent on viral thymidine kinase. It inhibits viral DNA polymerization by inhibiting the pyrophosphate binding site on the viral DNA-polymerase (Noble and Faulds 1998).

1.3 Life Cycle of Herpesvirus

1.3.1 Virion Structure

The infectious HSV1 virion has a diameter of about 225 nm and is composed of four structures (Grünewald et al. 2003; Roizman and Knipe 2001): the viral genome, the icosahedral capsid, the tegument, and the viral envelope. The viral genome has a size of 152 kb and encodes for about 84 proteins (Rajcani et al. 2004) whereof about 40 proteins build the structure of the virus.

HSV1 proteins are named either according to their position on an SDS gel (e.g. VP5, MW_{app} = 155 kDa, VP26, MW_{app} = 12 kDa), to the position of the ORF on the viral genomes unique long (UL) or unique short (US) region (e.g. UL25, US11) or to their function (e.g. UL41/vhs = virus host shut off protein). Viral glycoproteins have an additional own nomenclature (e.g. gB, gC, gD).

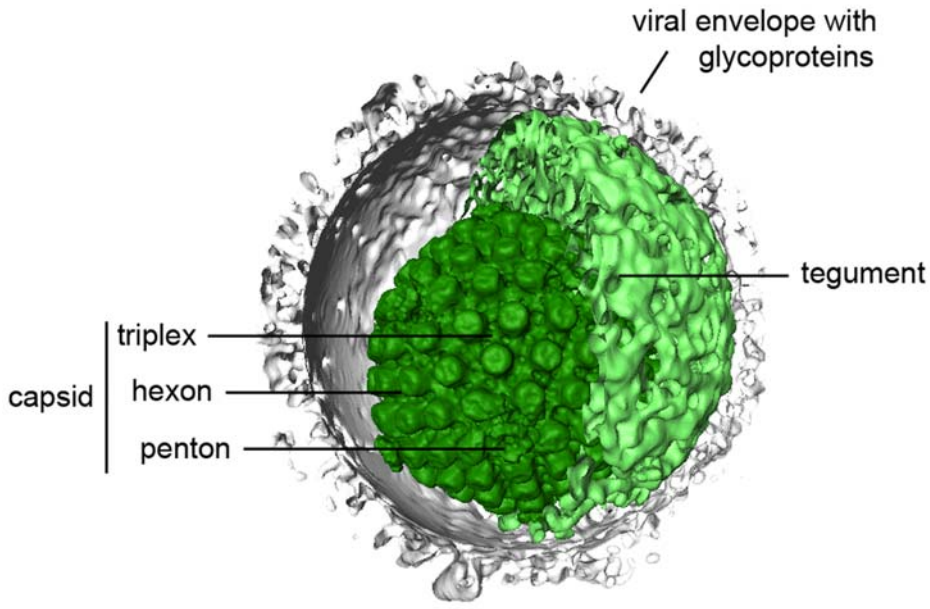

Figure 2: Cryoelectron microscopy tomogram of HSV1. The icosahedral capsid (dark green) is composed of triplices, hexons and pentons. The tegument (light green) has an asymmetric distribution: at the bottom, the capsid closely reaches the envelope, whereas at the top it is separated by about 30-35 nm of tegument. Viral glycoproteins are embedded into the viral envelope (grey). Image kindly provided by Kay Grünewald (Max Planck Institute of Biochemistry, Martiensried, Germany; Grünewald et al. 2003)

The three-dimensional structure of the HSV1 virion has been revealed by cryoelectron microscopy and 3D image reconstructions (Figure 2; Grünewald et al. 2003; Zhou et al. 1999; Zhou et al. 2000). The 5 nm thick viral membrane has a diameter of 170 to 225 nm, with viral glycoproteins protruding. Glycoproteins are important for attaching the incoming virus to the host cell plasma membrane, during virus assembly, trafficking and egress, and they also have immunomodulatory functions. The glycoproteins protrude from the viral membrane surface as spikes of 10 to 25 nm length and about 4 nm width (Grünewald et al. 2003; Reske et al. 2007; Spear et al. 2006). An amorphous protein layer called the tegument is located between the envelope and the capsid. It consists of about 20 different proteins. Based on assembly studies, the tegument proteins are divided into an outer shell containing mainly VP11/12 (UL46), VP13/14 (UL47), and VP22 (UL49); and an inner shell with close contact to the capsid which includes VP1-3 (UL36), UL37 and the kinase US3 (Mettenleiter 2002; Mettenleiter 2004).

The outer tegument dissociates after release of the capsid into the cytosol, while inner tegument proteins remain attached to the capsid until it reaches the nucleus (Granzow et al. 2005; Luxton et al. 2005; Sodeik et al. 1997). The two layers of tegument proteins can also be separated by detergent lysis of extracellular virions in the presence of different salt concentrations (Wolfstein et al. 2006). VP16 (UL48) is considered to be an adaptor protein between the inner and outer tegument layers, since it interacts with members of both (Vittone et al. 2005; Wolfstein et al. 2006). Examples of well characterized tegument proteins are VP16, a transactivator of immediate early viral transcription and UL41, the virus-host-shutoff factor (vhs), an RNase which degrades cellular mRNAs and stops host protein synthesis in infected cells (Zhang et al. 1991).

The capsid, which encloses the viral genome, has an eccentric position within the virus, with a proximal pole, where the distance between capsid and envelope is about 5 nm, and a distal pole, where the capsid and the envelope are separated by a 30 to 35 nm layer of tegument. The tegument is presumably attached to the capsid via the pentons and the adjacent hexons (Grünewald et al. 2003; Zhou et al. 1999; Zhou et al. 2000).

1.3.2 Capsid Assembly and DNA Packaging

Capsid assembly and genome packaging are crucial steps in virus assembly of double stranded (ds) DNA viruses (Mettenleiter 2006). Although dsDNA bacteriohages are quite distinct from the herpesviruses regarding their hosts, they do share similarities in capsid assembly and DNA packaging (Baines and Weller 2005; Baker et al. 2005; Catalano 2005; Duda et al. 2006). In the infected host of bacteriophages as well as of herpesviruses, capsid proteins are assembled into procapsids that further mature and are subsequently filled with viral concatameric genomes by specialized packaging and terminase machineries (Guo and Lee 2007).

The capsid with a diameter of 125 nm consists of 20 triangular faces, 11 pentagonal vertices and one portal complex at the 12th vertex. The capsid shell comprises four major proteins: VP5 (UL19), VP19C (UL38), VP23 (UL18), and VP26 (UL35; Duffy 2006; Newcomb et al. 1996; Roizman and Knipe 2001). Capsid assembly initiates with a spherical procapsid which self-assembles in the nucleus out of the proteins VP5, UL6, preVP22a, UL26.5 VP19C and VP23 (Singer et al. 2005). The major capsid protein VP5 assembles into both hexamers and pentamers (Figure 2). There are three types of capsomers: 150 VP5 hexons that form the faces and edges of the triangular faces, 11 VP5 pentons located at the vertices, and one UL6 portal complex at the 12th vertex (Cardone et al. 2007; Newcomb et al. 1996; Newcomb et al. 1999; Newcomb et al. 1994; Trus et al. 1996; Trus et al. 2004). On top of the VP5 hexons a hexamer of VP26 is located, which is not found on pentons (Wingfield et al. 1997). 320 triplexes, each consisting of two copies of VP23 and one copy of VP19C link adjacent capsomers (Chen et al. 2001; Homa and Brown 1997). A dodecameric ring of UL6 builds the 12th vertex, a portal. It most likely serves as an axial channel through which the concatameric viral DNA is tightly packaged (Booy et al. 1991; Cardone et al. 2007; Newcomb et al. 2005; Newcomb et al. 1996; Newcomb et al. 1999; Newcomb et al. 2001; Trus et al. 2004). The products of two further genes, UL26 (encoding a protease) and the UL26.5 (encoding the main scaffolding protein, VP22a), form the internal scaffold which is required for capsid assembly. The viral protease (UL26) cleaves both itself (to generate capsid proteins VP24 and VP21) and UL26.5 protein (generating VP22a) and is essential for DNA packaging, capsid maturation, and virus growth. Unlike VP21 and VP22a, which are removed from capsids upon DNA packaging, VP24 is quantitatively retained in mature, DNA containing capsids (Gao et al. 1994; Sheaffer et al. 2000).

Four capsid types are found in the nuclei of HSV1-infected cells during capsid assembly (Mettenleiter 2006). Capsids change either their size during maturation by expanding as shown for bacteriophages (Feis 2005) or changes their morphology from a rather spherical to angularized capsid as shown for herpesvirus (Baines and Weller 2005; Heymann et al. 2003). The so called short-lived procapsid matures into an angularized B-capsid that contains the scaffold proteins VP21 and VP22a. The so called A-capsids (abortive capsids) enclose neither scaffold nor DNA and are dead end products from unsuccessful DNA packaging. C-capsids lack scaffold proteins but do contain viral genomes (Homa and Brown 1997; Roizman and Knipe 2001).

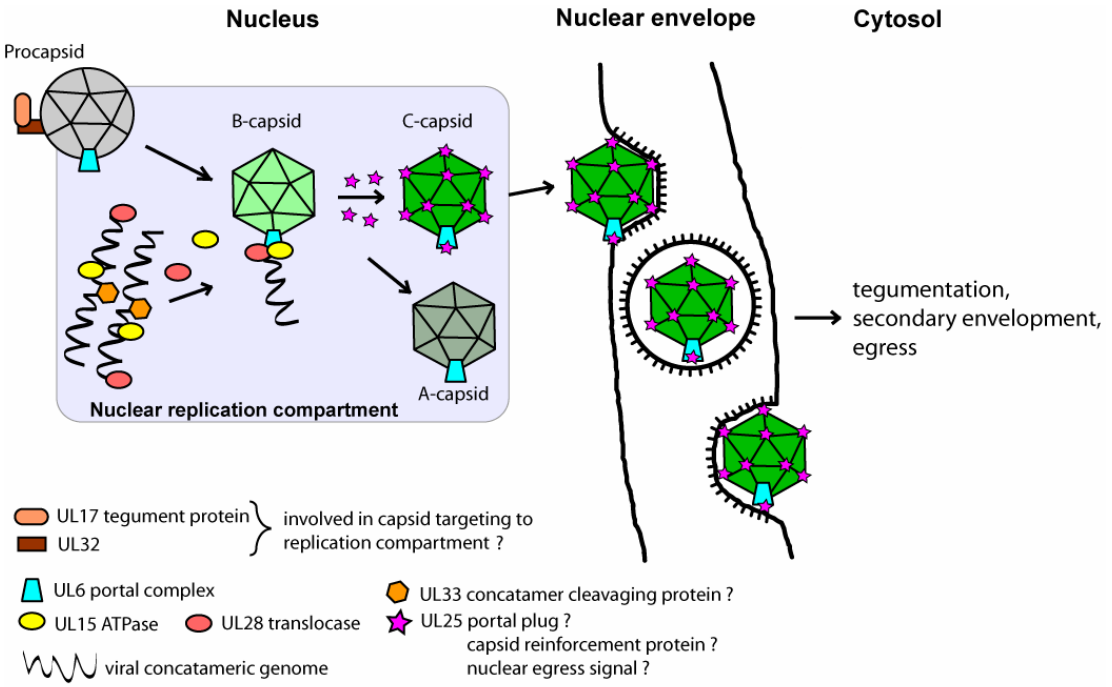

Figure 3: DNA packaging and capsid maturation: Packaging of viral DNA into the spherical procapsid begins with cleavage of the viral genome into concatamers presumably by UL32, UL28 and UL15 in the nuclear replication compartment. The procapsid may be targeted to the replication compartment by UL17 and UL32. The terminase complex is composed of the UL28 translocase and the UL15 ATPase that provides energy for packaging through ATP hydrolysis. This complex associates with the UL6 portal complex and packaging through portal is initiated. UL15 hydrolyses ATP, and thus provides the energy for packaging the viral DNA into the capsid. UL25 might be required for retaining the genome inside the capsid, stabilizes the capsids at their vertices and may provide an exit signal for nuclear egress. The DNA-containing capsid leaves the nucleus for further tegumentation, secondary envelopment and virus egress. Scheme derived and modified from Baines and Weller 2005; Beard et al. 2004; Beard et al. 2002; Klupp et al. 2006; Lamberti and Weller 1998; McNab et al. 1998; Newcomb et al. 2001; Stow 2001; Trus et al. 2007; Yang et al. 2007.

UL17 and UL32 are supposed to target procapsids to the nuclear sites of DNA packaging (Lamberti and Weller 1998). Packaging of viral DNA begins with specific binding of terminase proteins to the packaging initiation site of the viral concatemeric DNA (Figure 3). The genome is then packaged through a portal complex, also a common feature in bacteriophages and in herpesviruses (Casjens et al. 1992; Newcomb et al. 2001). The proteins UL6, UL15, UL17, UL25, UL28, UL32 and UL33 are essential for HSV1 DNA cleavage and packaging and located on the external surface of the capsid (Baines and Weller 2005; Wills et al. 2006). The terminase complex of UL15 and UL28 build a complex in the cytosol and interact with the portal complex in the nucleus (Yang et al. 2007). UL15, UL28 and possibly UL33 recognizes packaging signals on the viral DNA and cleaves the concatameric DNA into monomeric units (Beard et al. 2004; Beard et al. 2002). UL15 hydrolyses ATP, and thus provides energy for packaging the viral DNA into the capsid (Beard et al. 2002; White et al. 2003; Yu and Weller 1998). Especially UL6 and UL25 are structural proteins of the infectious virions but absent from L-particles which contain viral membrane and tegument proteins but neither capsids nor viral genomes (Dargan and Subak-Sharpe 1997; Taus et al. 1998; Thurlow et al. 2005). Only UL17 is also found in L-particles (Thurlow et al. 2005). UL25 performs a later function and may be required for retaining the genome inside the capsid by plugging the portal (McNab et al. 1998; Stow 2001). Moreover, after finishing the packaging process, heterodimeric UL25-UL17 complexes may be added at or near each of the capsid vertices to stabilize and reinforce the DNA-containing capsid prior to nuclear egress (Klupp et al. 2006; Newcomb et al. 2006; Trus et al. 2007).

1.3.3 Egress

After assembly and DNA packaging, capsids have to exit the nucleus for further maturation. The egress of herpesviruses might occur via three distinct pathways and is subject to controversy (Figure 4, Campadelli Fiume 2007; Campadelli-Fiume 2006; Enquist et al. 1998; Johnson and Spear 1982; Leuzinger et al. 2005; Mettenleiter et al. 2006; Mettenleiter and Minson 2006; Skepper et al. 2001; Wild et al. 2005).

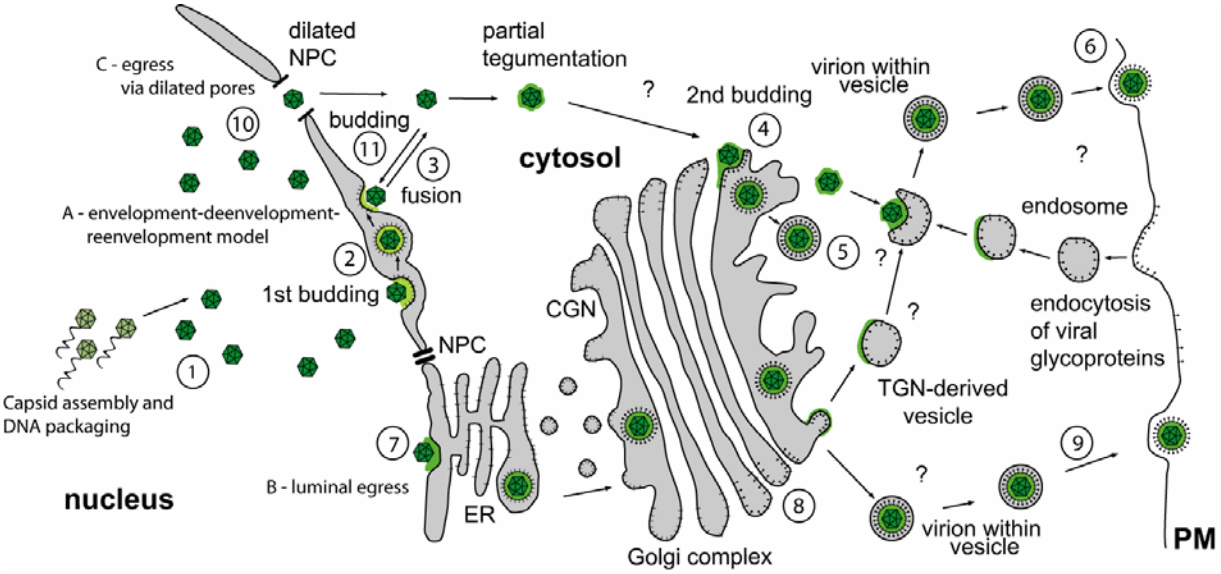

Figure 4: HSV1 egress. HSV1 capsids are assembled and the genome is packaged in the nucleus (1). According to the envelopment-deenvelopment-reenvelopment model (A), the capsids bud through the inner nuclear membrane into the perinuclear space, thereby aquiering a primary tegument and envelope (2), and then fuse with the outer nuclear membrane (3). Viral envelope proteins are modified and accumulate at the Golgi network. Tegumentation takes place at two sites, at the capsid and at an internal membrane, presumably the Golgi apparatus (GN; CGN – cis-Golgi network; TGN – trans-Golgi network), or vesicles from Golgi or endosomal origin. The partially tegumented capsid then buds into vesicles or into endosomes, so that an infectious virion inside a vesicle is formed (6). This vesicle fuses with the plasma membrane and releases the virion (7). In the luminal egress model (B), the mature capsid with tegument also buds into the perinuclear space (7). The capsid travels through the rough endoplasmic reticulum to the GN (8). The virion inside the vesicle might leave the cell via exocytosis (9). The latest model proposes that mature capsids leave the nucleus through dilated, impaired nuclear pore complexes (10). The capsid could then bud into the outer nuclear membrane (11) for further egress according to the luminal egress route (B) or for futher budding at the site of secondary envelopment (4-6). Scheme derived and modified from Enquist et al. 1998; Johnson and Spear 1982; Leuzinger et al. 2005; Mettenleiter and Minson 2006; Skepper et al. 2001; Wild et al. 2005 and kindly provided by Claus-Henning Nagel, Katinka Döhner and Beate Sodeik, Institute of Virology, Hannover Medical School.

A currently widely accepted model of nuclear capsid egress and HSV1 assembly is the **envelopment – deenvelopment – reenvelopment model** (Figure 4 A; Skepper et al. 2001), suggesting the formation of a primary virion with primary tegument and envelope. The DNA-filled C-capsid might acquire a nuclear egress signal via UL25/UL17 heterodimers on the capsid pentons to leave the nucleus (Trus et al. 2007). At the inner nuclear membrane, the protein complex of UL31 and the transmembrane protein UL34 sequester protein kinase C that subsequently phosphorylates lamin A/C and lamin B (Reynolds et al. 2004; Reynolds et al. 2001; Reynolds et al. 2002). Moreover, the viral protein kinase US3 also modifies lamin A/C (Mou et al. 2007). These processes disintegrate the nuclear lamina. The capsid can therefore get access to the inner nuclear membrane where it buds into the perinuclear space and acquires the primary tegument at least composed of UL31, the protein kinase US3 and the viral transcription factor VP16 (Bjerke and Roller 2006; Fuchs et al. 2002; Klupp et al. 2001; Naldinho-Souto et al. 2006; Ryckman and Roller 2004). The primary envelope protein UL34, but also the essential

glycoproteins gB and gH, as well as precursors of gD have also been detected on the primary virion in the perinuclear space (Campadelli-Fiume 2006; Farnsworth et al. 2007; Fuchs et al. 2002; Torrisi et al. 1992). Moreover, gM is incorporated in the membrane during budding at the inner nuclear membrane (Baines et al. 2007). Later, primary virions fuse their primary envelopes with the outer nuclear membrane or the endoplasmic reticulum membrane, presumably mediated via gB and gH, and release capsids into the cytosol which contain US3 and VP16 tegument proteins (Farnsworth et al. 2007; Granzow et al. 2004).

The **luminal egress model** proposes that mature capsids bud at the inner nuclear membrane and thereby acquire their final envelope. The virions would then travel through the perinuclear space into the rough endoplasmic reticulum. They might reach the Golgi apparatus and the trans-Golgi network within transport vesicles (Figure 4 B; Darlington and Moss 1968; Johnson and Spear 1982; Leuzinger et al. 2005). However, in this model tegumentation has to take place in the nucleus, because capsids never have access to the cytosol. This model is in conflict with data showing a subset of tegument proteins attached to the cytosolic tails of glycoproteins at the site of secondary envelopment (Harley et al. 2001; Mettenleiter 2006; Turcotte et al. 2005).

Both models were challenged by proposing that capsids may egress into the cytosol via **impaired and dilated nuclear pores**. Within this model, nuclear pores are believed to enlarge their diameter from 100 nm to about 700 nm and capsids leave the nucleus through those impaired pores (Figure 4 C; Leuzinger et al. 2005; Wild et al. 2005). The cytosolic capsids then either bud into the Golgi vesicles to follow the secretory pathway or into the outer nuclear membrane to travel through the perinuclear space and the endoplasmic reticulum to the Golgi apparatus or the trans-Golgi network. However, this hypothesis is intensively discussed since it is not in line with previous electron microscopy studies and mainly not consistent with the phenotypes of many mutant viruses that lack US3, UL31, UL34 or gB/gH (Farnsworth et al. 2007; Mettenleiter and Minson 2006; Reynolds et al. 2002), although minor nuclear membrane changes are observed during HSV1 infections (Haines and Baerwald 1976; Nagel, Döhner, Fathollahy, Strive, Borst, Messerle & Sodeik, accepted). Moreover, there is no evidence that nuclear transport factors interact with mature capsids that could support the egress via the dilated nuclear pore (Campadelli-Fiume 2006; Mettenleiter and Minson 2006).

According to the first model, the **envelopment – deenvelopment – reenvelopment model** the inner tegument proteins VP1-3 (UL36) and UL37 are attached to the capsids in the cytosol. In deletion mutants of HSV1 that lack the tegument proteins VP1-3 (UL36) or UL37, capsids devoid of tegument and envelope accumulate in the cytosol (Desai et al. 2001; Desai 2000). Viral glycoproteins together with a subset of outer tegument proteins like VP11/12 (UL46), VP13/14 (UL47), and VP22 (UL49) accumulate at sites of secondary budding, presumably vesicles or patches derived from trans-Golgi or endosomal origin (Figure 4, Granzow et al., 2001; Harley et al., 2001; Turcotte et al., 2005). During secondary budding into the lumen of these organelles via an interaction of inner and outer tegument the virions become fully assembled, and are then released into the extracellular space by fusion of virion-containing vesicles with the plasma membrane (Mettenleiter et al. 2006).

1.3.4 Attachment, Entry and Nuclear Tageting

Extracellular HSV1 virions make first contact with the cell by attaching at the plasma membrane with their envelope glycoproteins (Figure 5). Glycoprotein C (gC) or gB bind to cell surface via heparan sulphate or glycosamino glycans. These interactions, although not essential for infection, increase infection efficiency due to an enrichment of virions on the cell (Spear 2004; Spear et al. 2000; Spear and Longnecker 2003). For successful infection, gD has to bind one of the following secondary receptors (Campadelli-Fiume et al. 2007):

(I) the herpesvirus entry mediator (HVEM) which belongs to the tumor necrosis factor receptor family, (II) nectin-1, also called herpesvirus entry protein C (HveC) or poliovirus receptor-related protein-1, a cell-cell adhesion molecule of the immunoglobulin superfamily, or (III) 3-O-sulphated heparan sulphate (Shukla and Spear 2001; Tiwari et al. 2006). Moreover the type II transmembrane protein B5 whose viral ligand is not known is also involved in virus binding (Perez et al. 2005; Perez-Romero and Fuller 2005). Furthermore, the RGD motif of gH can interact with αvβ3 integrin (Parry et al. 2005).

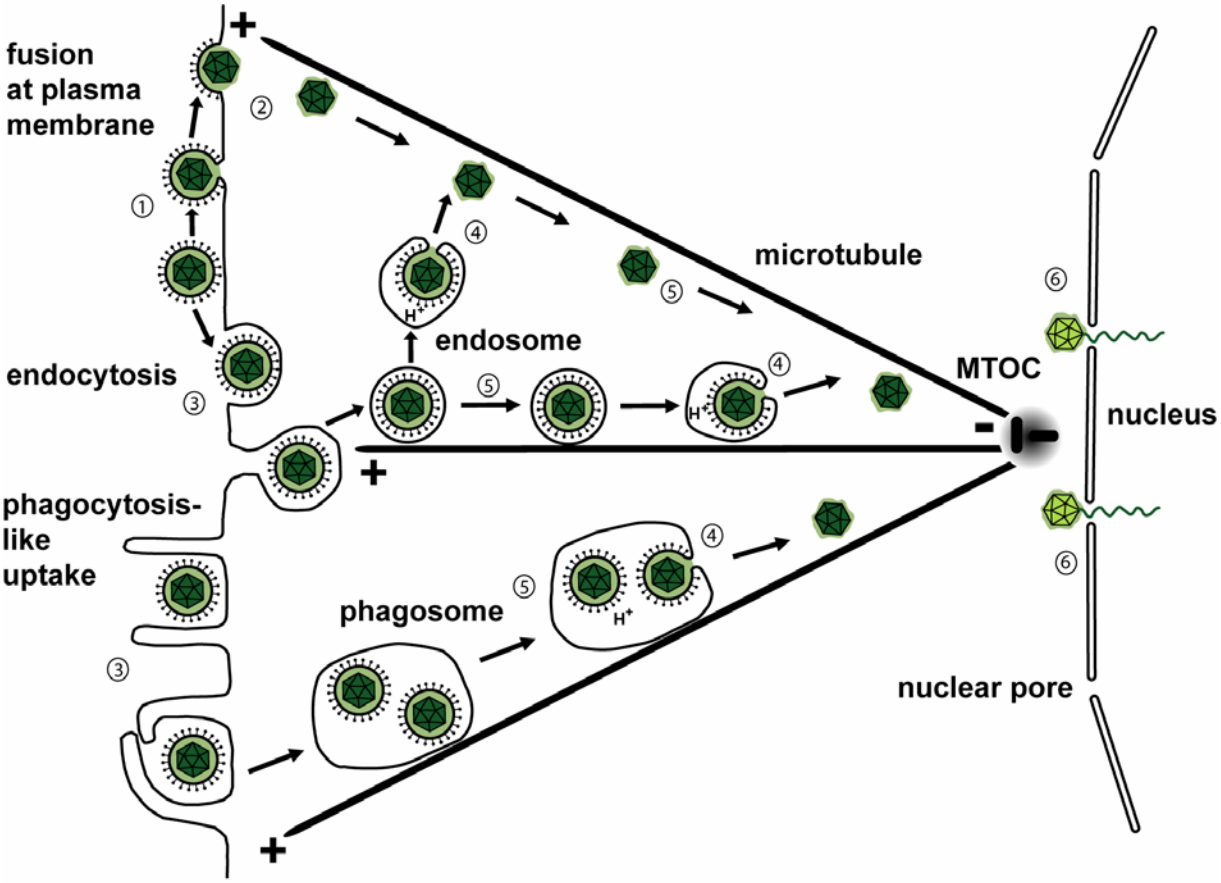

Figure 5: HSV1 entry. HSV1 envelope (black) glycoproteins mediate attachment to the host cell membrane (1). The virus enters many cell types by fusion of the viral envelope with the plasma membrane, thereby releasing the capsid (dark green) and tegument (light green) into the cytosol (2). Other cell types are entered by endocytosis or phagocytic-like uptake (3). By fusion of the viral envelope with the endosomal membrane capsid and tegument are released into the cytosol (4). The capsid with some tegument or an HSV1 virion inside an endocytic vesicle is then transported by the minus-end directed microtubule motor dynein and its cofactor dynactin to the MTOC (5). Finally, viral capsids arrive at the nuclear envelope. Importin β mediates binding to the NPC, and the viral genome is released into the nucleus for viral transcription and replication (6). Scheme derived and modified from Clement et al. 2006; Gianni et al. 2004; Koyama and Uchida 1987; Nicola et al. 2005; Nicola et al. 2003; Nicola and Straus 2004; Döhner and Sodeik 2005; Döhner et al. 2002; Sodeik et al. 1997 and kindly provided by Katinka Döhner and Beate Sodeik, Institute of Virology, Hannover Medical School.

After attaching to the plasma membrane, the viral capsid has to reach the nuclear pore compex (NPC) for genome uncoating. The viral envelope fuses either with the host cell plasma membrane, or with an endosomal or phagosomal membrane. Cell types such as Vero, BHK, HEp-2, COS and human dorsal root ganglion neurons are entered by fusion of the viral envelope with the plasma membrane (Koyama and Uchida 1987; Lycke et al. 1988; Sodeik et al. 1997; Wittels and Spear 1991). Other cell types, such as CHO-HVEM or HeLa cells are infected by endocytosis (Gianni et al. 2004; Milne et al. 2005; Nicola et al. 2005; Nicola et al. 2003; Nicola and Straus 2004). A phagocytic-like entry has been described for human corneal fibroblasts and CHO-Nectin cells (Clement et al. 2006). For fusion of the viral envelope with the host membrane, gD, gB and the heterodimer gH-gL are essential. Binding of gD to one of its receptors triggers a conformational change, which in turn results in interactions of gD with gB and/or gH-gL. gH-gL initiate hemifusion of the host membrane that is completed by gB (Gianni et al. 2006a; Gianni et al. 2006b; Gianni et al. 2005a; Gianni et al. 2005b; Spear et al. 2006; Subramanian and Geraghty 2007). The viral capsid inside the cytosol leaves some tegument proteins associated with glycoproteins at the plasma membrane, but some tegument proteins like VP1-3 (UL36) or US11 remain capsid-bound until arrival at the nucleus (Granzow et al. 2005; Luxton et al. 2006; Sodeik et al. 1997, Schipke and Sodeik; Janus, Döhner and Sodeik, personal communication).

HSV1 capsids use the minus-end directed molecular motor dynein and its cofactor dynactin to travel along microtubules, that are clustered with their minus end at the microtubule organizing center (MTOC; Döhner et al. 2005; Döhner et al. 2002; Radtke et al. 2006; Sodeik et al. 1997). The viral proteins mediating the interaction with dynein are unknown, but possible candidates are the tegument proteins VP1-3 (UL36) and UL37 (Luxton et al. 2006; Wolfstein et al. 2006). For pseudorabiesvirus, another α-herpesvirus infecting swine, it was shown that VP1-3 and UL37, but not VP16, VP13/14 and VP22 remain bound to capsids during the retrograde transport in axons (Granzow et al. 2005; Luxton et al. 2005; Luxton et al. 2006). *In vitro,* HSV1 capsids interact with dynein and dynactin and need the inner tegument for this interaction (Wolfstein et al. 2006). Capsids arrive at the MTOC, and from there they need to get further to the nuclear pore, presumably by using the plus-end directed microtubule motors of the kinesin family (Janus, Döhner, Büttner and Sodeik; personal communications). Moreover, capsids could also use nuclear import or export factors for their travel to the NPC (Hanz et al. 2003; Ojala et al. 2000; Radtke et al. 2006; Strunze et al. 2005).

1.3.5 HSV1 Genome Uncoating

Viruses that replicate their genomes in the nuclei of infected cells have to ensure that their genome is released into the nucleus and not into the cytosol. There, the genomes are either integrated into the host genome or maintained as an episome for transcription (reviewed in Greber and Fassati 2003). An important feature in this process is the nuclear pore complex (NPC). The NPC is a 125 MDa complex spanning the outer and inner nuclear membrane and thus providing a channel for nucleocytoplasmic trafficking. The entire pore has a diameter of about 120 nm whereas the inner diameter of the pore channel is about 40 nm (Pante and Aebi 1993; Pante and Kann 2002). In general, genome uncoating of nuclear replicating viruses follows one of the three pathways:

I. The viral capsid recruits nuclear import or export factors and thereby triggers its translocation through the pore to be disassembled in the nucleoplasm. Parvoviruses and hepatitis B virus pass the NPC channel prior to genome uncoating in the nucleoplasm (Kann 2004; Kann et al. 1999; Rabe et al. 2003; Vihinen-Ranta et al. 2002; Vihinen-Ranta et al. 2000).

II. The viral capsid disassembles in the cytosol and subviral genomic particles are further translocated through the pore into the nucleoplasm. Lentiviruses, such as the human immune deficiency virus 1 (HIV1) can infect non-dividing cells, whereas retroviruses can only enter cells that undergo mitosis. After cell entry, core disassembly and reverse transcription of the single strand RNA genome take place and the newly synthesized DNA associates with viral proteins to a preintegration complex which is then imported into the nucleus (Popov et al. 1998a; Popov et al. 1998b; Sherman and Greene 2002).

III. The viral capsid docks at the NPC and releases its genome either after disassembly of the capsid or by injecting it through the channel into the nucleoplasm (Greber and Fassati 2003). Incoming adenovirus capsids dock to the cytoplasmic fibrils of the NPC and interact with Nup214/CAN. Disassembly factors like histone H1, importin β, importin 7 and HSC70 are recruited and the viral genome is released into the nucleoplasm upon adenovirus capsid disassembly (Greber et al. 1997; Greber et al. 1996; Greber et al. 1993; Harel and Forbes 2001; Trotman et al. 2001). Incoming HSV1 capsids dock with the help of importin β at the NPC via the cytoplasmic fibrils with one penton facing the NPC (Granzow et al., 1997; Sodeik et al., 1997; Ojala et al., 2000). The interaction of capsid, supposedly by the protein VP1-3, and the NPC may lead to a destabilisation of the capsid so that the viral genome can de injected via the pore into the nucleoplasm for viral transcription and replication (Batterson et al. 1983; Ojala et al. 2000). The binding partner of the NPC with the HSV capsid is unknown but it is likely to be located at the cytoplasmic ring of the pore like Nup88/84, Nup214/CAN or Nup358/RanBP2 (Rabut et al. 2004, Trotman et al. 2001). The uncoating of the herpesvirus genome requires energy and cytosol and is temperature dependent (Newcomb et al. 2007; Ojala et al. 2000). The protein VP1-3 (UL36) is proposed to play a role during uncoating, since a temperature sensitive mutant of HSV1 (tsB7), which has a mutation in the UL36 gene, and also a UL36 mutant in pseudorabiesvirus, can bind at the NPC but are unable to inject the viral genome at the nonpermissive temperature (Batterson et al. 1983; Feldman et al. 1981).

An *in vitro* uncoating assay of viral C-capsids revealed that destabilizing the capsid with trypsin protease leads to uncoating where the viral genome is ejected as a single double helix, although it is still unknown whether the herpesvirus genome is released during cell entry through the UL6 portal complex (Newcomb et al. 2007). Released genomes were also observed via atomic force microscopy as rod shaped structures with a size of 130 x 30 nm, that enter the nucleoplasm via distorted nuclear pores (Shahin et al. 2006). In both cases, the viral genome is retained within the capsid, until its final destination, the NPC, is reached. After uncoating, empty capsids at the NPC or *in vitro* uncoated capsids still show an angularized morphology (Newcomb et al. 2007; Ojala et al. 2000; Sodeik et al. 1997).

1.3.6 Gene Expression, Transcription and Latency

After the the tegument protein VP16 (UL48) is imported into the nucleus and viral DNA is released into the nucleoplasm, viral gene expression commences. VP16 binds to the cellular transcription factors Oct-1 and HCF, and this complex activates the expression of the immediate early genes (α) genes ICP0, ICP4, ICP22, ICP27 and ICP47 by binding to TAATGARAT elements in their promoters (La Boissiere et al. 1999; Weir 2001). ICP4 together with viral genomes form intranuclear replication foci that are localized near promyelotic leukaemia (PML) nuclear bodies, also called nuclear domain (ND) 10. However, ICP0 degradates the PML protein by its E3-ubiquitin-ligase activity (Everett et al. 2004; Everett et al. 2003). The cooperation between nucleoprotein complexes, formed by immediate early transcription of incoming viral genomes, and ND10 structures finally results in the formation of intranuclear replication compartments that lack PML (Everett and Murray 2005).

HSV1 transcription is controlled in a cascade-like manner (Rajcani et al. 2004; Roizman and Knipe 2001; Sandri-Goldin 2007; Weir 2001). The immediate early (α) genes induce the expression of the early (β) genes which are needed for viral DNA-replication. Late (γ) genes, which are expressed after HSV1-DNA replication has started, include structural and packaging proteins. For replication the linear viral genome circularizes in the nucleus to a covalently closed form (Roizman and Taddeo 2007; Strang and Stow 2005; Yao et al. 1997). The HSV1 origin-binding protein UL9 binds to one or more HSV1 replication origins and opens the double strand. The HSV1 single-strand binding protein ICP8 (UL29) stabilizes the single DNA strands (Roizman and Knipe 2001). The helicase/primase complex of UL5, UL8 and UL52 then form the replication fork and the viral DNA polymerase UL30/UL42 synthesizes progeny DNA strands (Wilkinson and Weller 2003). Early in infection a rolling circle mechanism for replication of circular viral genomes was proposed (Roizman and Knipe 2001). In neurons, HSV1 establishes latent infections. No virions are produced, and circularized genomes remain silent in an episomal state. Latency-associated transcripts (LATs) are expressed during latency, representing a silent infection, that is ignored by the immune system (Bloom 2004). Besides LATs, also gB is present in neurons during latency, since CD8(+) T cells against a gB peptide block reactivation from latency in neurons **(**Khanna et al. 2003). Latency is probably induced by a block or impairment of immediate early gene expression (Preston 2000). Upon stress like UV-light or a compromised immune system, HSV1 reactivates and switches from latency to lytic replication (Khanna et al. 2004). New virions assemble and are transported back to the synapses of the innervating neurons of the initial site of infection. There epithelial cells and keratinocytes are infected again resulting in virus shedding and eventually recurrent diseases like cold sores (Steiner 1996).

Table 2: Overview of some HSV1 proteins involved in different stages of the viral life cycle;
modified and derived from Roizman and Campadelli Fiume 2007. Some proteins have also functions during other stages during the viral life cycle, but they are listed where they appear first. References for the protein functions can be found in the introduction.

Stage of HSV1 life cycle	Protein	Function
Capsid assembly	**VP5**	Major capsid protein; capsid hexons contain 6 copies, pentons 5 copies; 150 hexons and 11 pentons in total
	UL6	Builds the portal complex at a unique vertex of the capsid as a homododecameric protein complex
	VP19C	One copy of VP19c and two copies of VP23 build a triplex
	VP23	Part of the triplex that connects VP5 hexons and pentons, 320 triplices
	VP26	Small capsid protein binds as hexamer pentons but not hexons
	VP22a	Scaffold protein present in B-capsids; will be removed upon DNA packaging
DNA packaging	**UL32**	Involved in procapsid transport to the nuclear replication compartments for DNA packaging
	UL17	Targets the procapsid to the site of DNA packaging, presumably stabilizes capsids in a complex with UL25 after DNA packaging
	UL33	Presumably involved in concatamer cleveage of the viral DNA
	UL15	ATPase which provides energy through ATP hydrolysis for DNA packaging
	UL28	Translocase in complex with ATPase UL15, helps packaging the DNA through the UL6 portal complex
	UL25	Involved in capsid stabilization and might provide a nuclear exit signal once bound to C-capsids
Egress	**UL31**	Primary tegument protein, binds lamin A/C and directs envelopment a the inner nuclear membrane
	UL34	Primary envelope protein, needs UL31 for localization at the inner nuclear membrane, recruits protein kinase C for lamin phosphorylation
	US3	Serine/threonine protein kinase, dispensable for viral replication but blocks apoptosis, part of the primary and secondary enveloped virus
	VP16	Might connect inner and outer tegument, major transcriptional activator in complex with the cellular proteins Oct-1 and HCF
	VP1-3	Major tegument protein, essential for replication and egress of virions through the cytoplasm; ts mutant is deficient in DNA release into the nucleus at the nonpermissive temperature; putative receptor for microtubule motor
	UL37	Tegument protein that binds VP1-3, bind also DNA in the presence of ICP8 and is essential for virus replication
	VP13/14	Outer tegument protein, binds RNA and shuttles between cytoplasm and nucleus
	VP22	Tegument protein
Entry	**gC/gB**	Bind heparin sulfates on cells surface at initiate attachment of virus
	gD	Binds HVEM, nectin-1, 3-0-sulphated heparin sulfate for virus binding
	gB	Initiates hemifusion of viral and cellular membrane
	gH	Interacts with $\alpha v\beta 3$ integrin, essential for fusion
	gL	Essential for fusion
	vhs	Host shut off protein that mediated cellular RNA degradation
	US11	Virion associated US11 binds polyribosomes, late in infection it localizes to nucleoli
Gene expression, Replication, Latency	**ICP0**	Promiscuous transactivator of gene expression
	ICP4	Transactivator and repressor of viral gene functions
	ICP8	Required for viral DNA synthesis, single-strand DNA binding protein
	UL9	Origin binding protein
	UL5/8/52	Helicase/primase complex, new drug target (BAY-57-1293)
	UL30/42	DNA polymerase
	LAT	Latency associated transcript

1.4 The HSV1-UL25 Protein

1.4.1 General Properties of UL25

The UL25 gene is highly conserved among alphaherpesviruses (Rode 2003, Diploma thesis). The HSV1-UL25 protein is composed of 580 amino acids and has a calculated molecular weight of 62.6 kDa (McNab et al. 1998).

The crystal structure of an N-terminally truncated version of HSV1-UL25 (amino acids 134-580) has been recently resolved at a resolution of 2.1 Å (Figure 6, Bowman et al. 2006). It reveals a novel fold with a stable almost brick-shaped core of multiple α-helices and four β-sheets with many emanating flexible loops which may mediate UL25 functions. It folds into a structure with a distinct electrostatic distribution; the electronegative side might contribute for oligomerization and protein-protein interactions; the electropositive face could mediate DNA binding. Evolutionary trace analysis of UL25 and its homologues revealed important amino acids on the protein surface that may be crucial for binding associated proteins.

The functions of its homologues in human cytomegalovirus (HCMV-UL77) and in Kaposi´s sarcoma-associated herpesvirus (KSHV-ORF19) are unknown. For HCMV-UL77 a sequence identity to a pyruvoyl decarboxylase enzyme prosthetic group has been described, but its functional relevance for the viral life cycle remains unclear (Yoakum 1993).

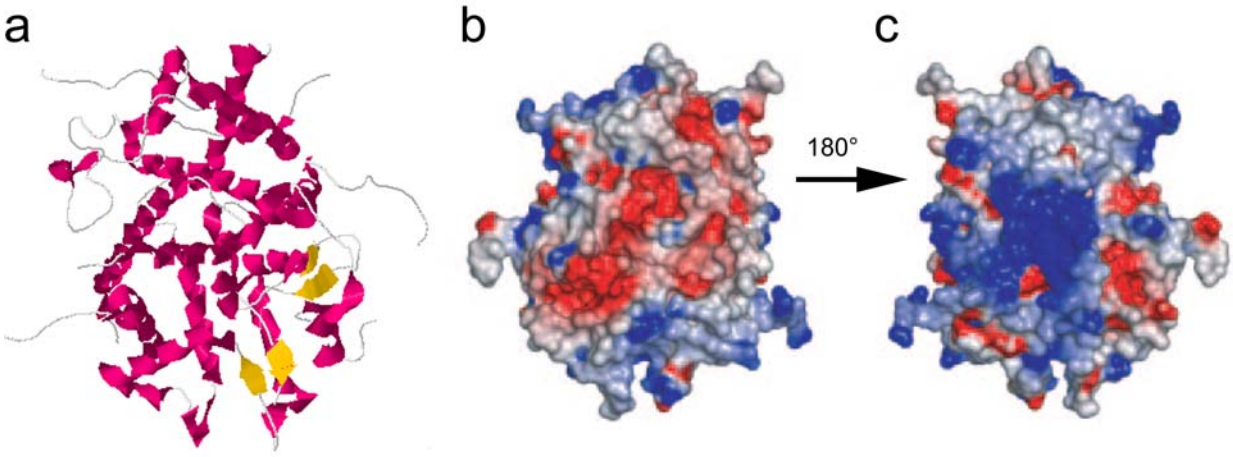

Figure 6: Crystal structure of HSV1-UL25 (aa 134-580): The structure of UL25 was resolved at a 2.1 Å resolution. A ribbon diagram (a) shows multiple α-helices (pink) and four β-sheets (yellow) in a brick-shaped core emanating flexible loops (from: http://oca.ebi.ac.uk/oca-bin/ccpeek?id=2F5U). The electrostatic surface representation shows the electronegative face (b) that might be involved in self oligomerization. The electropositive site (c) might be nessecary for DNA binding (from Bowman et al. 2006, Fig. 2, modified).

1.4.2 UL25 Functions During Capsid Assembly

Herpesviruses and some dsDNA bacteriophages such as T4, lambda or SPO1 share a common ancestry in capsid architecture and the process of DNA packaging (Baker et al. 2005; Duda et al. 2006; Murialdo 1991; Prevelige and King 1993). They all assemble spherical procapsids which then mature into angular capsids (Homa and Brown 1997; Prevelige and King 1993). After DNA packaging, the bacteriophages add scaffolding proteins to retain their DNA within the capsid (King et al. 1976; King et al. 1973; Lenk et al. 1975).

The UL25 protein of herpesviruses might provide a similar function, since it is required for efficient retention of the packaged viral genome inside the capsid. UL25 could seal the UL6 portal after the genome has been packaged (Figure 7 a; Desloges and Simard 2003; McNab et al. 1998; Ogasawara et al. 2001; Sheaffer et al. 2001; Stow 2001). However, in the absence of UL25, C-capsids are detected in HSV1 and PrV indicating packaging and encapsidation of viral DNA, albeit with reduced efficiency (Figure 7 b; Klupp et al. 2006; Stow 2001). Additionally, PrV-ΔUL25 capsids do not leave the nucleus (Klupp et al. 2006). These two proposed functions may not exclude each other (Figure 7 c). The copy number of UL25 correlates with the loss of scaffold protein during capsid maturation. Very little UL25 is found on procapsids that contain unprocessed scaffold. B capsids contain more UL25 and UL17, and the largest amount is found on C-capsids (Sheaffer et al. 2001; Thurlow et al. 2006; Trus et al. 2007). On PrV capsids the amount of UL25 on A- and C-capsids is higher than on B-capsids (Kaelin et al. 2000). A quantitative immunoblot showed that the capsid content of UL25 were 56, 20, and 75 copies per capsid in A, B, and C-capsids, respectively. Therefore about 5 copies per penton are found in C-capsids (Newcomb et al. 2006). Thus, removal of scaffold may allow more efficient binding of UL25 to capsids.

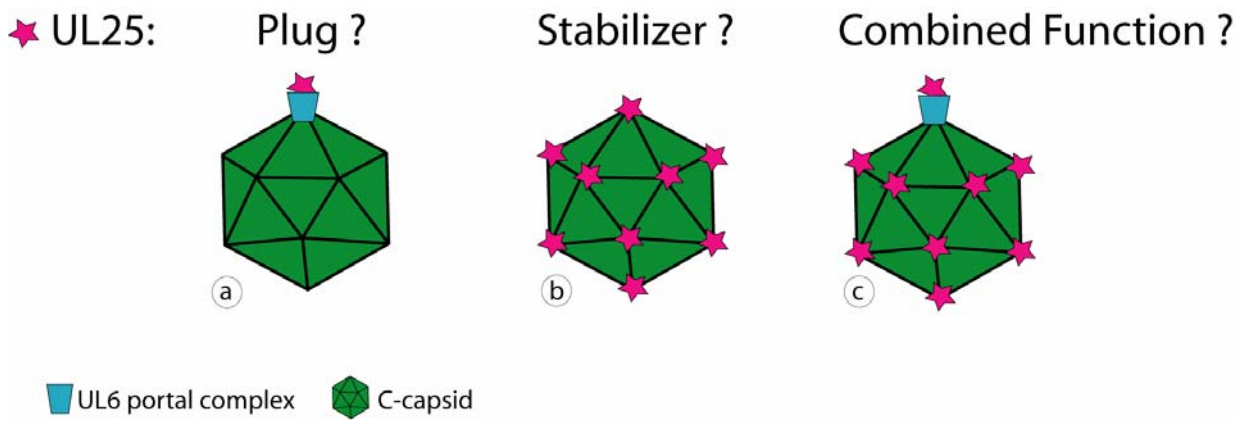

Figure 7: Proposed functions of UL25 during capsid assembly: The function of the UL25 protein during assembly is highly debated. Previous data suggested that UL25 might seal the channel of the UL6 portal complex after DNA packaging to retain the viral genome within the capsid (a). Recent data suggest that UL25, presumably in a complex with the tegument protein UL17 is subsequently added after DNA packaging to every vertex of the capsid for stabilization. Moreover only packaged capsids that contain UL25 may leave the nucleus for further maturation. Therefore UL25 was proposed to be a nuclear exit signal (b). Furthermore a combination of both functions would be possible. Scheme derived and modified from Desloges and Simard 2003; Klupp et al. 2006; McNab et al. 1998; Ogasawara et al. 2001; Sheaffer et al. 2001; Stow 2001; Trus et al. 2007.

Far western blot analysis proposed an association of UL25 with the capsid proteins VP5, VP19C and VP23. Moreover UL25 specifically binds herpesviral DNA (Ogasawara et al. 2001). The C-terminus ot the large tegument protein VP1-3 interacts with UL25. VP1-3 was proposed to initiate tegument assembly after nuclear egress of capsids, Therefore, UL25 may connect VP1-3 to capsids for recruitment of tegument proteins (Coller 2007).

A careful structural analysis of wild type virus C-capsids and A-capsids derived from UL25-deletion mutants revealed that there is a C-capsid specific component (CCSC) clustered at the vertices (Trus et al. 2007). Based on the size of this CSCC, a heterodimer of UL25 and the DNA packaging protein UL17 (Thurlow et al. 2005) most likely comprises this CSCC (Trus et al. 2007). UL25 remains associated with viral capsids after salt extraction suggesting a tight association of UL25 with the capsid (Wolfstein et al. 2006). UL25 and UL17 both play a role in capsid maturation and DNA packaging. In the absence of UL17, the levels of UL25 on the B-capsid were lower and vice versa (Thurlow et al. 2006; Thurlow et al. 2005), therefore UL25 and UL17 interactions are important for efficient incorporation of both proteins. UL25 and UL17 may be subsequently added to the C-capsid vertices to reinforce the structure and to give a signal for leaving the nucleus by budding through the nuclear membrane (Figure 7 b; Klupp et al. 2006; Thurlow et al. 2006; Trus et al. 2007). Regarding the common ancestry of bacteriopahges and herpesviruses (Baker et al. 2005), UL25 might be analogous to the lambda phage protein gpW, which is required for the stabilization of the phage head (Perucchetti et al. 1988).

1.4.3 UL25 Functions During Virus Entry

Studies on two temperature-sensitive HSV1-mutants, ts1204 and ts1208, that both have a mutation mapped in the UL25 open reading frame, suggest that UL25 may not only function in capsid assembly but also during cell entry. At the nonpermissive temperature of 39°C, the mutant ts1204 absorbed to the plasma membrane but failed to penetrate it. Upon superinfection with HSV2 also ts1204 could enter but lower amounts of capsids were generated. The mutant ts1208 penetrated the cell normally, but as for ts1204 formation of functional capsids was affected (Addison et al. 1984).

Since the PrV-UL25 protein seems to associate with microtubules after transient transfection, it was proposed that UL25 may be involved in microtubule mediated transport of incoming capsids from the cell periphery to the nuclear pores (Kaelin et al. 2000). In contrast to PrV-UL25, we showed that in living cells overexpressed GFP-tagged HSV1-UL25 was localized in the cytosol and to a lower extent in the nucleus but never on cytosceletal strutures (Rode 2003, Diploma thesis). Several fixation and permeabilization protocols for immunofluorescence labeling could maintain this localization, and overexpressed HSV1-UL25 did also not colocalize with actin, vimentin or microtubule filaments (Figure 8). Only after one protocol, pre-extraction in a microtubule stabilizing buffer and methanol fixation, we obtained a filamentous GFPUL25 pattern that partially overlapped with microtubules. This pattern differed from the *in vivo* localization as well as from the localization after several other fixation and permeabilization protocols therefore it was most likely a fixation artifact (Figure 8 k). After the harsh pre-extraction prior to fixation with methanol the negatively charged surface of the microtubules (Downing 2000) might interact with the electropositive side of the UL25 protein (Bowman et al. 2006).

Thus, in contrast to the filamentous pattern of PrV-UL25, most likely being a fixation artifact, transiently expressed HSV1-UL25 was localized in the cytosol and to a lower extent in the nucleus (Rode 2002, Internship report; Rode 2003, Diploma thesis).

If HSV1-UL25 had a function during nuclear targeting of capsids, UL25 in excess might act as a dominant negative inhibitor and compete with such a process. Cells overexpressing UL25GFP (Figure 9 b, f), GFPUL25, UL25 (not shown) or GFP (Figure 9 a, e; Rode 2003, Diploma thesis) were infected with HSV1 in the presence of cycloheximide to prevent new synthesis of viral proteins. At 1 h pi, the capsids were randomly distributed throughout the entire cytoplasm (Figure 9 c, d). Irrespective of the overexpressed protein, capsids accumulated at the nucleus at 3 h pi (Figure 9 g, h). Moreover, a tight association of UL25 with microtubules would rather be obstructive than beneficial for microtubule mediated transport, because it might disturb or hinder the binding and movement of dynein and its cofactor dynactin along microtubules. Thus, an excess of UL25 during the early phase of the HSV1 life cycle did not compete with capsid transport to the nucleus (Rode 2003, Diploma thesis).

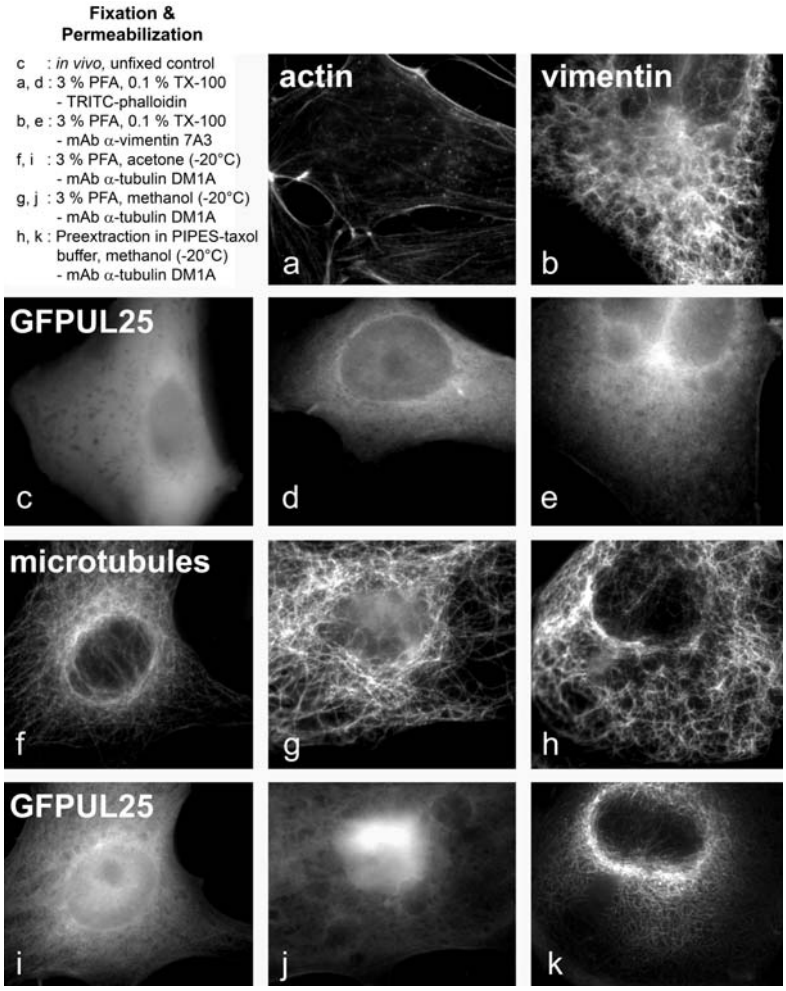

Figure 8: Cytosolic distribution of overexpressed UL25 *in vivo* and after different fixation and permeabilization methods. PtK2 cells were transiently transfected with GFPUL25. *In vivo* overexpressed GFPUL25 is present in the cytosol and to a lesser extent in the nucleus (c). Using the indicated fixation techniques (box), the localization of GFPUL25 is still cytosolic and nuclear like in living cells (d, e, i, j, k) and therefore not colocalizing with microtubules (f, g). Only after preextraction in a taxol containing PIPES buffer, followed by fixation with methanol GFPUL25 randomly overlapped with microtubules (h, k). No colocalization with actin (a) or vimentin (b) with GFPUL25 could be observed after PFA fixation and TX-100 permeabilization. Taken together all the observations obtained with several fixation and permeabilization techniques, GFPUL25 was localized in the cytosol and the nucleus (Rode 2002, Internship report; Rode 2003, Diploma thesis).

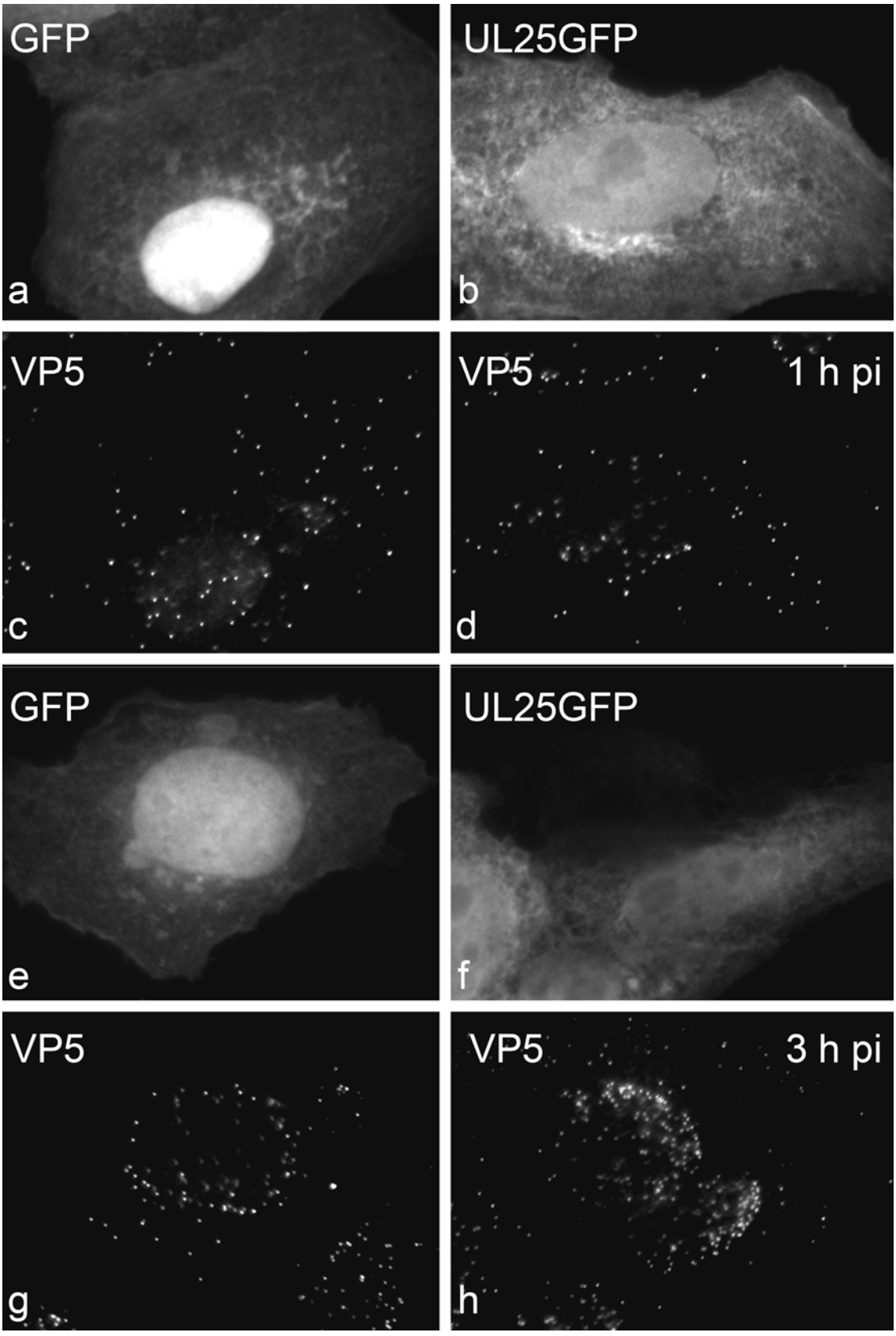

Figure 9: UL25 overexpression did not affect nuclear targeting. Capsids (c, d) were distributed over the entire cytosol at 1 h pi in untransfected, and GFP (a) or UL25GFP (b) expressing cells. Almost all capsids (g, h) accumulated at the nucleus at 3 h pi, while only few capsids remained in the cytosol, irrespective of the overexpressed protein (e, f). Similar results were obtained with GFPUL25 or UL25 (data not shown). Immunofluorescence microscopy of GFP (a, e) or UL25GFP (b, f) overexpressing Vero cells, infected with 70 PFU/cell in the presence of cycloheximide. The cells were PFA-fixed at 1 or 3 h pi and TX-100-permeabilized and labeled with a mouse anti-capsid antibody (mAb 5C10, c, d, g, h; Rode 2003, Diploma thesis).

1.5 Aim of the Study

Analysis of temperature-sensitive HSV1-UL25 mutants, ts1204 and ts1208, suggest a role for UL25 during entry, since those viruses failed to penetrate the plasma membrane and less capsids were produced upon subsequent virus propagation (Addison et al. 1984). Moreover, the UL25 protein of pseudorabiesvirus was suggested to be a microtubule motor receptor and to be involved in transport of capsids to the nucleus, since overexpressed PrV-UL25 seemed to associate with microtubules (Kaelin et al. 2000).

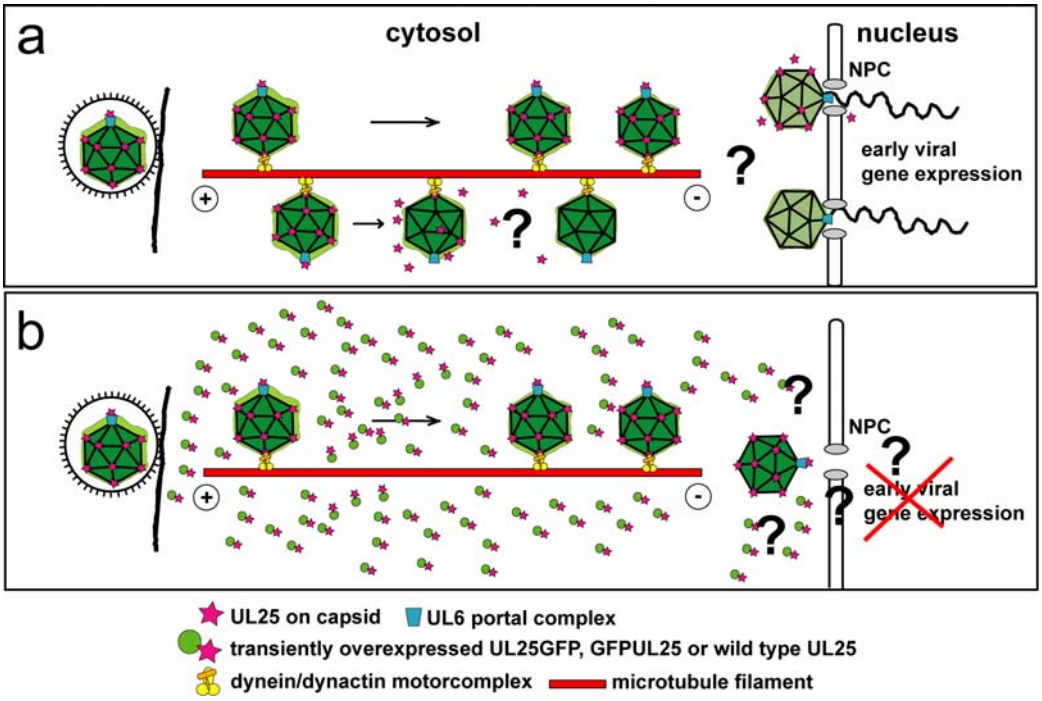

Figure 10: Analyzing the function of UL25 during entry: (a) What is happening to the capsid-associated UL25 on incoming viral capsids? Is it associated with the capsid until arrival at the nucleus or is it released during travelling to the nucleus? (b) In UL25 overexpressing cells, capsid transport to the NPC is not affected. Surprisingly, immediate early gene expression is reduced. What happened to the capsid and the viral genome? Why is no immediate early protein synthesized? What is the mechanism behind?

In my diploma work, I showed that overexpressed GFP-tagged HSV1-UL25 was localized mainly in the cytosol and to a lesser extent in the nucleus but never associated with the cytoskeleton (Figure 8, Rode 2003, Diploma thesis). Moreover, excess UL25 did not affect the nuclear targeting of incoming capsids during virus entry (Figure 9, Rode 2003, Diploma thesis). However, initial experiments suggested that overexpressed UL25 may inhibit immediate early gene expression, and that UL25 may target a step after capsid arrival at the nucleus but prior to immediate early gene expression (Figure 10 b; Rode 2003, Diploma thesis), and a phase of the HSV1 life cycle which is hardly characterized in molecular terms.

In this thesis, I determined for the first time the subcellular localization of UL25 during capsid assembly and nuclear egress to address when UL25 is attached to nuclear capsids (Figure 7). Moreover, I analyzed the fate of capsid-associated UL25 to test whether it remains associated with incoming viral capsids until arrival at the nucleus or whether it is released during capsid transport (Figure 10 a). The major tasks were to analyze the potential reduction of immediate early gene expression quantitatively, and to elucidate at which step the excess of UL25 may interfere with immediate early HSV1 gene expression (Figure 39).

2 Material and Methods

2.1 Chemicals

All chemicals were of molecular biology grade purity and purchased from the following companies unless otherwise indicated: Amersham (Amersham, Little Chalfont, UK), AppliChem (Darmstadt, Germany), Baker (Deventer, Netherlands), Fluka (Buchs, Switzerland), GE Healthcare (Freiburg, Germany), Gibco (Karlsruhe, Germany), ICN (Aurora, Ohio, USA), Invitrogen (Karlsruhe, Germany), Dianova (Hamburg, Germany), Merck (Darmstadt, Germany), Molecular Probes (Karlsruhe, Germany), New England Biolabs (Ipswich, MA, USA), Promega (Mannheim, Germany), Riedel de Haën (Seelze, Germany), Roche (Mannheim, Germany), Roth (Karlsruhe, Germany), Santa Cruz (Santa Cruz, CA, USA), Seromed-Biochrom (Berlin, Germany), Serva (Heidelberg, Germany), Sigma-Adrich (Steinheim, Germany).

Consumables were obtained from Amersham, BD Biosciences (Heidelberg, Germany), Beckman (Fullerton, CA, USA), Biozym (Hessisch Oldendorf, Germany), Corning-Costar (Schiphol, Netherlands), Eppendorf (Hamburg, Germany), Gilson (Middleton, WI, USA), Greiner (Frickenhausen, Germany), Pall (Pensacola, FL, USA), Pharmacia (New York, USA), Qiagen (Hilden, Germany), Sarstedt (Nümbrecht, Germany), Schleicher & Schuell (Dassel, Germany), or Whatman (Dassel, Germany).

2.2 Antibodies

Primary antibodies were either purchased or kindly provided by the indicated collegues and collaborators.

mAb 5C10 – α-VP5: Mouse monoclonal antibody against HSV1-VP5 hexons, obtained from B. Newcomb and J. Brown (University of Virginia, Charlottesville, VA, USA; Trus et al. 1992)

pAb NC-1 – α-VP5: Rabbit polyclonal antibody against HSV1-VP5, obtained from G. Cohen and R. Eisenberg (University of Pennsylvania, Philadelphia, USA; Cohen et al. 1980)

mAb H1.4 – α-VP5: Mouse monoclonal antibody against HSV1-VP5 (Biodesign & OEM Concepts of Meridian Life Science, Inc.; Saco, Maine, USA)

mAb LP12 – α-VP5: Mouse monoclonal antibody against immature VP5, obtained from A.C. Minson (University of Cambridge, UK; Döhner et al. 2006; Phelan et al. 1997)

pAb EC/R8-3 – α-UL25: Rabbit polclonal antibody against GST-UL25 (aa 341-580), obtained from E. Cantin (Department of Neurology, City of Hope National Medical Center, Duarte, California, USA; Ali et al. 1996)

pAb ID1 – α-UL25: Rabbit polclonal antibody against GST-UL25, obtained from D. J. Tenney (Bristol-Myers Squibb Pharmaceutical Research Institute, Wallingford, Connecticut, USA; Koslowski et al. 1997)

mAb IC9 – α-UL6: Mouse monoclonal antibody against UL6 coupled to a maltose binding protein tag, obtained from B. Newcomb and J. Brown (University of Virginia, Charlottesville, VA, USA; Taus et al. 1998)

mAb 11060 – α-ICP0: Mouse monoclonal antibody against ICP0, obtained from R. Everett (MRC Virology Unit, Glasgow, UK; Everett et al. 1991)

pAb SW7 – α-VP16: Rabbit polyclonal antibody against the thyroglobulin-conjugated carboxyl terminal amino acids 475 to 488 of VP16, obtained from D. J. Tenney (Bristol-Myers Squibb Pharmaceutical Research Institute; Weinheimer et al. 1992)

pAb α-p35/H5R – Rabbit polyclonal antibody against the vaccinia virus protein p35 obtained from J. Krijnse-Locker (University of Heidelberg, Germany; Tolonen et al. 2001)

pAb α-p16/A14L – Rabbit polyclonal antibody against the vaccinia virus protein p16, obtained from J. Krijnse-Locker, (University of Heidelberg, Germany; Salmons et al. 1997)

mAb 1501 – α-actin: Mouse monoclonal antibody raised against purified chicken gizzard actin (Lessard 1988).

mAb DM1A – α-tubulin: Mouse monoclonal antibody raised against human brain α–tubulin (amino acis 426-450; Upstate – Millipore, Billerica, Maryland, USA)

mAb 7A3 – α-vimentin: Mouse monoclonal antibody against vimentin (Kouklis et al. 1993)

mAb 414 – α-NPC: Mouse monoclonal antibody (ab24609) that reacts with NPC proteins which contain FG repeats; Nup358/RanBP, Nup214/CAN, Nup62, Pom121 and Nup153, Abcam, Cambridge, UK)

mAb 3E9 – α-importin β: Mouse monoclonal antibody that detects importin β/nuclear transport factor 97, raised against purified importin β from bovine erythrocytes (Abcam, Cambridge, UK)

mAb JL8 – α-GFP: Affinity purified mouse monoclonal antibody against full length GFP, affinity purified (Living color® Antibody, Clontech, Mountain View, California, USA)

pAb α-β-galactosidase: Rabbit polyclonal antibody against β-galactosidase (5-Prime – 3-Prime Inc., Boulder, CA, USA)

mAb α-NFκB: Mouse monoclonal antibody against NFκB (sc-372; Santa Cruz Biotechnology, Inc., CA, USA)

mAb α-IκB: Mouse monoclonal antibody against IκB (sc-847; Santa Cruz Biotechnology, Inc., CA, USA)

mAb α-STAT1: Mouse monoclonal antibody against STAT1 (sc-464; Santa Cruz Biotechnology, Inc., CA, USA)

mAb α-NFAT: Mouse monoclonal antibody against NFAT (sc-7294; Santa Cruz Biotechnology, Inc., CA, USA)

Secondary antibodies were isolated from antisera by immunoaffinity chromatography using antigens coupled to agarose beads and purchased from Jackson Immuno Research via Dianova, Hamburg, Germany.

Fluorescein Isothiocyanate (FITC)-conjugated AffiniPure Goat anti-Mouse IgG: Minimal cross-reaction to human, bovine, horse, rabbit and swine serum proteins

FITC-conjugated AffiniPure Goat anti-Rabbit IgG: Minimal cross-reaction to human, bovine and horse serum proteins

Lissamine Rhodamine Sulfonyl Chloride (LRSC)-conjugated AffiniPure Goat Anti-Mouse IgG: Minimal cross-reaction to human, bovine, horse, rabbit and swine serum proteins

LRSC-conjugated AffiniPure Goat Anti-Rabbit IgG: Minimal cross-reaction to human, mouse and rat serum proteins

Peroxidase-conjugated AffiniPure Goat anti-Mouse IgG/**Goat anti-Rabbit IgG** and

Alkaline phosphatase-conjugated AffiniPure Goat anti-Mouse IgG/Goat anti-Rabbit IgG: Antibody specificity is based on immunoelectrophoresis. The antibody reacts with the heavy chains on host IgG and with light chains to most host immunoglobulins. No antibody was detected against non-immunoglobulin serum proteins, but antibodies may cross react with immunoglobulins from other species.

2.3 Molecular Biological Techniques

All molecular biology techniques were performed according to Sambrook et al. 1989.

2.3.1 Bacterial Strains and Propagation

***E. coli* DH5α:** used for maintenance and cloning of plasmids (Grant et al. 1990)

Genotype: F- *deo*R *rec*A1 *end*A1 *hsd*R17 (r_{k}^{-}, m_{k}^{+}) *sup*E44 λ- *thi*-1 *gyr*A96 *rel*A1

***E. coli* DH10B:** used for maintenance and cloning of plasmids (Grant et al. 1990)

Genotype: F^{-} *mcr*A Δ(*mrr-hsd*RMS-*mcr*BC) Φ80*lac*ZΔM15 Δ*lac*X74 *rec*A1 *end*A1 *ara*Δ139 Δ(*ara*, *leu*) 7697 *gal*U *gal*K λ- *rps*L (Str^{R}) *nup*G

LB medium: 1% [w/v] peptone (Roth); 0.5% yeast extract (Roth); 0.5% NaCl; 1 mM NaOH; sterile

Overnight cultures from freshly picked colonies were usually grown in LB medium with the appropriate antibiotic at 37°C and shaken at 220 rpm in a Kendro incubator (Rodenbach, Germany). The amount of growth medium was chosen according to the recommendations of the manufacturer´s protocol. For cryoconservation, a 400 µl aliquot of bacteria from a 2 ml over night culture was mixed 1:1 with glycerol, snap frozen in liquid nitrogen, and stored at -80°C.

2.3.2 DNA Purification and Labeling Kits

Plasmid DNA and DNA probes were amplified and purified using the following kits according to the manufacturer´s instructions.

QiaPrep Plasmid miniprep kit	Qiagen, Heidelberg, Germany
GeneElute HP Plasmid midiprep kit	Sigma-Aldrich, Munich, Germany
Amersham Cy3-dCTP nucleotides	GE Healthcare, Freiburg, Germany

2.3.3 Expression Plasmids

The plasmid maps were constructed using the SIM Vector program (version 2, PREMIER Biosoft International, Palo Alto, CA, USA).

pEGFP-C1 encodes for the enhanced green fluorescent protein (GFP) and includes a C-terminal multiple cloning site. It includes a kanamycin resistance cassette for propagation in bacteria and a neomycin resistance cassette for eukaryotic selection (GenBank Accession #: U55763, Clontech, Saint-Germain-en-Laye, France).

pGFPUL25 encodes a N-terminal enhanced green fluorescent protein (GFP) fusion protein with the complete UL25 ORF (Müller 2000, Internship report). The plasmid with a size of 6.4 kb was constructed using pEGFP-C1 (Invitrogen) and a UL25-insert amplified from the HSV1(17^{+})-genom with *BamHI* and *EcoRI* restriction sites. It contains a neomycin resistance cassette for selection of stable cell clones in eukaryotic cell culture. The kanamycin resistence is important for the amplification in *E.coli*.

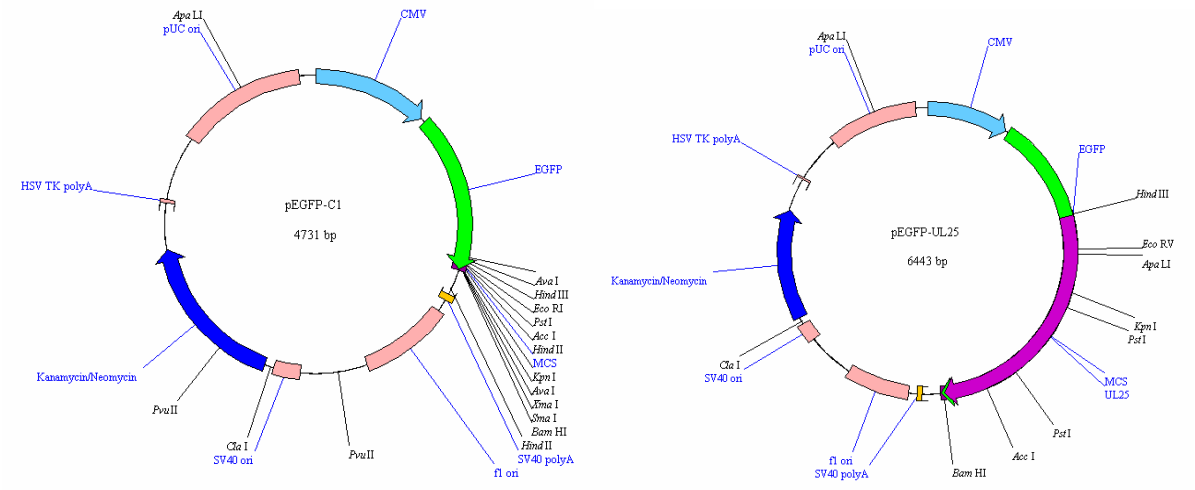

pUL25GFP encodes a C-terminal GFP fusion protein with the complete UL25 ORF (Rode 2002, Internship report). The plasmid has a size of 6.4 kb and was constructed using pEGFP-N1 and a UL25 insert amplified from cosmid 28 (Cunningham and Davison 1993) via *BamHI* and *XhoI* restriction sites. This plasmid also encodes for a neomycin- and kanamycin resistance cassette.

pcDNA3-UL25 was constructed from pcDNA3 (Invitrogen) and a UL25 insert amplified from cosmid 28 (Cunningham and Davison 1993) containing a Kozak consensus sequence (ACCATGG). This sequence facilitates the initital binding of mRNA to the small subunit of the ribosome and therefore improves expression levels (Kozak 1986). The insert was cloned into the vector using *BamHI* and *EcoRI*. The plasmid with a size of 7.1 kb and encodes for a neomycin- and an ampicillin resistance cassette (Rode 2003, Diploma thesis).

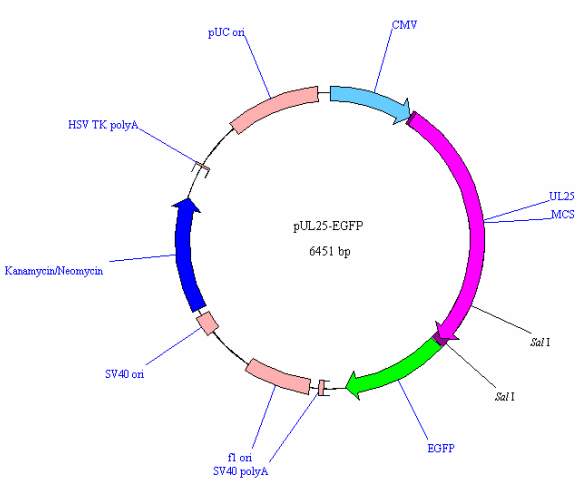

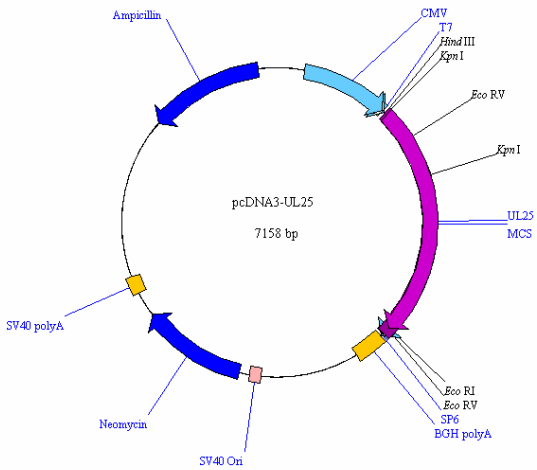

pGL2basic is a luciferase reporter plasmid (Promega, Madison, Wisconsin, USA). It lacks eukaryotic promoter and enhancer sequences. The expression of luciferase is dependent on the insertion and orientation of a functional promoter sequence upstream of the luciferase coding region.

pGL2b-cyclin E promoter contains the human cylin E promoter upstream of the luciferase gene in pGL2basic (Geng et al. 1996, kindly provided by M. Ottinger and T.F. Schulz, Institut of Virology, Hannover Medical School)

pGL2b-EBV cp2.0 contains 2 kb of the Epstein Barr Virus (EBV, HHV4) C promoter upstream of the transcriptional start site which contains the Epstein Barr Nuclear Antigen 2 (EBNA-2) responsive element. It lacks the EBV origin of replication and was cloned into pGL2basic (Ottinger 2005; kindly provided by M. Ottinger and T.F. Schulz, Institut of Virology, Hannover Medical School).

pGFP-Hunk encodes a N-terminal GFP fusion protein of Hunk (Ottinger 2005; kindly provided by M. Ottinger and T.F. Schulz, Institut of Virology, Hannover Medical School).

pTal and pSRE are plasmids which belongs to the Mercury Pathway Profiling Vector System (Clontech, Saint-Germain-en-Laye, France). These vectors contain specific responsive elements upstream of the TATA-like (TAL) minimal promoter element of HSV1 thymidine kinase with the exception of the negative control vector pTal. The specific serum responsive element (SRE) together with the Tal promoter regulates transcription of the reporter gene luciferase.

2.4 Eucaryotic Cell Culture

BHK-21 cells (American Type Culture Collection (ATCC) certified cell line (CCL)-10): Adherent kidney fibroblasts from syrian golden hamster (*Mesocricetus auratus)*

PtK_2 cells (NBL-5; ATCC no. CCL-56): Adherent kidney epithelial cells from potoroo *(Potorous tridactylis)*

Vero cells (ATCC no. CCL-81): Adherent kidney epithelial cells from african green monkey *(Cercopithecus aethiops*)

HeLa (ATCC CCL-2): Adherent cervical cancer epithelial cell from human (*Homo sapiens*)

HEK 293-T (ATCC CRL-11268): Human ephithelial kidney cells that were immortalized through transformation with adenovirus 5 and SV40 large T-antigen (*Homo sapiens*)

MEM (Cytogen)	Eagle's buffered salt solution, nonessential amino acids, glutamine, 2.2 g/l $NaHCO_3$
D-MEM (Gibco)	4.5 g/l glucose, GlutaMAX™, pyruvate (used for vaccinia virus infections)
RPMI1640/BSA (Cytogen)	supplemented with 0.1% BSA
Foetal calf serum (FCS; Gibco)	heat-inactivated for 30 min at 56°C
Trypsin/EDTA solution (Biochrom)	0.25%/0.02% in PBS, pH 7.4 (150 mM NaCl, 8 mM KH_2PO_4, 2 mM Na_2HPO_4) without Ca^{2+} and Mg^{2+}
Cycloheximide	100x, 50 mM stock solution in H_2O

For maintenance of cell lines the following media were used:

BHK-21, PtK_2, HeLa and HEK 293-T cells:	MEM supplemented with 10% FCS
Vero cells:	MEM supplemented with 7.5% FCS

Cells were grown in an incubator (Hera Cell, Kendro, Rodenbach, Germany) with a humid atmosphere and 5% CO_2 at 37°C. For maintenance cells were subcultured twice a week.

For long-term storage in liquid nitrogen, cells of a 10 cm dish were trypsinized and resuspended in 2 ml culture medium supplemented with double the amount of FCS relative to the growth medium and 10% DMSO, transferred into a cryo tube and frozen at -80°C for a few days prior to storage in liquid nitrogen.

To recover the cells, they were quickly thawed, resuspended and washed in pre-warmed culture medium. Cells were centrifuged at low speed in a cell culture centrifuge (1000 rpm, 10 min, RT, cell culture centrifuge 5810R, Eppendorf, Hamburg, Germany) and the pellet was resuspended in growth medium and plated in a tissue culture flask.

2.5 Virological Techniques

2.5.1 Viruses

HSV1 strain F: wildtype virus (ATCC VR-733)

HSV1 strain 17$^+$: fully sequenced wildtype virus (GenBank accession number X14112; McGeoch et al. 1988; McGeoch et al. 1986; kindly provided by J.H. Subak-Sharpe; MRC Virology Unit, Glagow, UK)

Vaccinia virus Strain Western Reserve: wildtype virus (ATCC VR-119, Parker et al. 1941; kindly provided by Jacomine Krijnse-Locker; University of Heidelberg, Germany)

Adenovirus-LacZ: this adenovirus encodes for β-galactosidase under an early adenoviral promoter (Schiedner et al. 2000; kindly provided by Florian Kreppel; University of Ulm, Germany)

2.5.2 Propagation of HSV1 and Quality Control of Virus Preparations

HSV1 was prepared as previously described (Döhner 2006; Döhner et al. 2002; Sodeik et al. 1997). All experiments were performed with virus stocks of passage number 3. BHK-21 cells were plated in 175 cm^2 flasks, grown to 90 to 95% confluency, washed with PBS, and then infected with a MOI of 0.01 PFU/cell. For infection, cells were incubated with 5 ml virus suspension in RPMI1640 containing 0.1% BSA (RPMI/BSA) for one hour on a rocking platform at room temperature to allow the virus to bind to the cells. Then 25 ml of culture medium were added, and the cells were further incubated at 37°C and 5% CO_2. The virus was harvested when nearly all cells had rounded up and could be detached from the flask by knocking them off. The time point of harvesting depended on the virus strain, and for wild-type strains it was between 48 to 60 hours post infection.

The medium containing the secreted extracellular virions and cells was spun at 4,000 rpm at 4°C for 10 min in a JA-10 rotor in an Avanti J-25 centrifuge (Beckman Coulter, Fullerton, CA, USA). The pooled supernatants containing the virions were transferred to Beckman Type 19 rotor bottles and centrifuged at 12.000 rpm at 4°C for 90 min in a Beckman L8-70 ultracentrifuge (Beckman Coulter, Fullerton, CA, USA). The virus pellets were resuspended in 1 ml MNT buffer (20 mM MES; 100 mM NaCl; 30 mM Tris; pH 7.4) and allowed to dwell at 4°C for 24 to 36 h. For further purification, the virus suspension was sonicated for 3 times 30 s in an ultrasonic bath, further resuspended by pipetting up and down with a molten glass pasteur pipette, and centrifuged for 5 min at 4.000 rpm in a 15 ml tube in an Eppendorf 5810R centrifuge. A 10 to 40% Nycodenz (Axis Shield PoC, Oslo, Norway) gradient in MNT was made using a Gradient Master™ Model 106 (Biocomp, Fredericton, Canada).

The supernatant was then loaded on top and spun at 20.000 rpm for 1 h 45 min in a SW28 ultracentrifuge rotor (Beckman Coulter, Fullerton, CA, USA). The virus band in the middle of the gradient was visible due to light scattering, harvested, aliquoted, snap-frozen in liquid nitrogen and stored at -80°C.

The quality of the gradient purified virus was analyzed by immunoflurescence where the nuclear targeting efficiency of the virus was elucidated. Moreover, virus titer was determined by plaque assays on Vero cells (Döhner et al. 2002).

With real time detection PCR the amount of viral genomes per particle was determined. A low PFU/particle ratio (~ 20-40) indicates a good quality virus preparation with good nuclear targeting efficiency (Döhner et al. 2006). Some of the virus preparations were examined according to all these quality control criteria. Not all virus preps could be analyzed by real time detection PCR method because they were already empty at the time of establishment.

Table 3: Quality of some gradient purified virus preparations used in this study:

HSV1(F)	Virus titer by plaque assay	Nuclear targeting efficiency	Genome/PFU (-DNAse)
12.09.04	$2.3 \cdot 10^8$ pfu/ml	+	32.4
14.10.05	$7.2 \cdot 10^8$ pfu/ml	+	29.9
13.01.06	$1.2 \cdot 10^8$ pfu/ml	+	20.0

2.5.3 Transient Transfections

Cells were seeded into or 48-well plates without cover slips or on 12 mm glass cover slips in 24-well plates at a density of about 1 to 2 x 10^4 cells per well or 3 to 4 x 10^4 cells per well, respectively or in 10 cm dishes with a cell density of 1 x 10^6. After 24 h, expression plasmids were transfected into cells with the calcium phosphate method (Döhner et al. 2002; Sambrook et al. 1989) or with the cationic liposomal-based GeneJuice (Novagen, Merck KGaA, Darmstadt, Germany) or Fugene transfection reagent (Roche, Mannheim, Germany) according to the manufacturer's instructions for 18 to 30 h depending on the following experiments.

2.5.4 Synchronised HSV1 Infection

For all entry experiments Vero, PtK_2 or HeLa cells were synchronously infected with HSV1, vaccina virus or adenovirus. The cells were plated one day before the experiment either in 24-well plates or 10 cm dishes, or two days before the experiment when cells were transfected prior to virus infection. The cells of one well or one dish were counted, and the virus suspension (200 µl/well for a 24-well plate or 500 µl for a 10 cm dish) containing the appropriate amount of PFU in RPMI medium supplemented with 0.1% [w/v] BSA was prepared. The cells were cooled on ice in RPMI medium/BSA for 20 min; the virus was added and allowed to bind at 4°C on a rocking platform for 1 to 2 h. For vaccinia virus infections, D-MEM without serum or BSA was used. After binding, unbound virus was removed by washing 3 times with RPMI medium/BSA and to start the infection growth medium at 37°C was added. For nuclear targeting experiments, the medium contained 0.5 mM cycloheximide which inhibits protein synthesis (Obrig et al. 1971). It is used here to prevent the synthesis of progeny viral proteins (Döhner et al. 2002, Sodeik et al. 1997). For gene expression experiments, growth medium without cycloheximide was used. Cells were incubated at 37°C, 5% CO_2 until fixation or harvesting. MOIs of 0.5 to 10 PFU/cell were used for HSV1 assembly, of 20 to 500 for HSV1 cell entry, of 2-10 to monitor HSV1 early gene expression (Döhner et al. 2002; Mabit et al. 2002; Sodeik et al. 1997), of 100 to monitor adenovirus gene expression (Schiedner et al. 2000) and of 60 to analyze vaccinia virus gene expression (Jensen et al. 1996; Schepis et al. 2006).

2.6 Protein Analysis

2.6.1 Preparation of Cell Lysates

Cells in a 10 cm dish were placed on ice, scraped into 300 µl (entry experiments) or 700 µl (assembly experiments) hot Laemmli sample buffer (5% glycerol, 58 mM SDS, 58 mM Tris-HCl, 30 µM bromophenol blue; 0.02% β-mercaptoethanol pH 6.8; Laemmli 1970) containing protease inhibitors at the indicated final concentrations (AEL – 0.05 mg/ml Apronitin, 0.01 mg/ml E-64, 0.05 mg/ml Leupeptin in H_2O; ABP – 0.01 mg/ml Antipain, 0.05 mg/ml Bestatin, 0.05 mg/ml Pepstatin in methanol; 0.16 mg/ml PMSF in isopropanol). Samples were transferred to a 1.5 ml tube on ice. To shear the DNA, samples were triturated 50x using a 25 µl Hamilton syringe (Bonaduz, Switzerland). The lysates were denatured at 95°C for 5 min and centrifuged for 10 min at 16.000 rpm at RT before loading onto an SDS gel or stored frozen at -20°C until use.

2.6.2 SDS-Polyacrylamide Gel Electrophoresis (SDS-PAGE) and Immunoblot

The buffer system described by Laemmli (Laemmli 1970) was used for discontinuous electrophoresis in the presence of SDS. The gels had a length of 8 cm, width of 10 cm, and a thickness of 0.75 mm (Hoefer™ SE250 mini vertical unit, Amersham, Little Chalfont, UK), or a length and width of 16 cm, and a thickness of 1.5 mm (Hoefer™ SE600 standard dual cooled electrophoresis unit, Amersham, Little Chalfont, UK). Molecular weight standards with 250, 150, 100, 75, 50, 37, 25, 15 and 10 kD bands (Precision Plus Protein Standard Unstained or Kaleidoscope, Bio-Rad) were used.

Proteins separated on SDS gels were transferred onto BioTrace®NT nitrocellulose membrane (Pall, Pensacola, Florida, USA) in transfer buffer (48 mM Tris, 380 mM glycine, 0.1% w/v SDS, 10% methanol) in a tank blot transfer unit (Amersham, Little Chalfont, UK) for 16 hours at 40 mM for small SDS gels and at 100 mA for large SDS gels (Burnette 1981).

The nitrocellulose membrane was stained with 0.2% Ponceau S in 3% trichloroacetic acid, destained in water or 1% [v/v] acetic acid, and the molecular weight markers were indicated. Unspecific binding sites on the membrane were blocked in PBST (PBS, 0.1% Tween-20) containing 5% milk (milk powder, Sucofin, Trade Service International, Zeven, Germany) for 1 h at RT. The membrane was incubated with an appropriate dilution of the primary antibody in PBST-milk for 2 h at RT on a rocking platform, washed 3 times with PBST and incubated with the appropriate secondary peroxidase- or alkaline phosphatase-coupled antibody in PBST-milk for 1 h at RT on a rocking platform. After washing 3 times with PBST, antibody labeled bands with peroxidase were detected using ten fold diluted SuperSignal® West Femto Maximum Sensitivity Substrate (Pierce, Perbio Science, Bonn, Germany) in a LAS-3000 documentation system (FujiFilm, Dusseldorf, Germany). Membranes labeled with alkaline phosphatase-coupled antibodies were equilibrated twice for 10 min in TSM (100 mM Tris, 100 mM NaCl, 5 mM $MgCl_2$, pH 9.5), and then the bands were visualised in a colour reaction in the dark with 0.165 µg/ml 5-bromo-4-chloro-indolyl-3-phosphatase and 0.305 µg/ml nitroblue tetrazolium salt in TSM. The reaction was stopped by washing with water.

2.6.3 Luciferase Reporter Assays

To assay promoter activity, Vero cells were seeded in 48 well plates and cotransfected 24 h later with the respective 210 ng UL25, GFP or Hunk expression plasmids and 40 ng luciferase expression plasmids (cf. chapter 2.3.3), either with the empty vector control or plasmids that contain promoter elements. 30 h post transfection, cells were washed with cold PBS and incubated for 10 min on ice with 75 µl/well Reporter Lysis Buffer (Promega, Mannheim, Germany; 25 mM Tris-phosphate, pH 7.8, 2 mM DTT, 2 mM 1,2-diaminocyclohexane-N,N,N´,N´-tetraacetic acid, 10% glycerol, 1% Triton X-100) and transferred into a 1.5 ml tube. Lysates were cleared by centrifugation for 1 min at 14.000 rpm and supernatants were transferred into a fresh tube. 20 µl of cleared lysate was added to 100 µl Promega Luciferase Assay Buffer (supplemented with Promega Luciferase Assay substrate that contains Mg^{2+}, ATP and D-Luciferin), vortexed and immediately measured in duplicates in a luminometer (LB9501, Berthold Lumat, Barsinghausen, Germany) for 10 seconds. Activities were calculated as fold induction compared to mock (empty vector) transfected cells. GFP together with the reporter plasmid was set as 1 (100%). The error bars represent the standard error of the mean.

2.6.4 Fluorescence Activated Cell Sorting (FACS)

GFP, UL25GFP or GFPUL25 overepressing Vero cells in a 10 cm dish were infected with HSV1(F) at an MOI of 500 PFU/cell for 2 h. Infected cells were washed with PBS, trypsinized and resuspended in 3 ml growth medium. 3 ml of 8% PFA and 0.1% glutaraldehyde in 400 mM cacodylate, pH 7.4 were added to the cell suspension, mixed and incubated for 20 min at RT. Cells were pelleted at 1.500 rpm for 10 min at RT and resuspended in 500 µl PBS containing 7.5% BSA.

FACS sorting was performed at the FACS Facility of Hannover Medical School by Dr. Matthias Ballmeier and Christina Reimer on a MoFlow FACS sorter (DAKO Cytomation, Glostrup, Denmark). GFP-positive single cells were sorted, collected and pelleted at 10.000 rpm for 5 min. The cell pellets were subsequently fixed with 1% glutaraldehyde in 200 mM cacodylate pH 7.4 for 1 h. The pellets were washed 3 times with 200 mM cacodylate pH 7.4. After every washing step, the cell pellets were centrifuged to maintain the pellets at the bottom of the tubes. Until embedding in epon for electron microscopy, the pellets were stored at 4°C.

2.7 In Situ Hybridization of Viral Genomes

2.7.1 Preparation of Viral DNA

Viral DNA was prepared from HSV1(F)-infected BHK-21 cells according to MacLean 1998. The cell suspension was mixed in a ratio of 1:1 with 1% (v/v) Triton X-100 in resuspension buffer (RSB; 10 mM Tris-HCl, 10 mM KCl, 1.5 mM $MgCl_2$, pH 7.5), vortexed and incubated on ice for 10 min to lyse the cells. Nuclei were pelleted from the lysate in a cell culture centrifuge (5810R, Eppendorf, Hamburg, Germany) for 10 min at 4.000 rpm and 4°C. The nuclei pellets were resuspended in 6 ml of 0.5% Triton X-100 in RSB and centrifuged. The supernatants were pooled, and the capsids were pelleted from the cytoplasmic lysate in a Beckman SW40Ti rotor (Beckman Coulter,

Fullerton, CA, USA) using a Beckman L8-70 ultracentrifuge at 30.000 rpm for 90 min at 4°C. The pellets were resuspended in 800 µl of NTE buffer (100 mM NaCl, 10 mM Tris-HCl, 1 mM EDTA, pH 7.4) and incubated overnight at 4°C. To solubilize capsids and release the viral DNA, 200 µl of a 5x SDS/EDTA solution (12.5% [w/v] SDS, 50 mM EDTA in NTE buffer) were added, carefully mixed by inversion and incubated at 37°C for 10 min.

The lysate was extracted twice with 1 ml phenol/chloroform/isoamyl alcohol by inverting 50 times and centrifuging for 5 min at 14.000 rpm. The DNA was precipitated from the aqueous phase by adding 800 µl isopropanol and centrifuging 15 min at 14.000 rpm. The DNA pellet was washed with 1 ml 70% [v/v] ethanol, dried and resuspended in 100 µl 10mM Tris-HCl, pH 8, 50 µg/ml RNase A at 4°C overnight. Viral DNA preparations were stored at 4°C to prevent shearing by ice crystal formation.

2.7.2 Synthesis of Cy3-labeled DNA Probes for *In Situ* Hybridization

In situ hybridization probes were generated using partially digested viral DNA and Cy3-labeled dCTP (GE Healthcare, Madison, Wisconsin, USA; Everett and Murray 2005). Viral DNA from HSV1(F) was incubated with DNase 1 (RQ1, 2 µu/µl; Promega, Madison, Wisconsin, USA) at 37°C for 30 min and analyzed on an agarose gel to check the amount of digestion. DNase 1 was heat inactivated and the digested viral DNA was subsequently used for nick translation.

For nick translation the digested DNA was diluted in nick translation buffer (0.05 M Tris-HCl, pH 7.2; 0.01 M $MgSO_4$; 1 mM Dithiothreitol) and incubated over night at 16°C with 200 mM dATP, dGTP and dTTP (Promega), as well as 5 nM Cy3-dCTP and 50 U of NEB-Taq Polymerase. The Cy3-labeled probe was purified by ammonium acetate-ethanol precipitation, and the pellet was resupended in TE buffer (10 mM Tris-HCl, 0.5 mM EDTA, pH 8.0), and stored in aliquots at -20°C (Everett and Murray 2005).

2.7.3 Agarose Gel Electrophoresis

Partially digested viral DNA was separated on 1% agarose gels in TAE (40 mM Tris; 40 mM acetic acid; 1 mM EDTA) using the Mini S/L gel system (Peqlab, Erlangen, Germany; Perfect Blue Mini S/L) at a constant voltage of 180 V. The Gene Ruler DNA Ladder Mix or the NEB ladders were used as molecular weight marker. Agarose gels contained 0.5 µg/ml ethidium bromide to visualize any DNA by ultraviolet light. For better visualization of the DNA bands, gels were eventually stained by soaking in 0.5 µg/ml ethidium bromide for 30 min and destained in H_2O for 30 min.

1kb DNA Ladder (New England Biolabs, Ipswich, MA, USA):
10.000, 8.000, 6.000, 5.000, 4.000, **3.000**, 2.000, 1.500, 1.000, 500 (sizes in bp)

100 bp DNA Ladder (New England Biolabs, Ipswich, MA, USA):
1.517, 1.200, **1.000**, 900, 800, 700, 600, **517, 500**, 400, 300, 200, 100 (sizes in bp)

6x DNA loading buffer: 30% [w/v] glycerol, 0.3% [w/v] bromophenol blue, 0.3% [w/v] xylencyanol

2.7.4 *In Situ* Hybridization of Infected Cells for Genome Detection

Ethanol-acetic acid fixed cells (c.f. 2.8.1) were prehybridized for 30 min at 37°C in hybridization buffer (50% [v/v] formamide, 10% [v/v] dextran sulfate, 4x SSC (0.6 M NaCl, 0.06 M Sodium citrate)) to quench unspecific crosshybridization in a humidified hybridization chamber. Formamide lowers the DNA melting temperature by breaking the hydrogen bonds of the two strands. Dextrane sulfate precipitates lipoproteins and inhibits RNases. Therefore the addition of dextrane sulfate enhances hybridization efficiency. Next, the coverslips were blotted dry and incubated at 42°C for 20 min. The probe (c = 0.1 µg/µl) was diluted 1:10 in hybridization buffer and a 5 to 7 µl spot was added to the coverslip. Then a 20x20 mm glas coverslip was placed on the cells and everything was fixed on a coverslide using Marabu´s fixogum rubber cement (Tamm, Germany). The coverslide was heated at 95°C for 4 min in a Thermocycler Cyclone 96 (PeqLab, Erlangen, Germany), followed by over night incubation at 37°C in a humidified chamber. The next day, the coverslips were washed 2 times with 2X SSC (0.3 M NaCl, 0.03 M Sodium citrate) at 60°C and once with 2xSSC at RT. Cells were further washed with PBS/1% FCS or PBS/0.5% BSA and either embedded for microscopy or labeled with antibodies (Everett and Murray 2005).

2.8 Microscopy

2.8.1 Fixation, Permeabilization and Antibody Labeling

Untransfected or transfected HeLa, PtK_2 or Vero cells were grown on cover slips (Ø 12 mm) prior to infection with HSV1 at different MOIs according to the experimental setup. At the end of the infection time, cells were washed once with PBS and then fixed using different protocols.

PFA fixation: Cells were fixed in 3% [w/v] PFA in PBS for 20 min at RT. After washing 3 x 5 min in PBS, any remaining PFA was inactivated by addition of 50 mM NH_4Cl in PBS for 10 min. Again, cells were washed 3 x 5 min in PBS. Cells were permeabilized in 0.1% [v/v] TX-100 in PBS for 4 min and washed 3 x in PBS (Sodeik et al. 1997).

PHEMO fixation: Cells were washed once in PBS at 37°C, fixed for exactly 10 min in PHEMO-Fix (68 mM Pipes; 25 mM Hepes, pH 6.9; 15 mM EGTA; 3 mM $MgCl_2$; 10% DMSO; 3.7% PFA; 0.05% glutaraldehyde; 0.5% TX-100), washed twice for exactly 5 min in PHEMO buffer (68 mM Pipes; 25 mM Hepes, pH 6.9; 15 mM EGTA; 3 mM $MgCl_2$; 10% DMSO) at 37°C, and washed twice in PBS. Incubating in 50 mM NH_4Cl in PBS for 10 min, and washing 3 times in PBS inactivated any remaining PFA. PHEMO fixation fixes and permeabilizes cells in one step (Döhner et al. 2002).

***In Situ* fixation**: Cells were washed with PBS containing 1% FCS or 0.5% BSA and fixed for 5 min in 95% [v/v] ethanol/5% [v/v] acetic acid at -20°C. Cells were then washed 3 times with PBS/FCS or PBS/0.5% BSA (Everett and Murray 2005).

EM fixation: Trypsinized, infected cells were resuspended in the same volume of 8% PFA, 0.1% glutaraldehyde in 400 mM cacodylate, pH 7.4 and incubated for 20 min at RT. After pelleting and resuspending the cells in PBS/7.5% BSA, FACS sorting was performed.

Sorted cells were then again fixed with 1% glutaraldehyde in 200 mM cacodylate pH 7.4 for 1 h. Later the pellets were washed 3 times with 200 mM cacodylate pH 7.4. After every washing step, the cell pellet was centrifuged again for maintaining the pellet at the bottom of the tube. Until epon embedding for transmission electron microscopy, the pellets were stored at 4°C until further processing for transmission electron microscopy.

Fixed samples were subsequently labeled with antibodies as previously described (Döhner et al. 2006; Döhner et al. 2002; Sodeik et al. 1997) and embedded in ProLong Gold Antifade mounting medium (Molecular Probes-Invitrogen, Karlsruhe, Germany) or in Mowiol (6 g glycerol; 2,4 g Mowiol; 6 ml H_2O; 12 ml 0,2 M Tris; pH 8,5), supplemented with 25 – 50 mg/ml 1,4-Diazabicyclo [2,2,2]octane as an antifade reagent.

2.8.2 Epifluorescence and Confocal Microscopy

Cover slips were observed and images were taken using an Till-Photonics-Axiovert 200M or an Axiovert Observer microscope (Zeiss, Göttingen, Germany) equipped with a plan-apochromat 63x/1.40 Oil or 100x DIC objectives (Zeiss), a 150 W xenon lamp (Polychrome IV, TillPhotonics, Gräfeling, Germany) or a mercury lamp (Zeiss Observer) as a light source and appropriate filter sets (Table 4). Images were taken with a Till Imago QE CCD camera (TillPhotonics) using the TillVision software (version 4.0, TillPhotonics) or with the Zeiss AxioCam HRm (Zeiss Observer) camera using the Axiovision software (version 4.6.3.0 SP1, Zeiss). Confocal sections were recorded with a Zeiss LSM 510 Meta confocal microscope using a plan-apochromat 63x/1.40 Oil objective (Zeiss), an argon laser (Argon 2 – 458 nm, 477 nm, 488 nm and 514 nm spectral lines) and helium-neon lasers with either 543 nm (HeNe1) or 633 nm (HeNe2) spectral lines. Images were taken with the Carl Zeiss Laser Scanning Microscope LSM 520 software (Zeiss, version 3.2 SP2).

All images were further processed with MetaMorph (version 5, Meta Imaging Software, Molecular Devices, Downingtown, PA, USA), ImageJh (version 1.36b, Wayne Rasband, NIH, USA, http://rsb.info.nih.gov/ij/), Zeiss LSM Image Browser (Zeiss, version 3,5,0,3,7,6) or Adobe Photoshop (version 6, Adobe Systems, San Jose, CA, USA).

Table 4: Filter sets

Microscope	Filter set	Excitation filter	Dichroic mirror	Emission filter
Till Photonics	DAPI/Hoechst	SP 410	LP 410	LP 420
	GFP	SP510	LP 490	BP 535/550
	Rhodamine	Sp540	LP 565	LP 610(675
Observer	GFP – FS 38 HE	BP 470/40 (HE)	FT 495 (HE)	BP 525/50 (HE)
	Rhodamine – FS 43 HE	BP 550/25 (HE)	FT 570 (HE)	BP 605/70 (HE)
	Cy5 – FS 50	BP 640/30	FT 660	BP 690/50
LSM Meta	GFP – FS09	BP 450 - 490	FT 510	LP 515
	Rhodamine – FS15	BP 546/12	FT 580	LP 590

2.8.3 Transmission Electron Microscopy

Glutaraldehyde fixed, FACS sorted GFP-, UL25GFP- or GFPUL25 overexpressing, HSV1-infected cells were washed 3 times for 10 min with membrane pure water to wash out the cacodylate. For contrasting the specimen, pellets were incubated with a water based solution containing 1% osmium and 1.5% $K_3(Fe^{3+}(CN)_6$ for 1 h at RT. Later cells were washed 4 times 10 min with membrane pure water at RT and once with 50% ethanol at RT to remove residual osmium. The pellets were further contrasted with 0.5% uranylacetate in 50% ethanol at RT over night, followed by dehydration with a graded ethanol series at room temperature (2 x 10 min 50% ethanol, 2 x 20 min 75% ethanol, 2 x 10 min 90% ethanol, 2 x 10 min 100% ethanol (absolute, over molecular sieve), 1 x 15 min 100% ethanol (absolute), 1 x 60 min 100 % ethanol (absolute). Cells were then transferred into a fresh reaction tube and incubated for 20 min at RT with propylenoxide (absolute, over molecular sieve).

The dehydrated, osmium contrasted specimens were infiltrated with a 1:1 mixture of epon resin and propylenoxide over night at RT. The epon/propylenoxide mixture was replaced by fresh epon after 3h for again 3h and again after 1h. Polymerization occurs at 60°C for about 115 h.

Ultrathin sections were cutted with a Leica Ultramicrotom. The sections have a thickness of 50 to 80 nm. Sections were stained with uranylacetate and lead citrate according to Reynolds 1963 (1.33 g $Pb(NO_3)_2$, 1.76 g $(C_6H_5Na_30_7)x2H_20$, 8 ml 1N NaOH, 42 ml membrane pure H_20, light and air protected) placed on a formvar coated copper grid and examined with a Zeiss EM 10 CR electron microscope at an acceleration voltage of 80 kV. Pictures were scanned and further processed using Adobe Photoshop (version 6, Adobe Systems, San Jose, CA, USA).

3 Results

3.1 The Subcellular Localization of UL25 During the HSV1 Life Cycle

3.1.1 UL25 Associated with Capsids During Capsid Assembly and Egress

The UL25 protein is required for efficient retention of the viral genome inside the capsid, possibly by sealing the UL6 portal complex after packaging (Ali et al. 1996; McNab et al. 1998; Ogasawara et al. 2001). Alternatively, UL25 may stabilize the capsid at the pentons (Trus et al. 2007), since it has been localized on capsids with 5 copies per capsid penton (Newcomb et al. 2006). Recent studies revealed that UL25 might reinforce the capsid structure and give a signal for nuclear egress (Klupp et al. 2006; Trus et al. 2007). Moreover, UL25 remains associated with viral capsids after salt extraction with 1M KCl suggesting a tight association of UL25 with the capsid (Wolfstein et al. 2006).

In the first set of experiments, I determined the expression kinetics of UL25, UL6 and VP5 during capsid assembly and egress. Vero cells were synchronously infected with HSV1 at an MOI of 10 PFU/cell and harvested for SDS-PAGE and immunoblot analysis at various times post infection (Figure 11). UL25 as well as the portal protein UL6 were first detected at 6 to 7 h pi. The appearance of the proteins fits to their characteristics, since they belong to the family of late (γ)-proteins with a weak transcription promoter (Rajcani et al. 2004). For efficient synthesis they need high genome copy numbers. VP5 belongs to the leaky-late ($\beta\gamma$)-protein family (Huang and Wagner 1994; Rajcani et al. 2004) and can be detected already 4 to 5 h pi, although some of the VP5 detected at 4 h pi may also represent the inoculum. The actin loading control showed that similar amounts of cells (~ 0.5 x 10^5 per lane) were loaded.

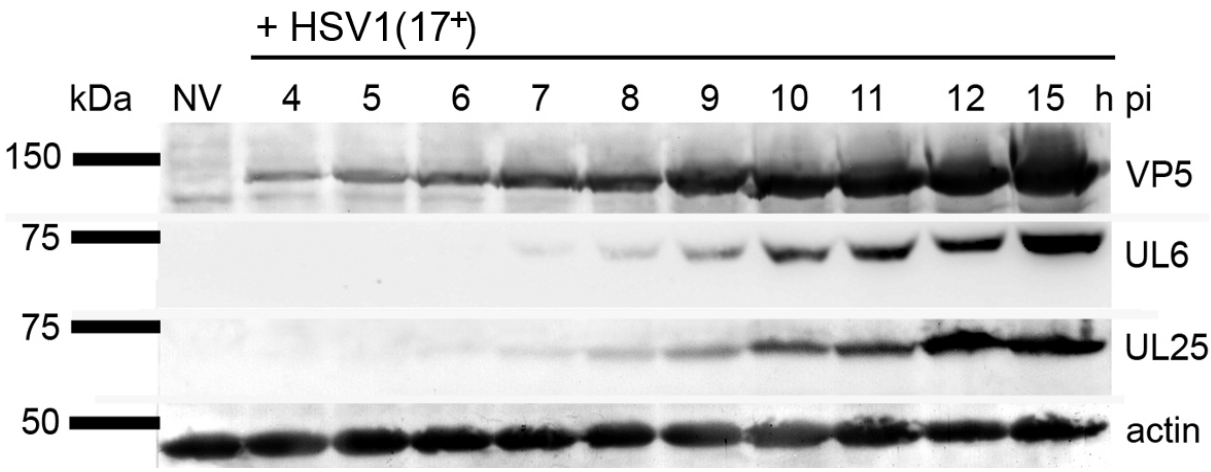

Figure 11: Expression kinetics of capsid proteins during assembly. UL25 and UL6 were first detected at 6 to 7 h pi, whereas VP5 was already detected at 4 h pi. Vero cells were synchrounosly infected with HSV1(17+) with an MOI of 10 PFU/cell for 4 to 15 hours. Cells were harvested in hot Laemmli-buffer, separated on a 7-15% SDS polyacrylamide gel and transferred onto nictrocellulose. The blot was subsequently probed with pAb UL25-EC, mAb UL6-IC9, pAb VP5-NC1, and mAb1501 against actin as a loading control.

Next, Vero cells were infected with an MOI of 10 PFU/cell, fixed, and analyzed by immunoflurescence microscopy, either wide field (Figure 12, Figure 13) or confocal laser scanning microscopy (Figure 14, Figure 15). The cells were labeled with the mouse monoclonal antibody mAb 5C10 directed against VP5-hexons (Döhner et al. 2006; Newcomb et al. 1996; Trus et al. 1992), with the mouse monoclonal antibody LP12 that recognizes an immature VP5 epitope (Döhner et al. 2006; Phelan et al. 1997) or another mouse monoclonal antibody H1.4 against VP5 in combination with the the rabbit polyclonal antibody UL25-EC (Ali et al. 1996) or the rabbit polyclonal antibody UL25-ID1 (Koslowski et al. 1997) both generated against recombinant GST-UL25.

Newly synthesized capsids detected by mAb 5C10 were distributed as dot-like structures in nuclear, viral replication compartments at early time points (Figure 12 d, g, j). The mAb LP12 gave a more diffuse labeling of the nucleus (Figure 12 e, h, k). The mAb H1.4 seemed to recognize both populations of VP5 (Figure 12 f, i, l); dotted indicative for capsids and diffuse nuclear labelling, although the overall labelling intensity was weaker than with the other α-VP5 antibodies. All mAbs detected an increasing amont of VP5 over time (Figure 12), but only mAb 5C10 detected capsids in the cytoplasm at later time points (Figure 14 c, arrows). This data is consistent with the suggestion that mAb 5C10 detects mature epitopes on capsids (Trus et al. 1992,Döhner et al. 2006). UL25 was detected using pAb UL25-ID1 (Figure 13, left panel; corresponding VP5-5C10 labeling of VP5 can be found in Figure 12 left panel) or pAb UL25-EC (Figure 13, right panel).

Both antibodies labeled UL25 during early time points of assembly rather dotted than diffuse. These data indicate that UL25 antibodies rather bind capsids that were detected by mAb 5C10 and not with mAb LP12 or mAb H1.4 (Figure 13 c, d, e, f, g, h). To obtain an even more detailed picture, the same experiment was analyzed by confocal laser scanning microscopy. At 9 h pi, capsids in the nucleus and in the cytoplasm were labeled by mAb 5C10 and colocalized with UL25 (UL25-EC, Figure 14 a, b, c-inset; UL25-ID1, Figure 15 a, b, c-inset). mAb LP12 or mAb H1.4 detected only nuclear but no cytoplasmic capsids, both of which contained UL25 (cf Figure 14 and Figure 15 d, e, f-inset; g, h, i-inset).

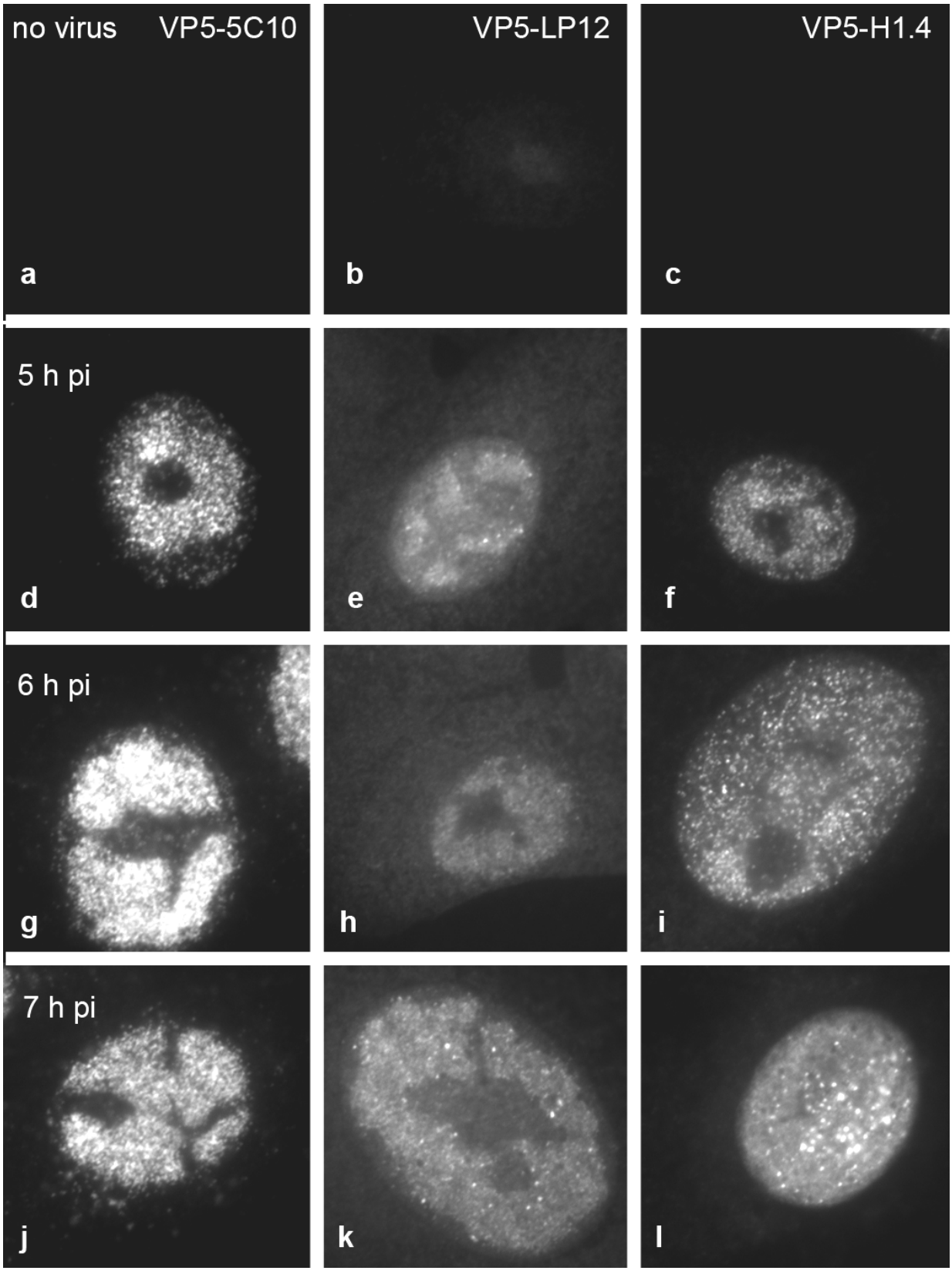

Figure 12: Different VP5 antibodies labeled different populations of nuclear capsids. Newly synthesized capsids were revealed as dot like structures in viral replication compartments in the nucleus at early time points using mAb VP5-5C10, that recognizes mature VP5 epitopes on hexons (d, g, j). The VP5 antibody LP12 gives a prominent diffuse and slightly dotted pattern (e, h, k). The VP5 antibody H1.4 labeled VP5 which was clustered in dots but also difuse VP5 in the nucleus (f, i, l). Vero cells were synchronously infected with HSV1 (F) with an MOI of 10 PFU/cell. At several times pi, the cells were fixed with 3% PFA and permeabilized with 0.1% TX-100. VP5 was visualized with the indicated antibodies.

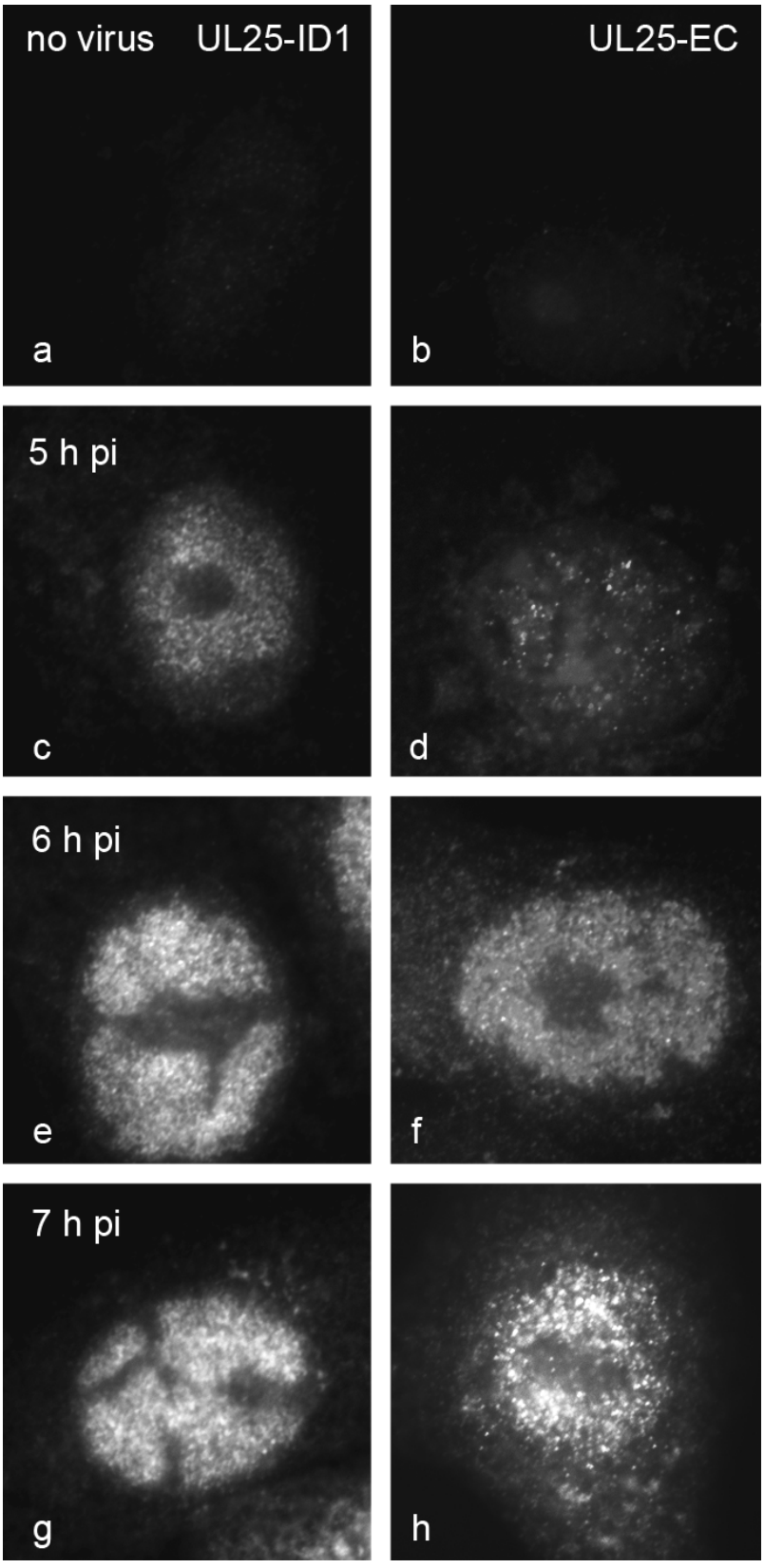

Figure 13: Newly synthesized UL25 accumulated in replication compartments and gave a similar labeling pattern than capsids labeled with VP5-5C10. Newly synthesized UL25 was detected with the polyclonal antibody UL25-ID1 more diffuse in the nucleus at early time points (c) but getting more dotted at later time points (e, g). Same UL25 distributions were observed with the polyclonal antibody UL25-EC (d, f, h). The localization of UL25 was similar to the capsid antibody VP5-5C10 (cf. corresponding VP5 staining in Figure 12 a, d, g, j to a, c, e, g). Vero cells were synchronously infected with HSV1(F) with an MOI of 10 PFU/cell. At several hours pi, cells were fixed with 3% PFA, permeabilzed with 0.1% TX-100 and labeled with the indicated antibodies.

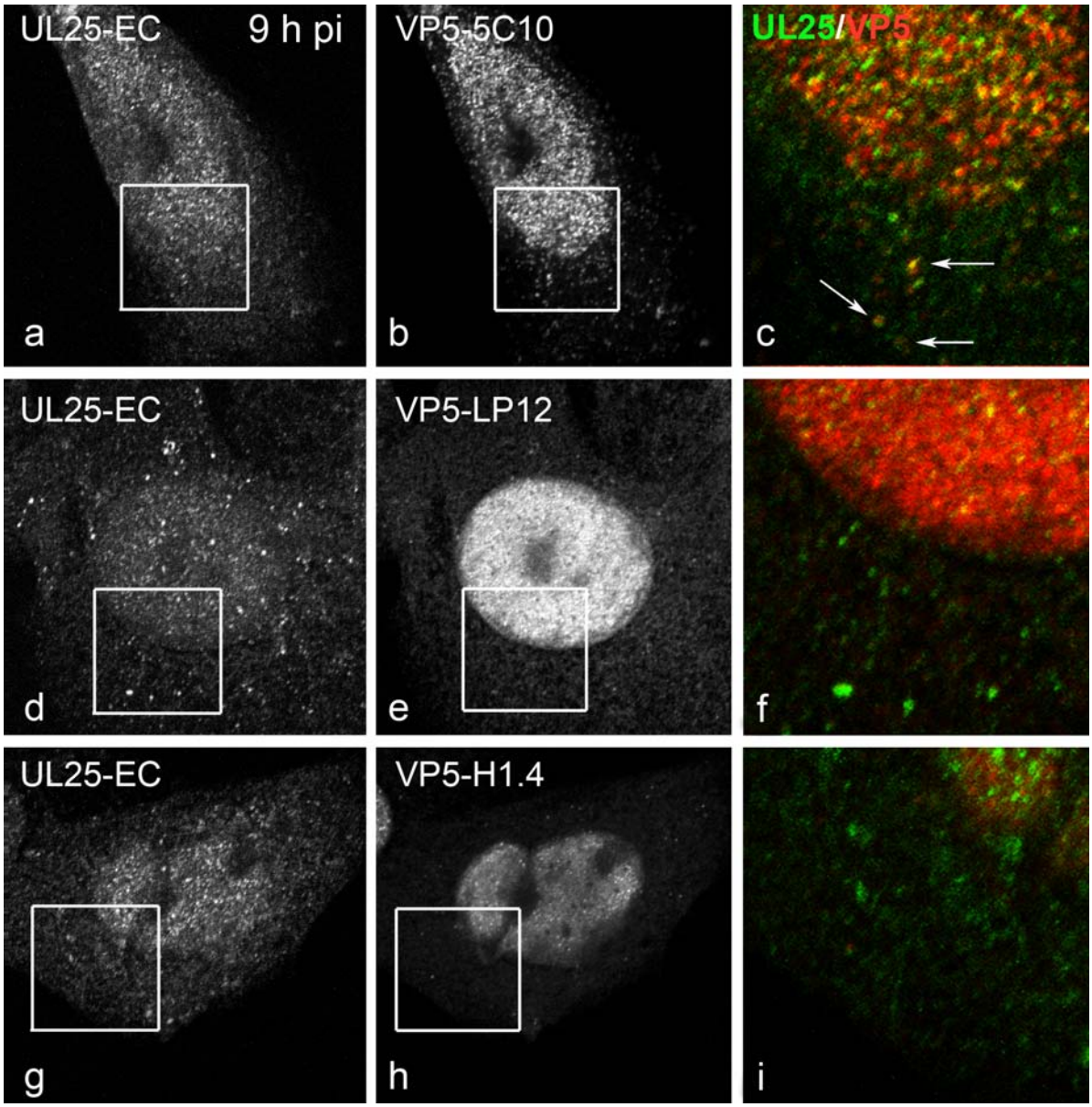

Figure 14: UL25 was associated with maturing particles during capsid egress. UL25 (pAb UL25-EC) colocalized with some of the capsids labeled with VP5-5C10 during assembly in the nucleus and in the cytoplasm (a, b, c-inset, arrows), but not with VP5-LP12 (d, e, f-inset) or VP5-H1.4 (g, h, i-inset). Vero cells were synchronously infected with HSV1(F) with an MOI of 10. At 9 h pi, cells were fixed with 3% PFA, permeabilized with 0.1% TX-100 and labeled with antibodies directed against UL25 or VP5. Confocal sections through the nucleus of 0.5 µm thickness were analyzed.

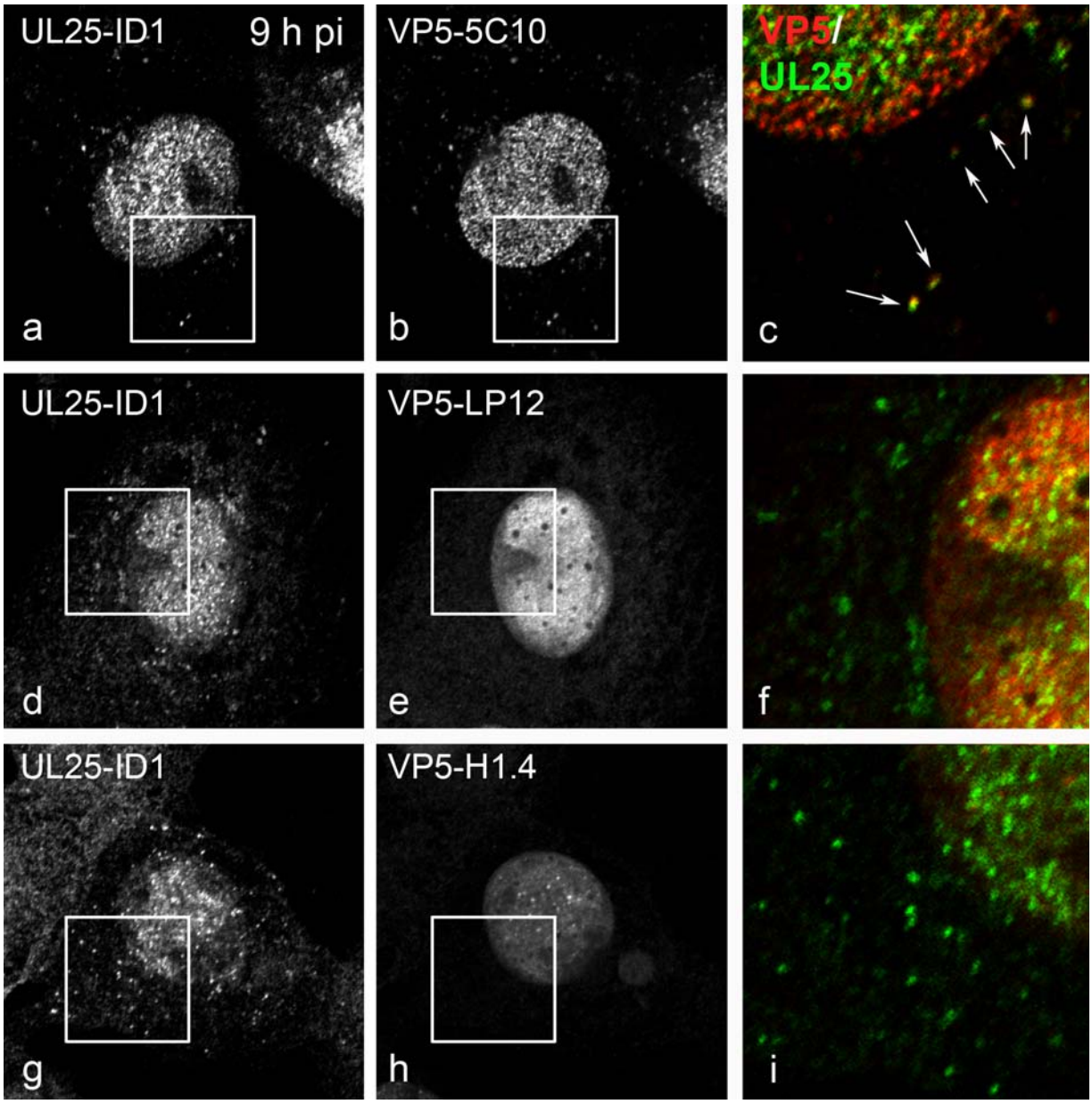

Figure 15: UL25 was associated with maturing particles during capsid egress. UL25 (pAb UL25-ID1) colocalized with most of the capsids labeled with VP5-5C10 during assembly in the nucleus and in the cytoplasm (a, b, c-inset, arrows), but not with VP5-LP12 (d, e, f-inset) or VP5-H1.4 (g, h, i-inset). Vero cells were synchronously infected with HSV1(F) with an MOI of 10. At 9 h pi, cells were fixed with 3% PFA, permeabilized with 0.1% TX-100 and labeled with antibodies directed against UL25 or VP5. Confocal sections through the nucleus of 0.5 µm thickness were analyzed.

3.1.2 HSV1-UL25 Remained Capsid-Associated until Arrival at the Nuclear Pore

During cell entry many tegument proteins dissociate from the incoming capsids, while others remain associated until the capsids dock at the nuclear pores (Morrison et al. 1998; Ojala et al. 2000; Sodeik et al. 1997). The temperature-sensitive HSV1 mutant virus 1204 attached to the plasma membrane but failed to penetrate it (Addison et al. 1984). Moreover PrV-UL25 was suggested to be a microtubule motor receptor (Kaelin et al. 2000), therefore the subcellular localization of incoming HSV1-UL25 during cell entry was determined.

To detect incoming HSV1 proteins by immuno blot, cells were infected with HSV1(17^+) at an MOI of 200 PFU/cell (Figure 16 g). Virus infected cells were harvested in hot sample buffer containing protease inhibitors to prevent proteolytic cleavage. The input lane represented the inoculum, whereas the lanes from 0 to 3 h pi represented the bound and internalized virus. UL25 and VP5 protein levels remained constant over time and were not degraded. The actin loading control showed that similar numbers of cells (~ 2 x 10^5 per lane) were loaded. Thus, UL25 was recruited onto capsids during capsid assembly in the nucleus, and remained capsid-associated during virus egress, and also during the transport of incoming capsids from the cell periphery to the nuclear pores.

Moreover, Vero cells were infected with HSV1 at an MOI of 70 PFU/cell in the presence of cycloheximide to prevent synthesis of progeny virus proteins, fixed and labeled with the mouse monoclonal antibody VP5-5C10 and the rabbit polyclonal antibody UL25-ID1. Capsids as well as UL25 were distributed throughout the entire cytoplasm at 1 h pi (Figure 16 a, b) and UL25 remained capsid-associated (Figure 16 c, inset). At 3 h pi, UL25 had reached the nuclear envelope together with the capsid (Figure 16 d, e, f, inset).

Since PrV-UL25 was suggested to be a microtubule motor receptor (Kaelin et al. 2000), cells overexpressing HSV1-UL25 were analyzed for capsid transport to the nucleus. If UL25 would interact with a microtubule motor, overexpressed UL25 might interfere with this hypothetical interaction. Nuclear targeting of incoming HSV1 capsids was not impaired in the presence of excess UL25 (cf. chapter 1.4, Figure 9). During the entire HSV1 life cycle, neither newly synthesized UL25, nor incoming UL25, or overexpressed UL25 colocalized ever with microtubules, actin or vimentin (Rode 2003, Diploma thesis). Moreover, neither UL25 nor VP5 were degraded during HSV1 cell entry, suggesting that intact capsids with UL25 reached the nucleus.

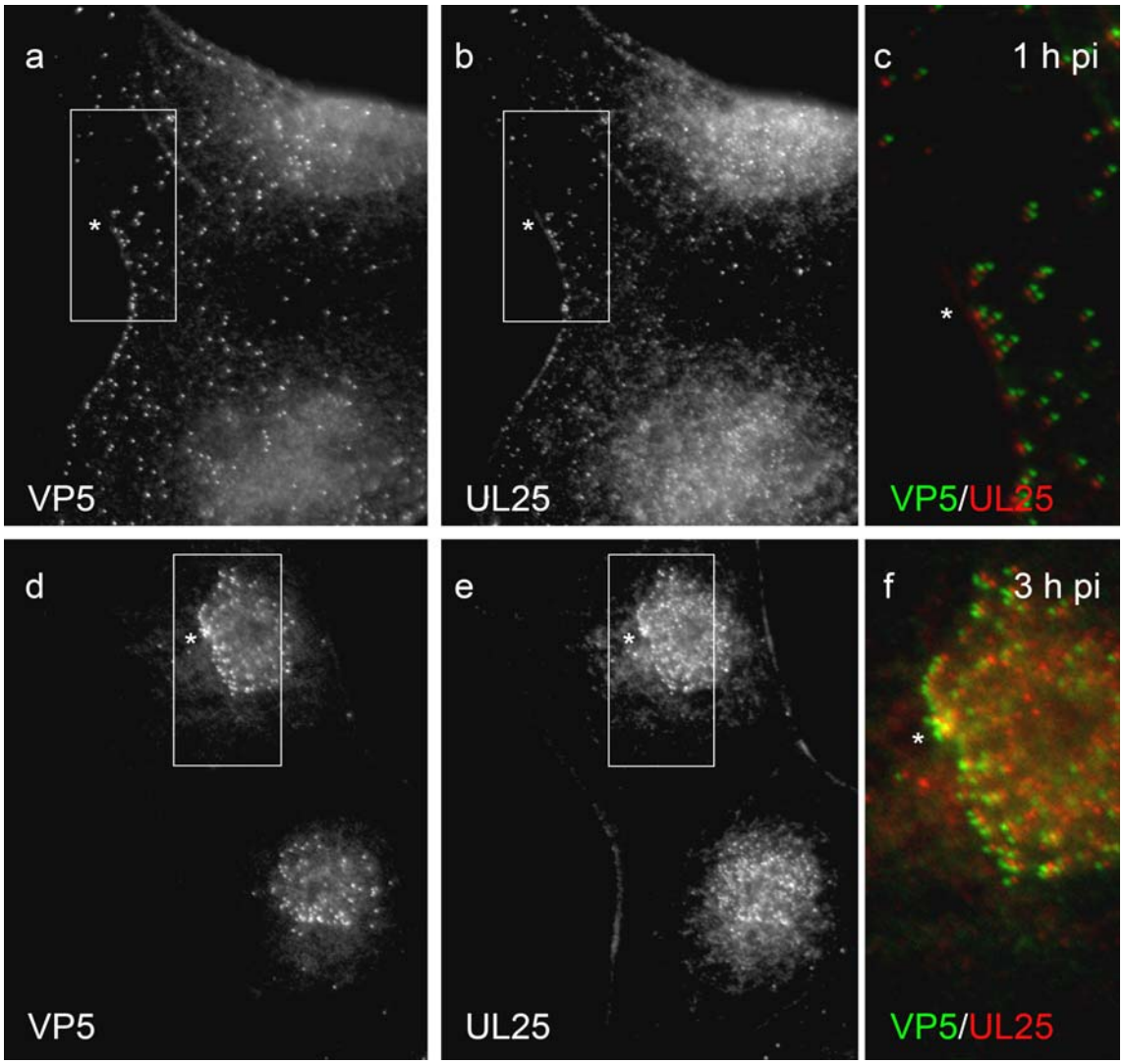

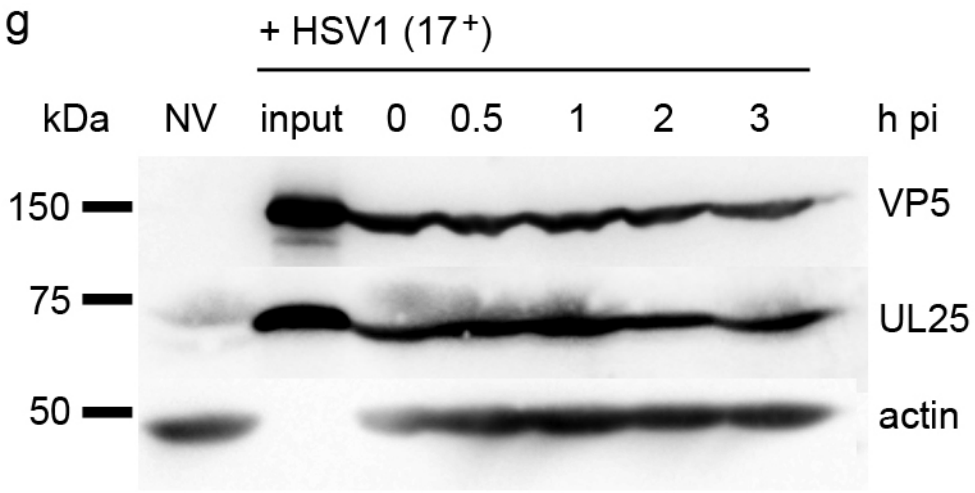

Figure 16: UL25 colocalized with incoming capsids during entry and was not degraded. At 1 h pi capsids labeled with anti-VP5 were distributed in the cell (a) and colocalized with UL25 (b, c-inset). After 3 h pi capsids (d) accumulated at the nuclear rim, where they still colocalized with UL25 (e. f-inset). UL25 remains associated with incoming capsids during entry. The western blot showed that VP5 and UL25 were not degraded during virus entry (g). The input lane represents the amount of virus that was added to the cells. After 2 hours binding on ice, unbound virus was washed away and the incoming capsids were assayed from 0 to 3h pi. Vero cells were infected with HSV1(F) with an MOI of 70 (a-f) or with HSV1(17+) with an MOI of 200 (g). Capsids were labeled with mAb 5C10 against mature VP5 hexons (a, d) for immunofluorescence or with the rabbit polyclonal antibody VP5-NC1 for western blot. The blot was probed with mAb1501 against actin as a loading control. UL25 was detected with a rabbit polyclonal antibody ID1 against UL25 (b, e, g) after the indicated time points.

3.2 Transiently Overexpressed UL25 During Virus Infection

3.2.1 Immediate Early HSV1 Gene Expression was Reduced

To test whether overexpressed UL25 had any effect on any of the subsequent steps of the HSV1 life cycle after the capsid had reached the nucleus, I analyzed the expression of immediate early proteins, which are the first proteins to be expressed after a cell is successfully infected with HSV1 (cf. chapter 1.3.6).

GFP or UL25GFP-transfected Vero cells were infected, fixed and labeled with antibodies directed against ICP0 (Figure 17), ICP4, ICP8, ICP22 or ICP27 (not shown). Untransfected as well as GFP expressing cells (Figure 17 a, b; circled cells) showed a typical punctuate distribution of ICP0 in the nucleus (Figure 17, dashed lines). However, cells expressing UL25GFP, indicated by the circled cell (Figure 17 c, d) showed a reduced synthesis of immediate early HSV1 proteins. ICP0 was reduced in UL25GFP or GFPUL25 transfected cells by 60% at 2 h pi and by 40 to 50% at 3 h pi when compared to GFP-expressing cells. The ICP0 expression in wild type UL25-overexpressing cells was reduced by 70% at 2 h pi and by 50% at 3 h pi compared to untransfected cells (Figure 18).

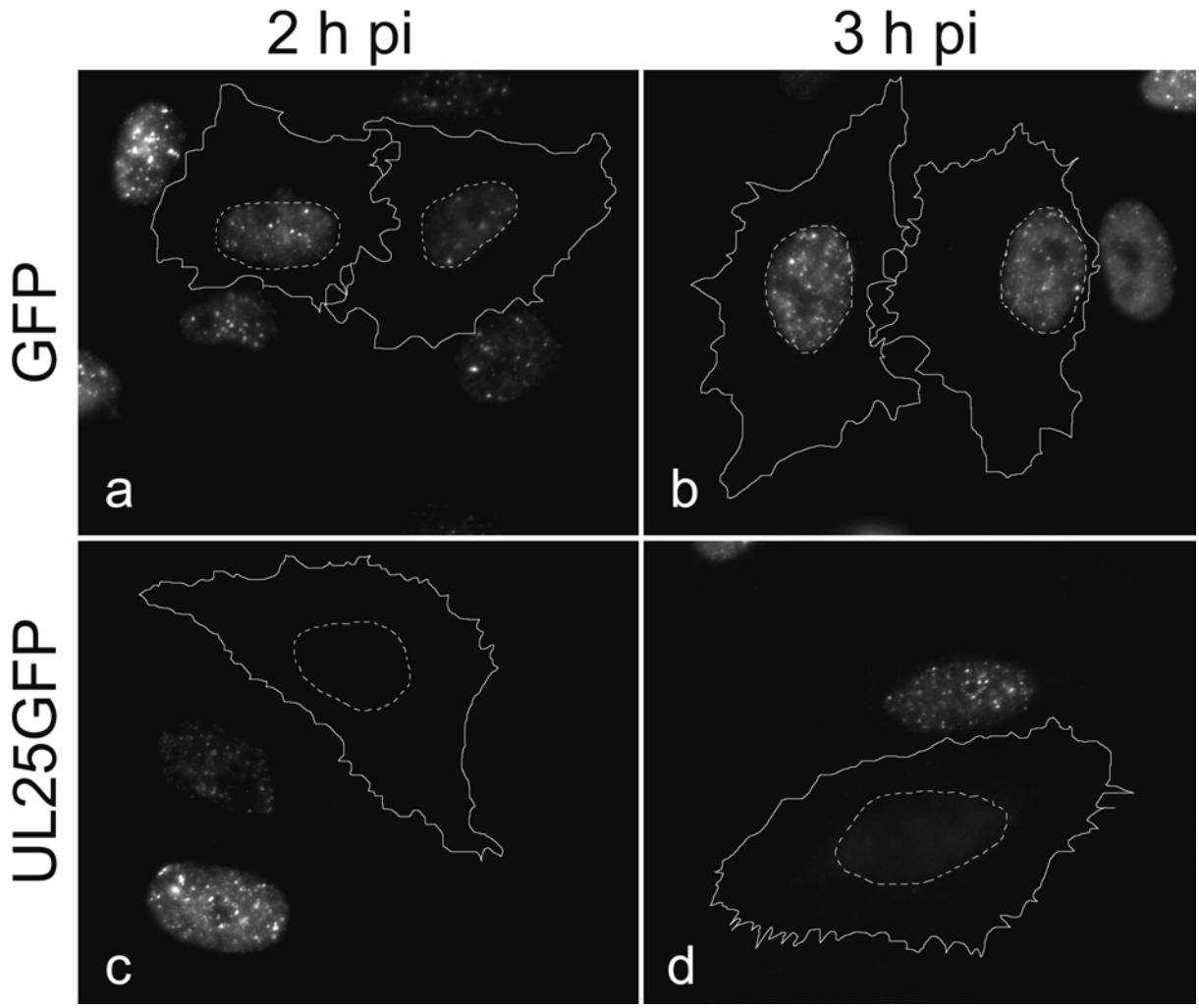

Figure 17: UL25 overexpression reduced HSV1 immediate early viral gene expression. GFP and untransfected cells expressed ICP0 in the nucleus (a, b), whereas UL25GFP expressing cells did not or to a lesser extent (c, d). Immunofluorescence microscopy of GFP (a, b) or UL25GFP (c, d) overexpressing Vero cells infected with 2 PFU/cell. The cells were fixed at 2 (a, c) or 3 h pi (b, d) with 3% PFA, permeabilized with 0.1% TX-100 and labeled with the mAb11060 against ICP0 (a-d). The circled cells represent the cells overexpressing either GFP or UL25GFP; the dashed line indicates the position of the nuclei of the transfected cell.

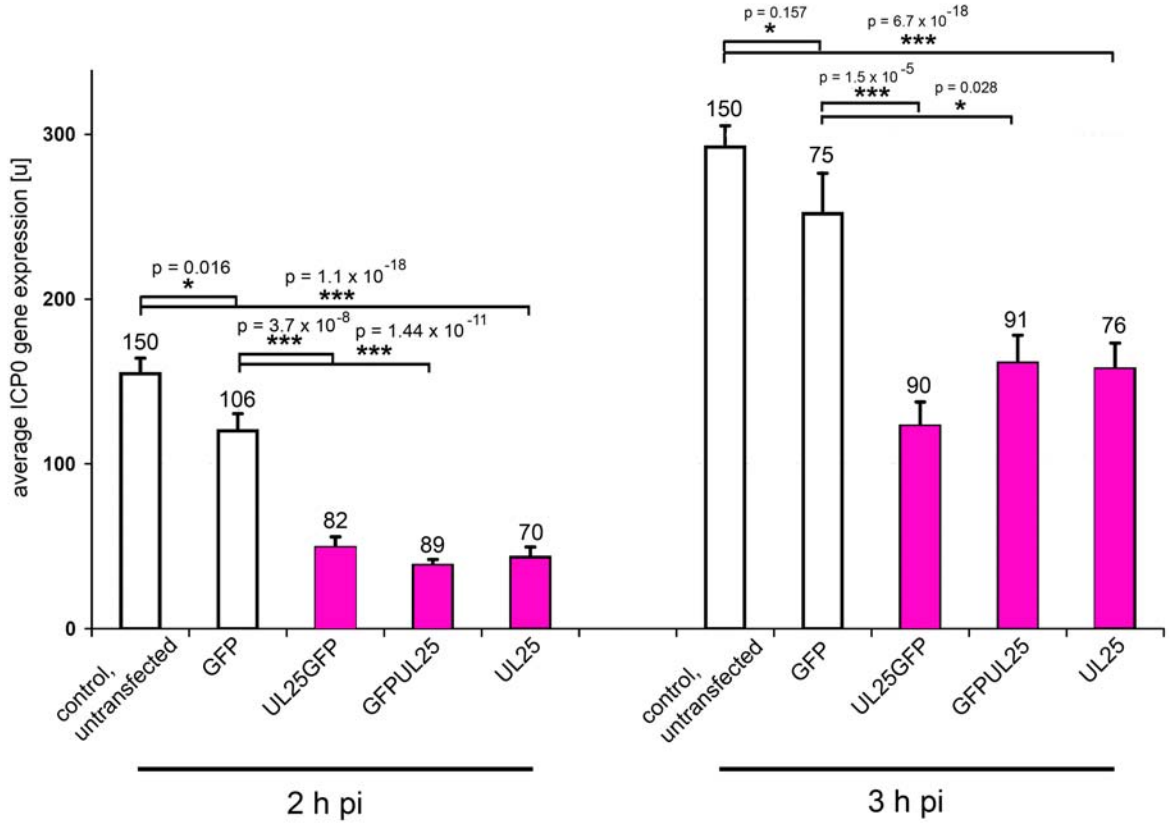

Figure 18: Quantification of reduced immediate early HSV1 gene expression. The quantification showed that ICP0 was significantly reduced by 60% at 2 h and by 40 to 50% at 3 h pi in cells expressing UL25EGFP or GFPUL25 compared to GFP-expressing cells. Compared to untransfected cells, UL25 expression reduced the ICP0 signal by 70% and 50% at 2 and 3 h pi, respectively. Statistical analysis using the two-sided Student´s t-test showed that the reduction of ICP0 in cells overexpressing wild type UL25 or GFP-tagged UL25 was significant. The fluorescence intensity of cytosolic UL25GFP, GFPUL25 or UL25, nuclear ICP0 was measured using the "region tools" of the Meta Morph software (Universal Imaging Corporation, West Chester, PA, USA version 5.0). Cells expressing GFP or labeled with UL25 above the threshold of 200 units were considered to be transfected. The background gray values of cells not expressing ICP0 ranged from 250 to 290 units, and were substracted to determine the relative fluorescence intensity. The numbers above the error bars (standard error of the mean) represented the number of analyzed cells.

3.2.2 Subcellular Localization of Importin β

Incoming capsids require the nuclear transport factor importin β to bind specifically to the nuclear pore (Ojala et al. 2000). Since UL25 might interfere with this process, the subcellular localization of importin β was analyzed after overexpression of UL25GFP, UL25 or GFP as a control. In untransfected cells, importin β was localized in the cytosol and at the nuclear envelope. In some cells, importin β had accumulated in aggregates around the nuclear peripherie (Figure 19 b, d, l). In cells overexpressing GFP, the subcellular localization of importin β was not changed (Figure 19 a, b, c, d). Cells overexpressing UL25GFP (Figure 19 e, f) or UL25 (Figure 19 i, j) showed a similar distribution of importin β as the cells overexpressing GFP or untransfected cells.

However, the labeling intensity for importin β was reduced if the cells were simultaneously labeled with α-importin β and α-UL25 (UL25-EC, cf. Figure 19 b, d, f, h with Figure 19 j, l). A stronger extraction of cytosolic importin β by the PHEMO protocol did also not reveal an altered localization of importin β in UL25 overexpressing cells (Figure 19 g, h, k, l). Compared to PFA fixed and TX-100 permeabilzed cells, the PHEMO fixation resulted in a stronger extraction of cytosolic importin β, whereas the fraction of importin β that was localized at the nuclear envelope remained.

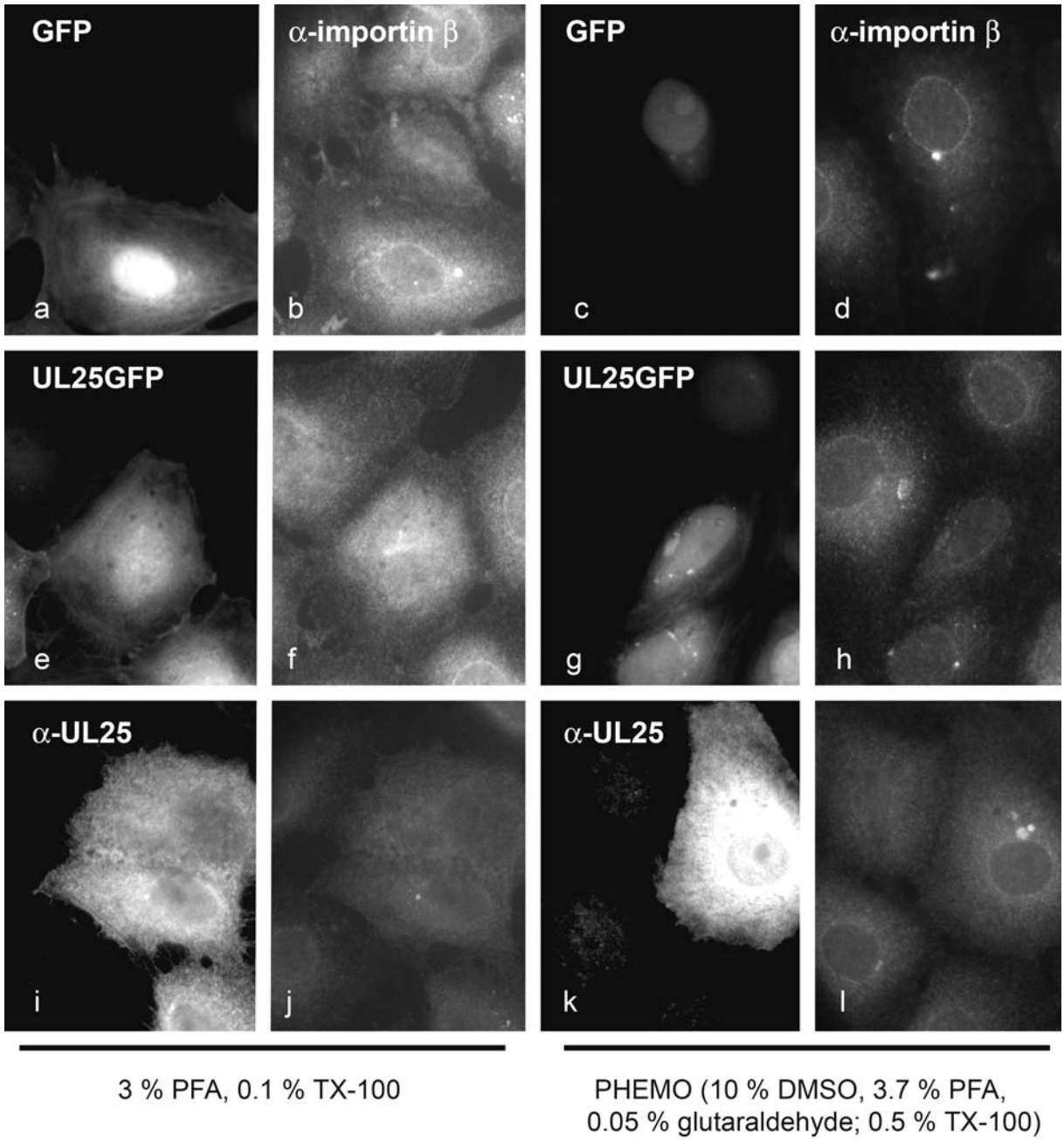

Figure 19: The subcellular localization of importin β was not changed in UL25 overexpressing cells. Importin β was localized in the cytosol and at the nuclear rim (b, d, f, h).The labeling of importin β was a bit weaker when cells were additionally stained with α-UL25 (j, l). A stronger extraction of cytosolic importin β also did not reveal an altered localization of importin β in UL25 overexpressing cells. The stronger extraction by the PHEMO fixation leads to a clearer importin β labeling at the nuclear rim. Cells overexpressing GFP (a, c), UL25GFP (e, g) or UL25 (i, k) were fixed with 3% PFA and permeabilized with 0.1% TX-100 (a, b, e, f, i, j). Alternatively, cells were fixed and permeabilzed in one step using the PHEMO fixative (c, d, g, h, k, l), which extracts the cytosol more than the PFA fixation.

3.2.3 The Nuclear Pore Network

After genome uncoating, transcription and replication of viral genomes commences. A decreased gene expression might be the result of a defective capsid docking and uncoating process at the NPC. The nuclear pore network was analyzed in cells overexpressing GFP, UL25GFP, GFPUL25 or wild type UL25 using an antibody directed against FG-domains that are present in many nucleoporins.

There was no difference in the dotted and nuclear rim localization of nucleoporins between GFP expressing and untransfected cells (Figure 20 a, e). Cells with excess UL25GFP (Figure 20 b, f), GFPUL25 (Figure 20 c, g) or wild type UL25 (Figure 20 d, h) showed a similar nucleoporin localization as GFP-expressing (Figure 20 a, e) and untransfected cells.

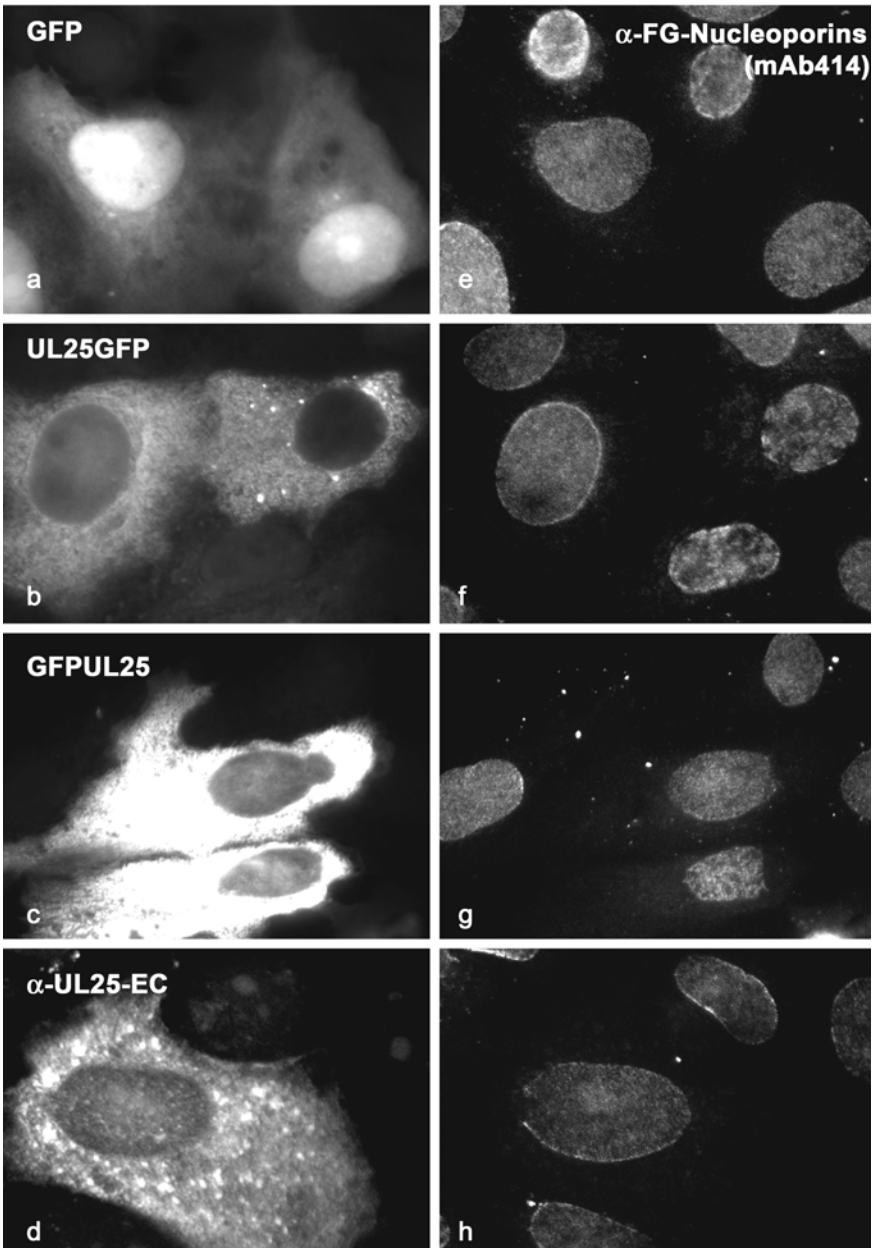

Figure 20: Overexpressed UL25 did not affect the nuclear pore network. All transfected cells (a, b, c, d) showed a dotted rim staining of nucleoporins (e, f, g, h), similar to untransfected cells that were found adjacent to the transfected cells. UL25 overexpression did not change the appearance of NPC. The nuclear rim staining of the antibody was not disturbed by UL25. Cells overexpressing GFP, UL25GFP, GFPUL25 or UL25 were fixed with 3% PFA and permealized with 0.1% TX-100. NPCs were labeled with a monoclonal antibody that recognizes FG-repeats within many nucleoporins. UL25 was visualized with the rabbit polyclonal antibody UL25-EC.

3.2.4 Nuclear Import of the Major Transcriptional Activator VP16

The HSV tegument protein VP16, also known as Vmw65 or α-TIF activates transcription of the viral immediate early genes and is essential for efficient virus replication (Greaves and O'Hare 1990). It is also essential for virus assembly (Weinheimer et al. 1992). Unlike other transcriptional transactivators, VP16 does not bind DNA by itself but interacts with two cellular proteins, Oct-1 and HCF. This complex binds to a TAATGARAT motif, found in all HSV1 immediate early enhancers (Rajcani et al. 2004). A mislocalization of the incoming heterotrimeric VP16 transactivation complex could result in an inefficient transactivation of viral gene transcription which would lead to a reduced early viral gene expression.

To analyze the subcellular localization of incoming VP16, GFPUL25 overexpressing cells were infected with HSV1 at a MOI of 100, PFA fixed and labeled for VP16 (Figure 21). Incoming VP16 had accumulated in the nucleus at 2 h pi. The presence of GFPUL25 did not reduce the nuclear import of VP16 (Figure 21 d). At 3 h pi and 4 h pi, VP16 was mainly present in the nucleus, indicating that most of the capsid associated VP16 had reached the nucleus (Figure 21 e, f). To quantify the amount of VP16 in the nucleus, grey values of the nuclei were measured in GFPUL25 transfected and untransfected cells. The signal within the nucleus was highest at 2 h pi and decreased slightly over time (Figure 21, Figure 22). The signal intensity was similar in GFPUL25 transfected cells compared to untransfected cells (Figure 22). Thus, an impaired nuclear accumulation of VP16 seemed not to be the explanation for the lower immediate early gene expression in UL25 overexpressing cells.

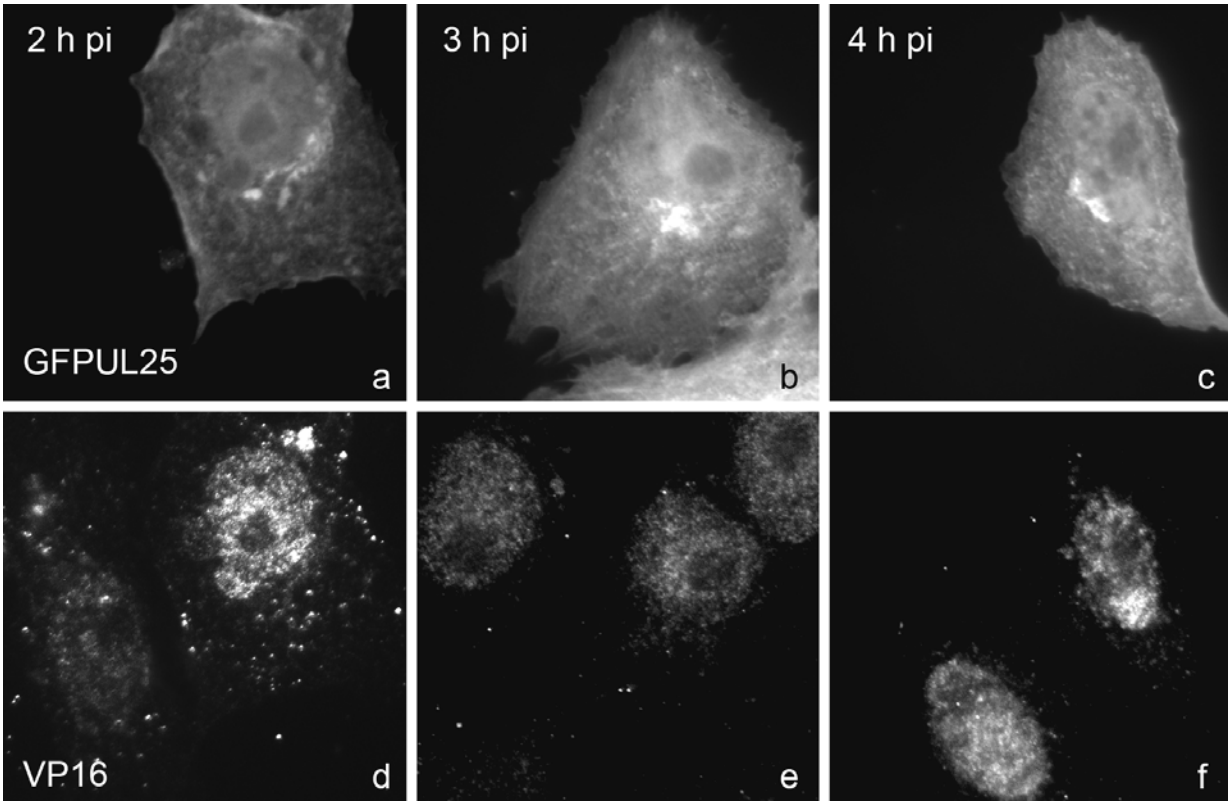

Figure 21: The accumulation of the major transcriptional activator VP16 was not influenced by excess UL25. VP16 was already accumulating in the nuclei of infected GFPUL25 transfected cells and neighboring untransfected cells (a, d) at 2 h pi. 3 h pi and 4 h pi, VP16 was mostly present in the nucleus, indicating that most of the incoming VP16 had reached the nucleus (IF Fig. e, f). GFPUL25 overexpressing cells were infected with HSV1(F) with an MOI of 100 PFU/cell, fixed with 3% PFA after 2h, 3h or 4 h pi and permeabilized with 0.1% TX-100. VP16 was labeled with the rabbit pAb SW7.

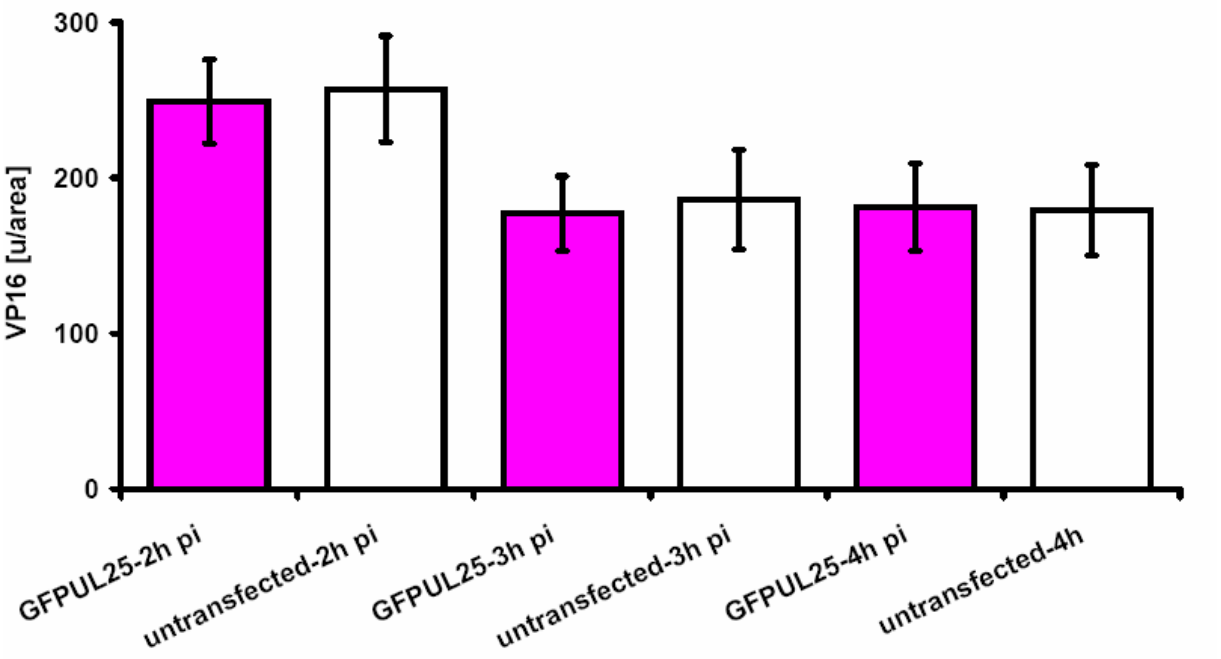

Figure 22: Nuclear targeting of VP16 in the presence of UL25. The quantification showed that the amount of VP16 was not changed in the presence of GFPUL25 (pink bars) compared to untransfected cells (white bars). The fluorescence intensity of nuclear VP16 was measured using the region tools of the Image Jh software (NIH, USA, version 1.35j). The nuclear background value of uninfected cells was substracted from the fluorescence intensity of nuclear VP16.

3.2.5 Transactivation of Cellular and Herpesviral Promoters

Transcription factors are proteins which help to recruit the RNA polymerase II, which transcribes all protein-coding genes in eucaryotes, place the RNA polymerase II correctly onto the promotor, aid in seperating the two DNA strands to initiate transcription, and release RNA polymerase II from the promoter into the elongation mode once transcription had been initiated (Nikolov and Burley 1997; Roeder 1996). The reduction in early viral gene expression by excess UL25 might be the result of mislocalized transcription factors, or a disturbed transcription initiation or elongation process in general e.g. by inhibiting the binding of the RNA polymerase to the promoter region on the DNA.

The transcription factor NFκB (nuclear factor-κB) is a latent gene regulatory protein which is involved in cellular responses to stimuli such as stress, cytokines, free radicals and bacterial or viral antigens. In unstimulated cells, the NFkB dimers are sequestered in the cytoplasm. NFκB translocation to the nucleus is induced and precedes the late phase of HSV1 replication and transcription. Moreover the translocation of NFκB to the nuclei of infected cells is necessary to prevent apoptosis during HSV1 infection (Goodkin et al. 2003).

The JAK (Janus Kinases)-STAT (Signal Transducer and Activator of Transcription) pathway is activated, e.g. by interferons. HSV1 suppresses the interferon signaling pathway by inhibiting the phosphorylation of the transcription factor STAT and JAK during early infection (Yokota et al. 2001).

The transcriptional activation by NFAT (nuclear factor of activated T cells) is efficiently blocked at early stages of HSV1 infection and may constitute an immune evasion strategy for herpesviruses or might promote viral replication (Scott et al. 2001).

The subcellular localization of the cellular transcription factors NFκB (Figure 23 b, d) and its inhibitor IκB (Figure 23 f, h), STAT (Figure 23 j, l) and NFAT (Figure 23 n, p) was analyzed in the presence of overexpressed GFP or UL25GFP to address whether UL25 alone can influence their intracellular distribution. 24 h post transfection transcription factors were labeled with specific antibodies (cf. chapter 2.2) and analyzed by immunofluorescence microscopy. None of the tested transcription factors or the inhibitor IκB showed a relocalization in GFP (Figure 23 a, e, i, m) or UL25GFP transfected cells (Figure 23 c, g, k, o) compared to untransfected cells.

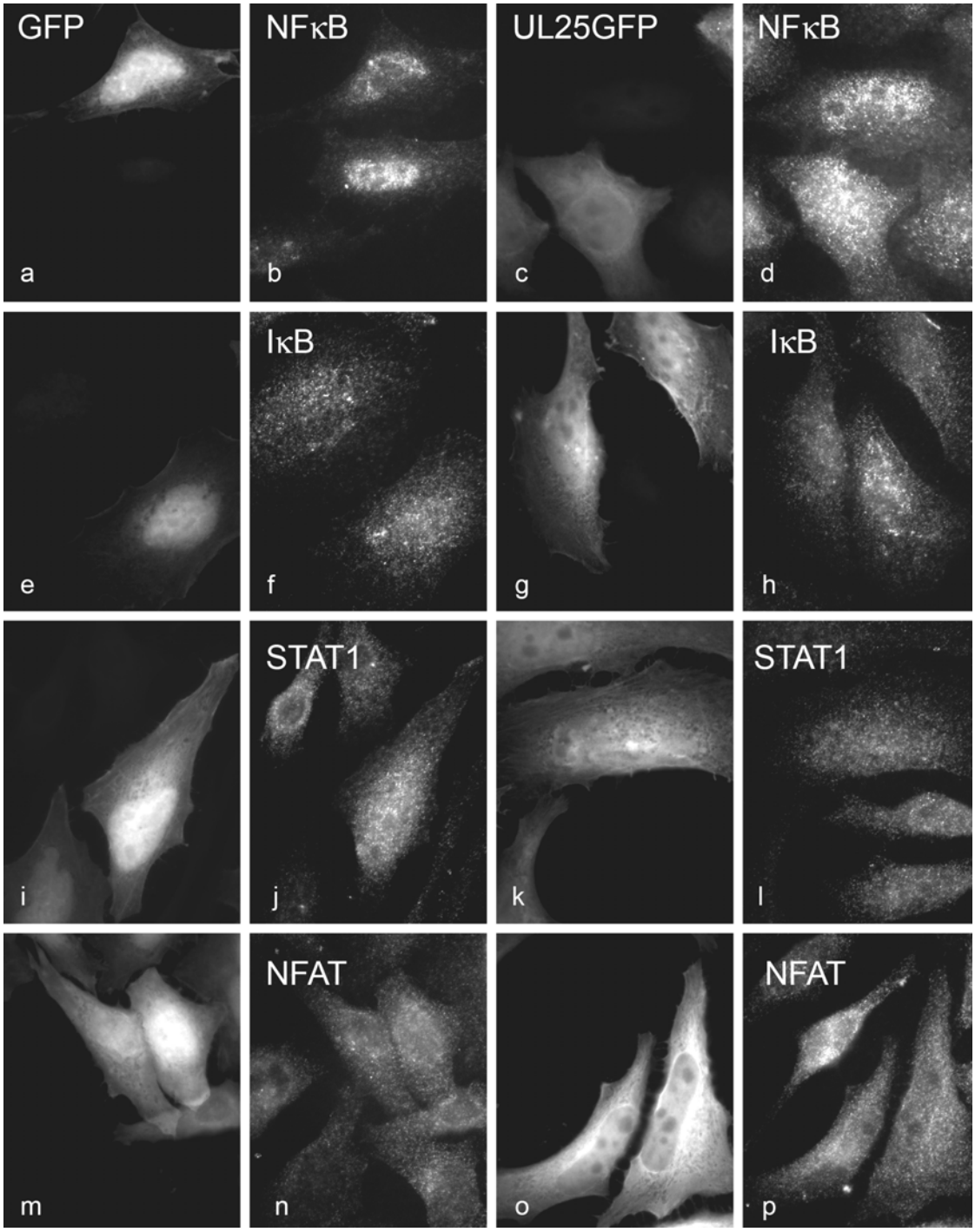

Figure 23: The subcellular localization of cellular transcription factors was not changed by overexpressed UL25. The localization of the cellular transcription factors NFκB (b, d), IκB (f, h), STAT1 (j, l) and NFAT (n, p) in GFP (a, e, i, m) or UL25GFP (c, g, k, o) overexpressing cells was not impaired, compared to untransfected cells. Vero cells were transiently transfected with GFP or UL25GFP. After 3% PFA fixation and 0.1% TX-100 permeabilization, cells were labeled with specific antibodies against NFκB, IκB, STAT1 or NFAT.

Next, the activation of cellular or herpesviral promoters in the presence of overexpresed UL25 was tested using luciferase reporter assays (cf. chapter 2.6.3). Cells overexpressing the luciferase encoding vector pGL2, that lacks promoter elements as a control (Figure 24 a) or containing a cyclin E promoter (Figure 24 b) together with increasing amounts of GFP (white), UL25GFP (pink) or GFP-Hunk (blue) were analyzed for luciferase activity. Since the plasmid dilution of GFP, UL25GFP or GFP-Hunk would result in less transfectable plasmid per well, the difference in plasmid amount was supplemented with the vector pcDNA3. Therefore a transfection with 250 ng pcDNA3 was performed without any pGL2, pGL2-Cyclin E, GFP, UL25GFP or GFP-Hunk to test whether this had any influence on the reporter assay. As expected for a functional assay, no luciferase activity was measured (Figure 24 b). The Hunk protein served as a positive control since it can activate the cyclin E promoter (Dey et al. 2000; Ottinger 2005). Expression of GFP and GFP-Hunk had no effect on intrinsic pGL2 luciferase activity. In contrast, high amounts of UL25GFP decreased an intrinsic residual promoter activity of pGL2 encoded luciferase (Figure 24 a). Cells cotransfected with pGL2-Cyclin E promoter and increasing amounts of GFP did not activate cyclin E promoter. GFP-Hunk was able to activate luciferase expression driven by cyclin E promoter revealing that the assay was working. Moreover, UL25 did not influence cyclin E promoter induced luciferase activity (Figure 24 b).

Further, a herpesviral promoter element derived from the Epstein Barr Virus (cf. Table 1) was tested. The vector pGL2b-EBV cp contains the EBV C promoter of the Epstein Barr Nuclear Antigen 2 (EBNA2) responsive element. The EBNA2 protein acts as a transcriptional activator of several viral and cellular genes and is necessary for immortalization of human primary B lymphocytes, a prerequisite for establishing latency (Meitinger et al. 1994; Ottinger 2005). Cells overexpressing pGL2-EBV-cp with increasing amounts of GFP did not exhibit enhanced luciferase expression driven by the EBV-cp promoter. Cells overexpressing UL25GFP decreased the promoter activity of EBV-cp (Figure 25).

The activation of luciferase was also analyzed with the vector pTal that contains the TATA-like (TAL) region of HSV thymidine kinase (TK) minimal promoter. Luciferase expression needs to be activated by promoter elements. The SRE (cloned in the pTal backbone) activates the transcription factors Elk-1/STAT which are important for the mitogen activated kinase/c-Jun kinase signalling (MAPK/JNK) pathway. Cells overexpressing pTAL or pSRE together with increasing amounts of GFP (white) or UL25GFP (pink) were analyzed for luciferase activation. GFP neither influences the intrinsic residual luciferase activity of pTal nor the SRE driven luciferase activity. The medium and highest concentration of UL25GFP resulted in a reduced luciferase activity irrespective whether there is a promoter element present or not (Figure 26). Therefore the reduction in luciferase expression by excess UL25 is not depending on the transcriptional activation by the SRE.

Disturbing specific promoter activation seemed not to be the reason for a lower gene expression in the presence of excess UL25, instead a general reduction of intrinsic transcription activity was observed.

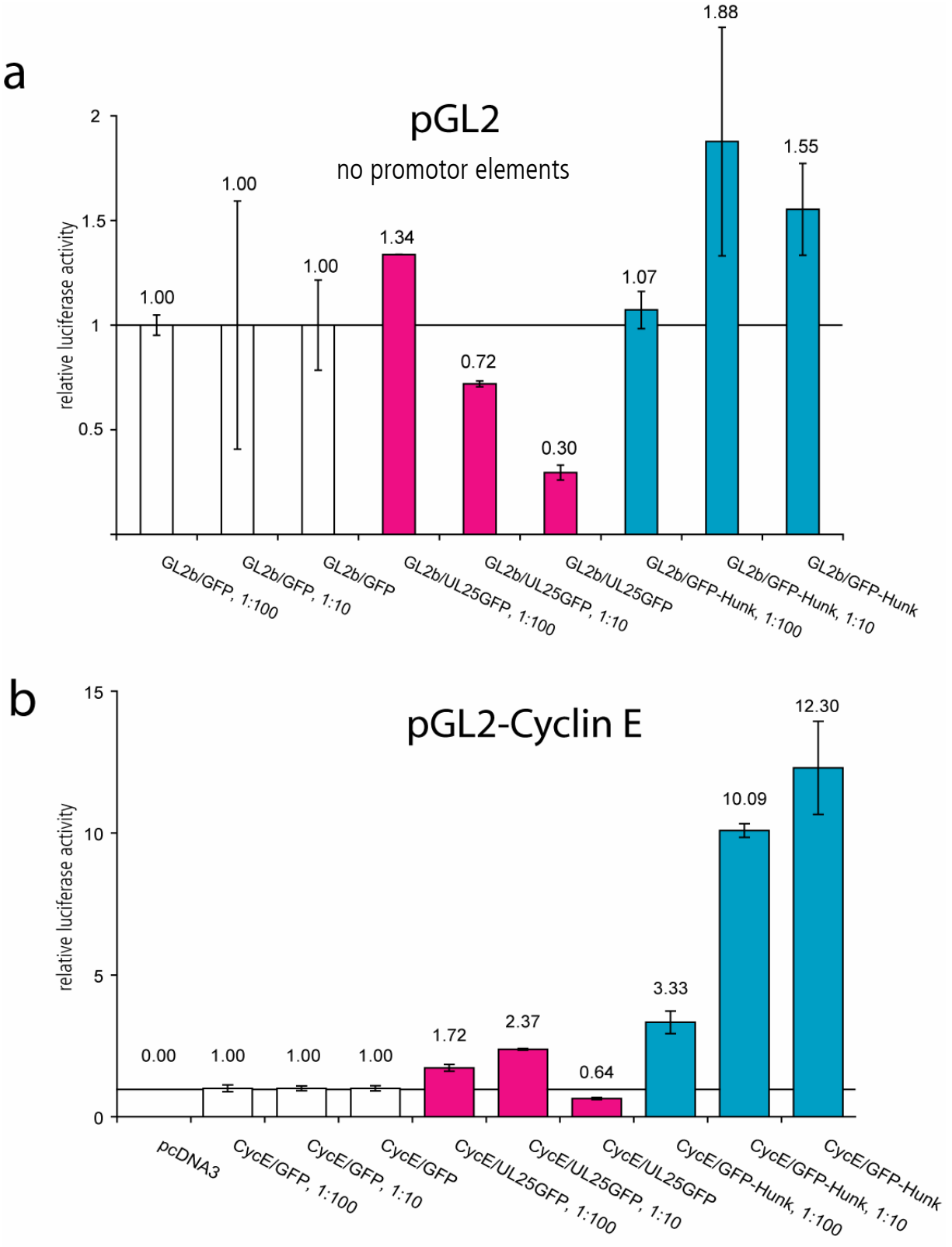

Figure 24: The activity of the cyclin E promoter was not specifically altered by overexpressed UL25GFP. Cells cotransfected with pGL2 (a) or pGL2-Cyclin E promoter (b) and increasing amounts of GFP (white bars), UL25GFP (pink bars) or GFP-Hunk (blue bars) were analyzed for the luciferase activity encoded by the pGL2 vector. The highest concentration of UL25GFP decreased the intrinsic residual promoter activity. The overexpression of GFP-Hunk only resulted in very weak activation for all three concentrations tested. Cells cotransfected with pGL2-Cyclin E promoter with increasing amounts of GFP or UL25GFP did not activate or reduce the luciferase expression driven by the cyclin E promoter. As a control, GFP-Hunk was able to activate luciferase expression driven by cyclin E promoter. Cells only overexpressing the empty vector pcDNA3 did not give a luciferase signal. Cells expressing the indicated plasmids for 30 h were lysed in reporter lysis buffer, mixed with luciferin containing substrate and measured in a luminometer.

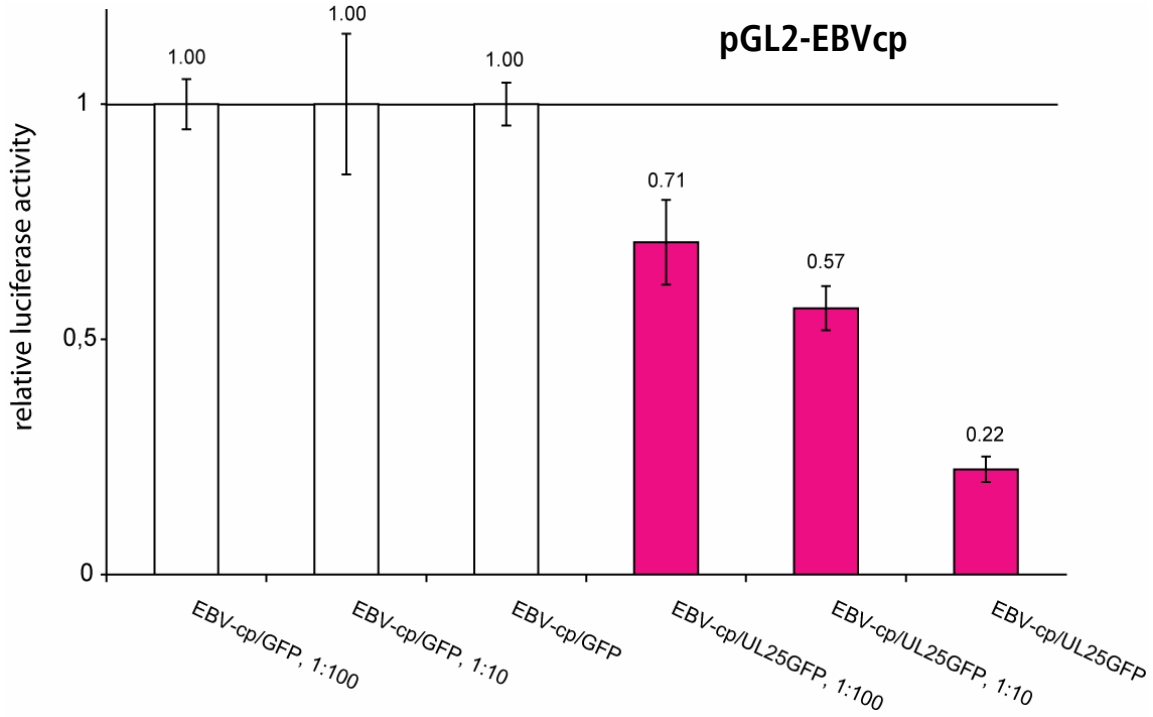

Figure 25: The repression of EBV-c promoter was not specifically caused by high amounts of overexpressed UL25GFP. Cells cotransfected with pGL2-EBV-cp promoter and GFP (white bars) or UL25GFP (pink bars) were analyzed for the luciferase activity encoded by the pGL2 vector. Cells coexpressing high concentrations of UL25GFP and luciferase under the control of an EBV-cp promoter showed a repression of luciferase. Cells expressing the indicated plasmids for 30 h were lysed in reporter lysis buffer, mixed with luciferin containing substrate and measured in a luminometer.

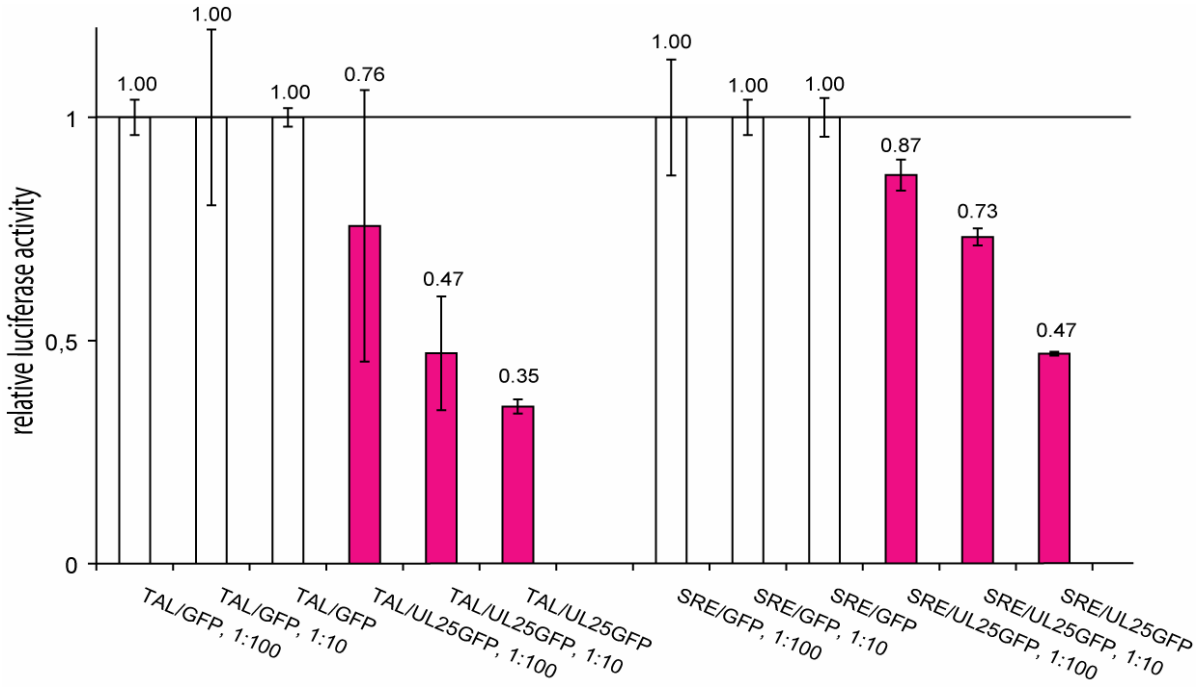

Figure 26: The residual promoter activity was repressed by overexpressed UL25GFP independently of the serum responsive element. Cells cotransfected with pTAL or pSRE (that contains a serum responsive element cloned in pTAL) and increasing amounts of GFP (white bars) or UL25GFP (pink bars) were analyzed for the luciferase activity. Overexpression of GFP neither influenced the intrinsic residual luciferase activity of pTal nor the SRE driven luciferase activity (white bars). The highest concentration of UL25GFP repressed the intrinsic residual luciferase activity of pTAL. The medium and highest concentration of UL25GFP resulted in less luciferase activity in the presence of the SRE. Cells expressing the indicated plasmids for 30 h were lysed in reporter lysis buffer, mixed with luciferin containing substrate and measured in a luminometer.

3.2.6 Late but Not Early Protein Synthesis of Vaccinia Virus was Slightly Impaired

Poxviruses, like vaccinia virus (VV) are unique among DNA viruses, as they replicate their DNA in the cytoplasm indepently of the nucleus and NPCs. Nevertheless, VV has also evolved ways to use the host cell to optimize their cytoplasmic DNA replication and to ensure that this process occurs at the right time and place (Schramm and Locker 2005). To test whether UL25 blocked protein synthesis in general, we infected GFP (Figure 27 a, c) or UL25GFP (Figure 27 e, g) overexpressing Hela cells with VV at an MOI of 60 PFU/cell (Schepis et al. 2006). As a marker for early VV gene expression p35/H5R protein, the late VV gene transcription factor 4 which accumulates in replication compartments next to the nucleus, was used (Kovacs and Moss 1996; Tolonen et al. 2001). For late VV gene expression the protein p16/A14L of VV was analyzed (Salmons et al. 1997). The protein p16/A14L is the major membrane protein of the first infectious form of VV, the intracellular mature virus and during assembly of VV it is located at the ER-Golgi compartment in perinuclear areas (Sancho et al. 2002).

Compared to the untransfected cells (Figure 27 b, f), VV replication compartments were assembled next to the nuclei at 3 h pi, and contained similar amounts of p35 irrespective of which protein was ectopically expressed. At 7 h pi, GFP overexpressing cells and untransfected cells showed similar amounts of p16 in juxtanuclear VV replication compartments (Figure 27 d). In contrast, in cells overexpressing UL25GFP the synthesis of p16 was slightly reduced compared to control cells (Figure 27 h, asterisk). Early protein synthesis per se was not impaired by excess UL25, but UL25 seemed to interfere with a late step during VV maturation by an unknown mechanism.

3.2.7 Adenovirus Mediated Transgene Expression was not Influenced

Like herpesviruses, adenoviruses (Ad) are replicating their genomes in the nucleus. Ad capsids travel to the nucleus and release their viral genome through the nuclear pores into the nucleoplasm for viral DNA transcription and replication (Trotman et al. 2001). To test whether UL25 influences gene expression of Ad, I infected GFP (Figure 28 a, e) or UL25GFP (Figure 28 c, g) overexpressing Hela cells with Ad encoding for β-galactosidase under an early adenoviral promoter (Schiedner et al. 2000).

At 12 h pi, the cells were fixed and labeled with an antibody to β-galactosidase to monitor the progress of Ad infection. Similar amounts of β-galactosidase were detected in untransfected, GFP or UL25GFP overexpressing cells (Figure 28 f, h). This indicated that the cell entry, uncoating and gene expression of Ad was functional in UL25 overexpressing cells. Thus, we concluded that in the presence of HSV1-UL25, not only Ad protein translation is functional, but also Ad uncoating at the nuclear pore, Ad genome import through the NPC, Ad mRNA synthesis and export into the cytosol.

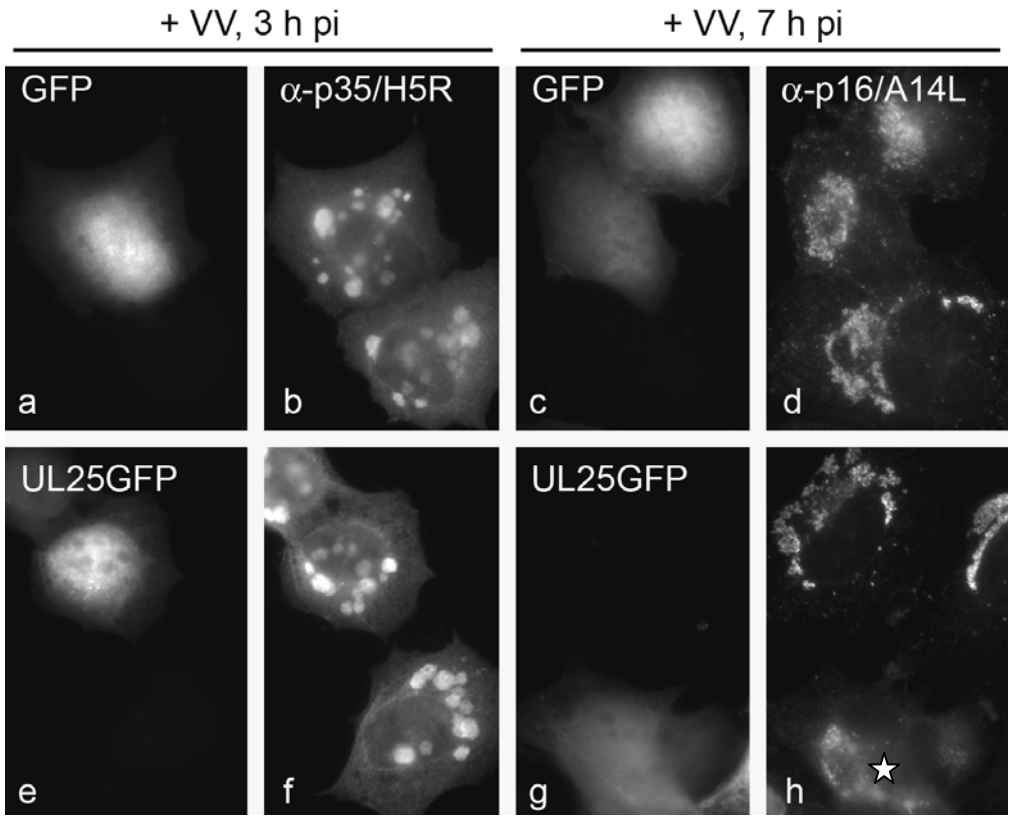

Figure 27: Excess UL25 did not influence early VV gene expression, but late VV gene expression was reduced. The early VV protein p35/H5R (b, f) was expressed 3 h pi in VV replication compartments that were located adjacent to the nuclei of infected cells irrespective, whether GFP (a) or UL25GFP (e) were overexpressed. At 7 h pi, only in GFP (c) overexpressing cells similar amounts of the late protein p16 (d) were detected in VV replication compartments next to the nuclei compared to the untransfected cells. Interestingly, in cells overexpressing UL25GFP (g) synthesis of p16 was slightly reduced, compared to adjacent untransfected cells or GFP expressing cells. GFP or UL25GFP overexpressing Hela cells were infected with VV strain WR with an MOI of 60 PFU/cell. 3 and 7 h pi, cells were fixed with 3% PFA and permeabilized with 0.1% TX-100 and labeled with antibodies against the early VV protein p35/H5R or the late VV protein p16/A14L monitor the progress of VV infection.

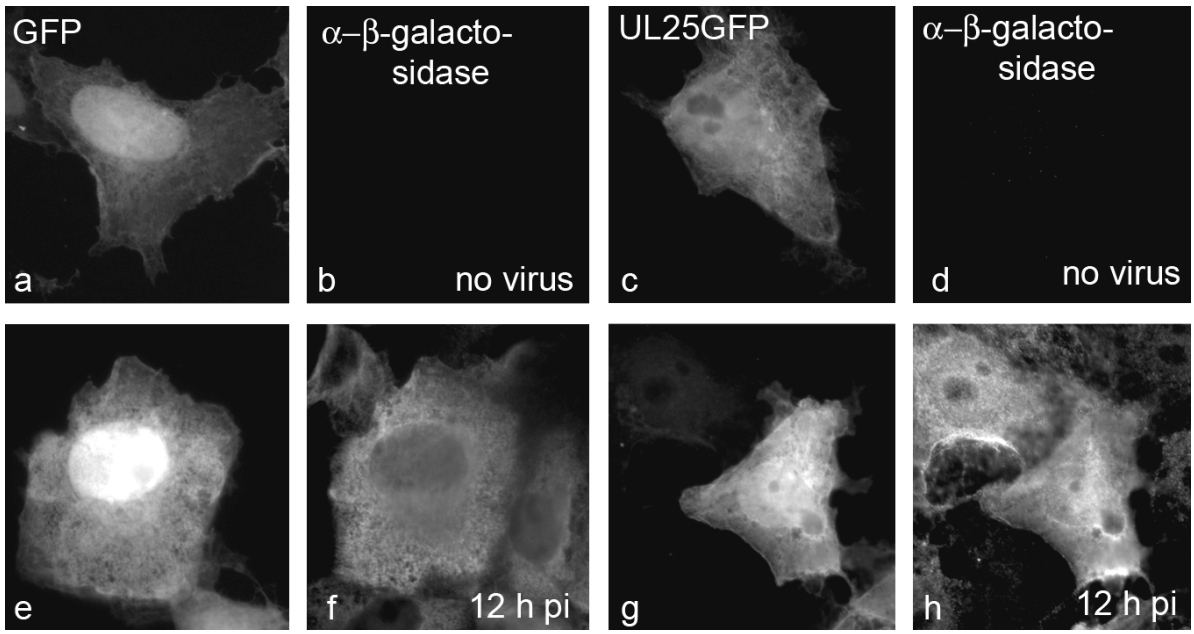

Figure 28: Excess UL25 does not impair adenovirus infection. The expression of β-galactosidase was detected in adenovirus infected cells irrespective of the overexpressed protein (f, h). GFP or UL25GFP overexpressing Hela cells were infected with adenovirus at an MOI of 100 PFU/cell encoding for β-galactosidase under an early adenoviral promoter. 12 h pi the cells were fixed with 3% PFA and permeabilized with 0.1% TX-100 and labeled with an antibody to β-galactosidase to monitor the progress of Ad infection.

3.2.8 Uncoating of HSV1 Genomes

If overexpressed UL25 would have disturbed the uncoating process, immediate early viral gene expression would be reduced. In this scenario excess UL25 could act as a dominant-negative inhibitor of the viral genome uncoating at the NPC.

To address whether capsids at the NPC of UL25 overexpressing cells still contained genomes, I performed transmission electron microscopy (EM). GFP fluorescence cannot be detected by EM. Therefore GFP or GFP-tagged UL25 overexpressing infected cells were seperated from untransfected cells prior to processing for EM. To this end, Vero cells were transfected with GFP, UL25GFP or GFPUL25 for 24 h and infected with HSV1 at a MOI of 500 PFU/cell. After trypsinization and fixation, the cells were sorted by FACS (Figure 29 a). The total cell population (blue) as well as the population of single cells (red) are depicted as an histogram, which displayed the number of cells at the y-axis and the cell size on the x-axis (Figure 29 b). Untransfected or GFP-transfected, uninfected cells were treated the same way as the transfected, infected cells and used for calibrating the FACS machine (Figure 29 c, upper two rows). Cells above a certain threshold were sorted and collected as GFP-positive cells (Figure 29 c, green), fixed again and further processed for epon embedding and EM analysis (cf. chapter 2.6.4). Single Vero cells (Figure 29 c, red) were further analyzed according to their GFP fluorescence (Figure 29 c, green). Very low GFP-expressing cells mixed with large untransfected cells were omitted (Figure 29 c, grey). Reanalyis of the GFP-positive sorted fraction by FACS revealed an enrichment of 98% GFP-expressing cells (not shown).

In ultrathin-epon sections of FACS enriched cells overexpressing GFP (Figure 30 a), UL25GFP (Figure 30 b) or GFPUL25 (Figure 30 c), the subcellular localization of capsids and whether they contained the HSV1 genome or not were analyzed at 2 h pi. Capsids at the nucleus were located at the NPC (Figure 30, asterisks). The majority of capsids at the nucleus were empty, thus they had already uncoated their genome (Figure 30 a, b, c). Rarely, capsids contained their genome at the NPC or were empty in the cytosol (not shown).

I quantified the frequency of capsid populations at the nuclear membrane or in the cytosol and differentiated for every cell population whether they contained their genome or not (GFP, UL25GFP, GFPUL25; Figure 31).

In GFP and GFPUL25 overexpressing cells, around 60 to 70% of all capsids at the NE were empty without genomes and around 30% were cytosolic, DNA containing capsids. The remaining 10% were either empty capsids in the cytosol or full capsids at the NE. In UL25GFP overexpressing cells, the amount of empty capsids at the NE was reduced to 40%. But while the fraction of full capsids at the NE remained relatively constant, the number of full capsids in the cytosol had increased (Figure 31 a). The amount of empty capsids in the cytosol was comparable to that of GFP or GFPUL25 expressing cells.

To test whether the uncoating event at the NPC was influenced by overexpressed UL25, the capsid population at the NE was divided in subpopulations (Figure 31 b). The total amount of capsids was comparable in all three cell populations transfected with GFP, UL25GFP or GFPUL25. Comparable amounts of capsids at the nuclear membrane were in close proximity to the outer nuclear membrane but without a NPC beneath irrespective of the overexpressed protein. At the NPC the number of empty capsids was equal in all cell populations, and therefore uncoating seemed to be unaffected by overexpressing UL25 (Figure 31 b).

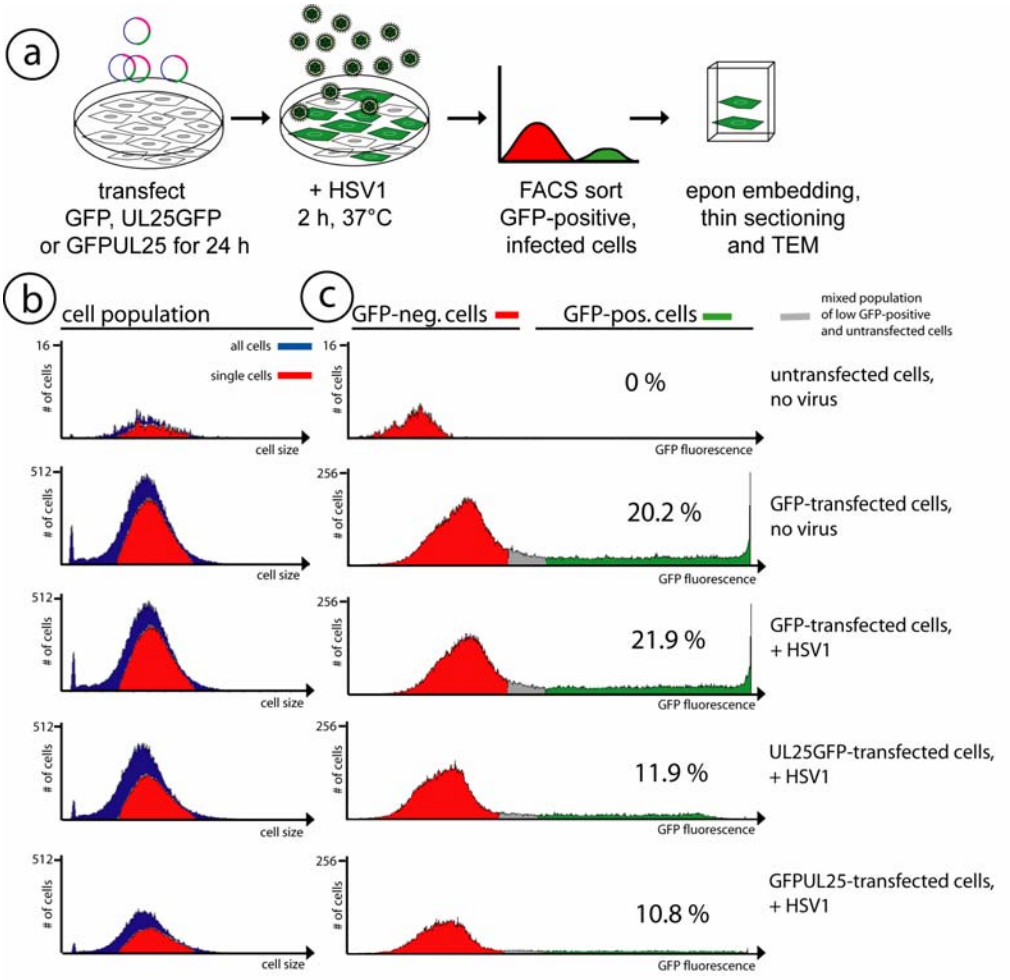

Figure 29: Experimental setup and FACS results prior to epon embedding for transmission electron microscopy. For EM, GFP or GFP-tagged UL25 overexpressing infected cells were separated from untransfected, infected cells. Vero cells were transfected for 24 h, infected with HSV1(F) at an MOI of 500 PFU/cell, trypsinized and fixed prior to FACS sorting. GFP-positve sorted cells were embedded in epon resin and further processed for EM analysis (a). The amounts of single cells were determined by plotting the number of cells according to their size (b, Adams 2005). The blue colored cell population represented all counted cells, the red population the single cells. Single cell populations were further analyzed according to their GFP fluorescence (c). For FACS calibration untransfected and GFP transfected cells were used (c, upper two rows). Untransfected cells (red), cells that express low amounts of GFP and bigger untransfected cells (grey) were not taken into the sort. GFP-positive sorted cells (green cell population and percentage) were further processed for epon embedding and EM analysis. Histograms were created and modified using WinMDI version 2.8 (http://facs.scripps.edu; by J. Trotter).

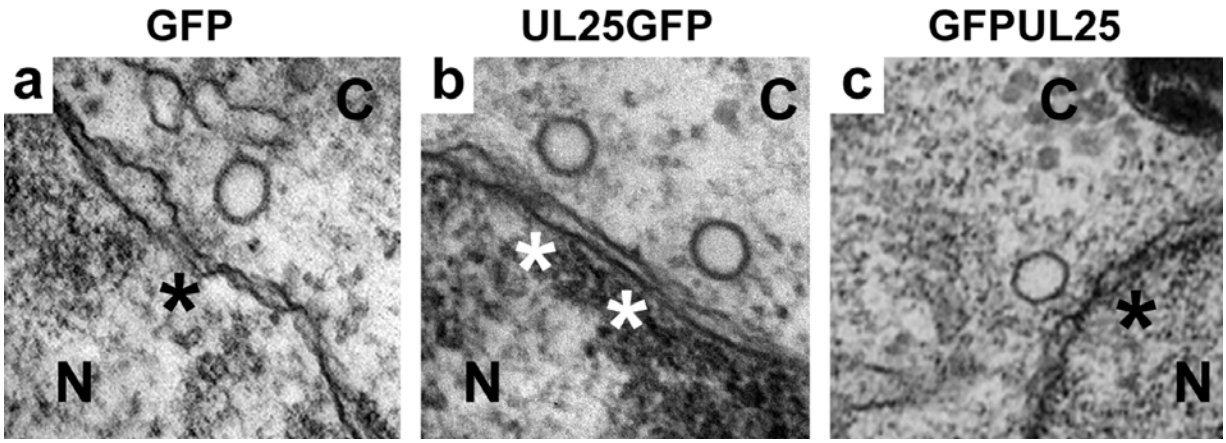

Figure 30: Empty capsids were found at the NPC in GFP, UL25GFP or GFPUL25 overexpressing cells. Ultrathin epon sections with a width of 50 to 80 nm were analyzed by EM and the localization of capsids at the nucleus (N) and in the cytosol (C) were analyzed. Capsids at the nucleus were located at the NPC (a, b, c; asterisks) indicating that the genome was released irrespective of the overexpressed protein. Cells sorted for GFP (a), UL25GFP (b) or GFPUL25 (c) by FACS were embedded in epon, and ultrathin sections were made, contrasted in lead nitrate and analyzed at a Zeiss electron microscope.

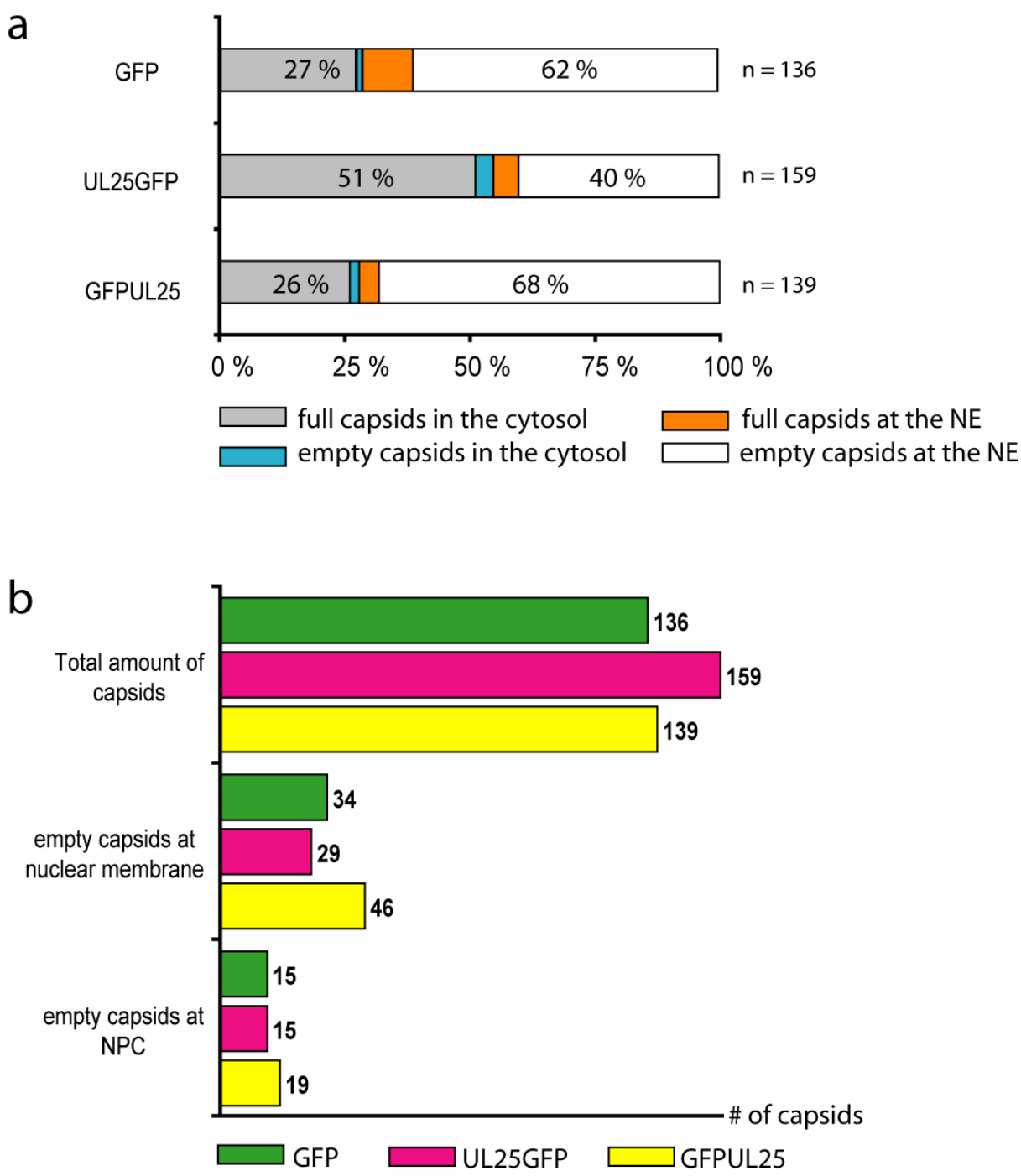

Figure 31: Quantification of the capsid subpopulations in GFP, UL25GFP or GFPUL25 overexpressing, HSV1 infected cells. Each capsid population was quantified by counting capsids for analyzing whether overexpression of UL25 influences the subcellular localization of capsids. First, the amount of empty (blue) and full (grey) capsids in the cytosol or at the nuclear envelope (NE, orange, white) were counted (a). In GFP and GFPUL25 overexpressing cells, around 60% of all capsids found at the NE were empty (white bars) and around 30% were cytosolic capsids that still contained their genome (grey bars). The remaining 10% were either empty capsids in the cytosol (blue bars) or full capsids at the NE (orange bars). In UL25GFP overexpressing cells the amount of empty capsids at the NE was reduced to 40%. But while the fraction of full capsids at the NE remained relatively constant, the number of full capsids in the cytosol increased. The amount of empty capsids in the cytosol and full capsids at the NE was comparable to GFP or GFPUL25 expressing cells. To determine, whether the uncoating event at the NPC was influenced by overexpressed UL25 the capsid population at the NE was further differentiated in subpopulations "empty capsids at the NPC" and "empty capsids at the nuclear membrane" compared to the "total amount of capsids" (b). The amount of capsids was comparable in all three analyzed cell populations of GFP (green bars), UL25GFP (pink bars) or GFPUL25 (yellow bars). The number of capsids at the NPC was equal in all cell populations.

3.2.9 Subcellular Localization of Incoming Viral Genomes

The reduction in viral gene expression in the presence of UL25 (Figure 17, Figure 18) might be the result of a defective translocation of the viral genome during the uncoating event (cf. chapter 4; Figure 39). To localize the viral genome in UL25 transfected cells, I combined *in situ* hybridization (Everett and Murray 2005) with transient transfection and virus infection. The probe for *in situ* hybridization was prepared using a nick translation procedure according to Everett and Murray 2005 (cf. chapter 2.7).

Briefly, HSV1(F) DNA isolated from infected cells was partially digested by DNase I, which has an endonuclease activity to generate single strand nicks. Those single strand breaks were then filled with fluorescently Cy3 labeled dCTP nucleotides by the 5´-3´polymerase activity of the Taq DNA polymerase. The aim was to produce DNA fragments with a size of 0.5 to 1 kb. This size of DNA fragments is well suited for random hybridization of the DNA template (R. Everett, MRC, Glasgow, personal communication). Viral DNA was incubated at 37°C with 1:1000 (1 µu/µl) diluted DNase for 0 to 30 min (Figure 32) and analyzed on an agarose gel. 25 min incubation was sufficient to achieve a partial DNA digest that results in DNA fragments of about 0.5 to 0.8 kb. Still a lot of undigested viral DNA was present above 8 kb. Therefore the dilution of DNase was modified (Figure 33). A 1:300 dilution of DNase resulted in a digest of viral DNA to fragments of 1.5 kb to 0.1 kb. A 1:600 dilution of DNase resulted in a complete digestion of the small fragments but also to a better digest of the higher DNA fragments. Therefore for further DNase digests a dilution of 1:500 (2µu/µl) was used. The *in situ* hybridization probe was prepared according to the manufacturer´s protocol (cf. chapter 2.7.2). To test the specificity of the Cy3-labeled HSV1(F)-DNA probe, Vero cells were infected with HSV1(17^+) with an MOI of 10 PFU/cell for 8 or 12 hours. Fixation and hybridization with the probe were performed as described (cf. 2.7.4).

Uninfected cells showed no Cy3 labeling in the nuclei (Figure 34 a), which were localized by DIC (Figure 34 b, d, f). Cells infected for 8 h showed replication compartments in the nuclei that were labeled by the HSV1(F)-Cy3 probe (Figure 34 c) and egressing particles were detected in the cytoplasm (Figure 34 c, inset). 12 h pi, the replication compartments became more prominent and many egressing viral particles could be detected as dotted particles in the cytoplasm of the infected cells (Figure 34 e, inset).

Next I tested whether incoming viral genomes were recognized by the HSV1(F)-Cy3-probe. Therefore Vero cells were infected with HSV1(F) with different MOIs and hybridized with the probe at 1 or 3 h pi (Figure 35). Uninfected cells showed very little background labeling derived from the probe (Figure 35 a). In cells infected with an MOI of 20 PFU/cell, there was a punctuate signal throughout the entire cell (Figure 35 b) that accumulated at the nuclear envelope at 3 h pi (Figure 35 c). Increasing the MOI from 20 PFU/cell to 50 PFU/cell (Figure 35 d, e) or 100 PFU/cell (Figure 35 f, g) resulted in an increased labeling of incoming viral genomes.

Cells were infected with an MOI of 70 PFU/cell, fixed, hybridized and labeled with an antibody directed against UL25 to determine the subcellular localization of the incoming genomes relative to the incoming viral capsids. I used the UL25 antibody because previous experiments had demonstrated that it recognized its epitope after many different fixation techniques (cf. Figure 8). Uninfected cells showed little background after labeling with the Cy3-probe and the UL25-antibody (Figure 36 a, b). At 1 h pi, viral capsids labeled for UL25 were distributed

throughout the cell (Figure 36 d). Viral genomes were also distributed throughout the cell (Figure 36 e) and some genomes colocalized with capsids (Figure 36 f, arrows). At 3 h pi, more viral genomes than capsids accumulated at the NE (Figure 36 g, h). While some capsids with their genomes were still in the cytoplasm (Figure 36 i, arrow), capsids at the nuclear envelope did not contain genomes and many genomes at the nucleus did not colocalize with capsids (Figure 36 i, asterisk). Thus, capsid and genome might have separated at the nuclear envelope, indicating that the capsid had released its genome.

To adress whether overexpressed GFP-tagged or wild type UL25 might interfere with nuclear import of incoming viral genomes, the overexpressed protein was detected using antibodies since the GFP-fluorescence was not maintained after fixation with ethanol and acetic acid. (Figure 37 m, n, o). Antibodies directed against GFP or UL25 were tested in PFA-fixed (Figure 37 left) or ethanol-acetic acid fixed cells (Figure 37 right). GFP, UL25GFP, GFPUL25 overexpressing cells could easily be identified by GFP fluorescence after PFA fixation and TX-100 permeabilization or labeling with an antibody against GFP after ethanol-acetic acid fixation (Figure 37 a, b, c). The antibodies against UL25 (ID1; Figure 37 f, g, h, r, s, t; EC Figure 37 j, k, l, v, w, x) recognized cells overexpressing UL25GFP, GFPUL25 or UL25 after PFA fixation and TX-100 permeabilization or after ethanol-acetic acid fixation, but did not react with GFP (Figure 37 e, i, q, u). Thus using these antibodies, the subcellular localization of the viral genomes could then be analyzed in UL25 overexpressing cells.

Next, the subcellular localization of incoming viral genomes was detected in UL25 overexpressing cells. Therefore the cells were transfected with GFP, UL25GFP or GFPUL25. 24 h later, cells were infected with HSV1(F) at an MOI of 70 PFU/cell and after 3 h pi fixed with ethanol-acetic acid. *In situ* hybridization of viral genomes was performed with a Cy3-labeled HSV1(F)-DNA probe as described in chapter 2.7.4, followed by an immunolabeling with antibodies against UL25 or GFP (not shown). Confocal sections of 700 nm were generated and slices through the nuclei of infected cells were analysed for the amount of Cy3-labeled HSV1(F) genomes in transfected and untransfected cells (Figure 38). Cells overexpressing GFP showed a punctuated genome labeling within the nucleus at 3 h pi like neighboring untransfected cells (Figure 38 a, circled cell) but some genomes were also found in the cytosol. In cells overexpressing UL25GFP, GFPUL25 or UL25 the amount of genomes in the nuclei (asterisks) was reduced compared to untransfected cells and genomes had accumulated in the cytosol and in the nuclear peripherie (Figure 38 b, c, d).

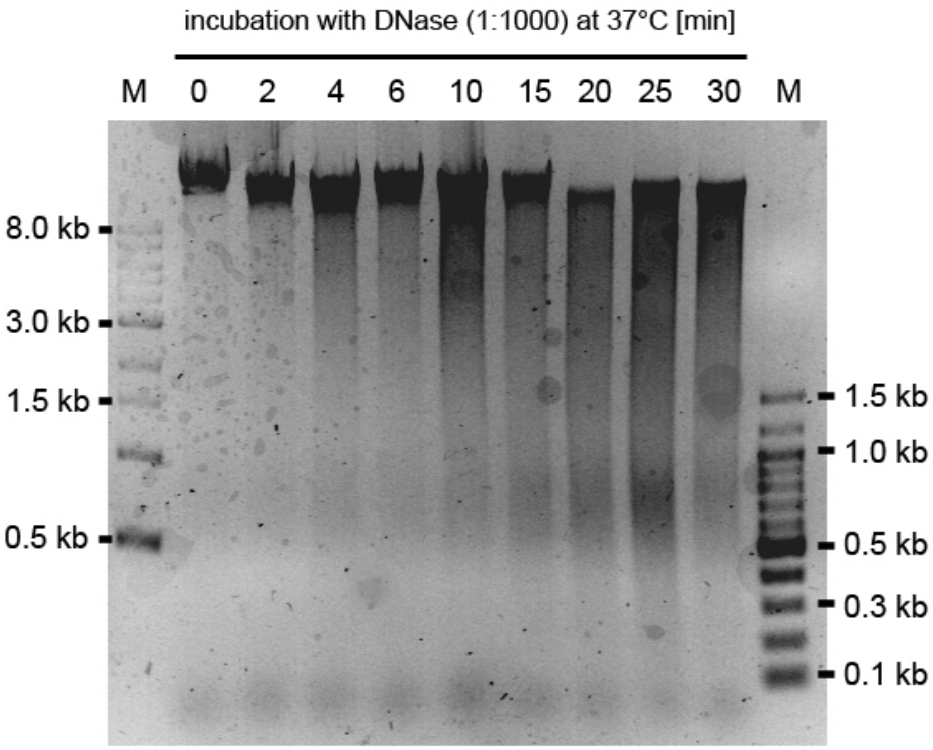

Figure 32: Optimizing the incubation time for the partial DNase digest to get the appropriate DNA fragments for the DNA-probe. 8 µg/lane HSV1(F)-DNA were digested with DNase (1 µu/µl) for the indicated time at 37°C to optimize the digestion time in order to get a DNA smear around 0.5 kb. After digesting the viral DNA for 25 min, a smear of bands around 0.5 to 0.8 kb appeared. The big band of undigested viral DNA above 8 kb indicated that there was still a lot of undigested DNA. Prolonging the incubation time to more than 25 min resulted in a loss of the 0.5 to 0.8 kb DNA bands; therefore the concentration of DNase in the reaction needed to be increased to digest more viral DNA in the time of 25 min.

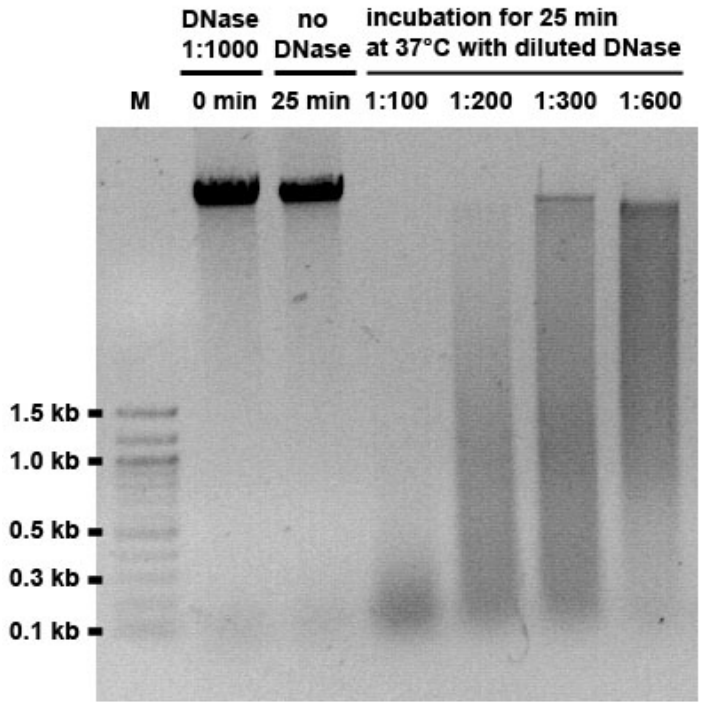

Figure 33: Optimizing the DNase dilution of the partial DNase digest to get the appropriate DNA fragments for the DNA-probe. 8 µg/lane HSV1(F)-DNA were digested with DNase at a diliution from 1:100 to 1:600 for 25 min at 37°C to optimize the amount of the DNA smear around 0.5 kb. After digesting the viral DNA for 25 min a smear of bands around 0.5 to 1.5 kb appeared at a DNase concentration of 1:300 to 1:600. Therefore the optimal DNase concentration was obtained by a dilution of 1:500 (2 µu/µl).

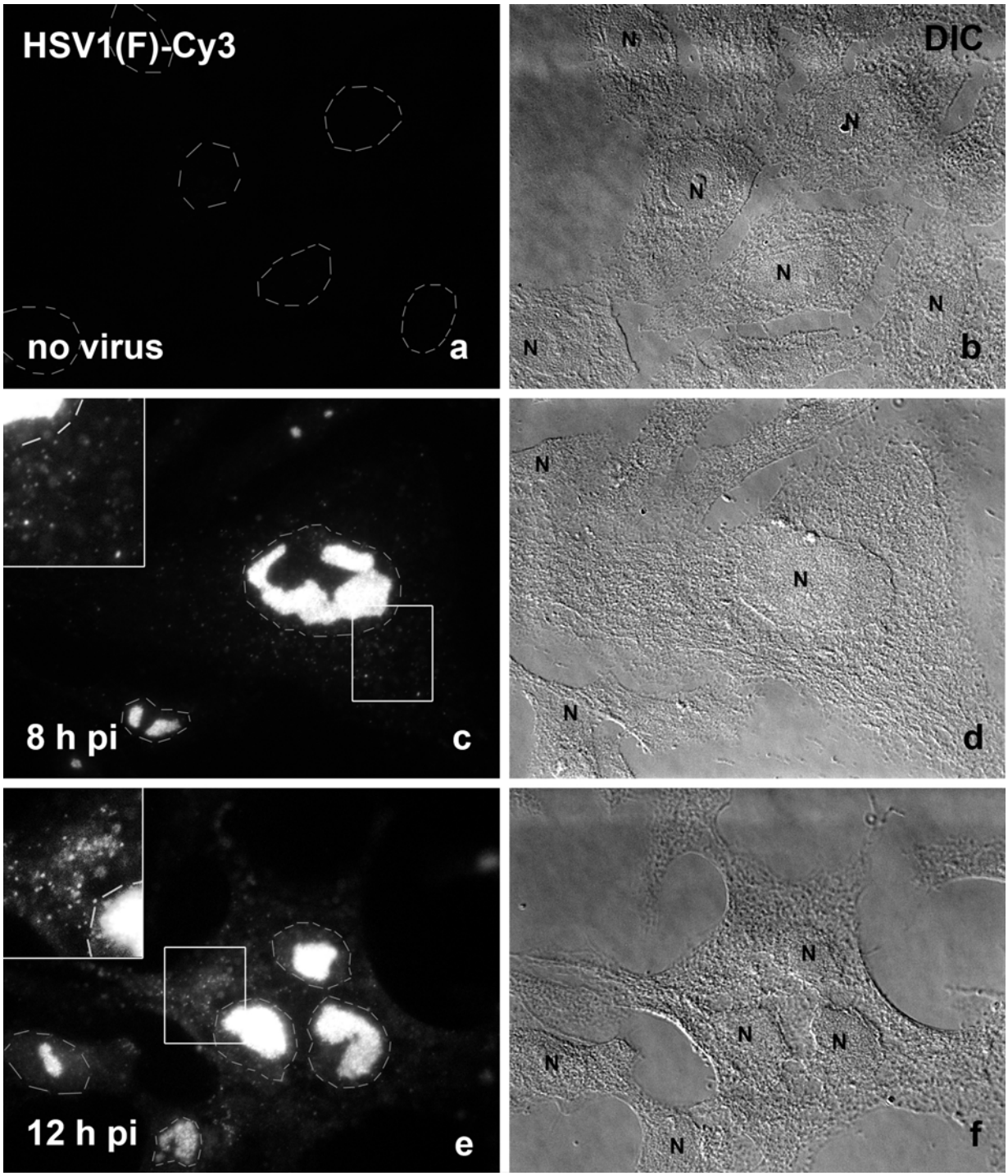

Figure 34: *In situ* hybridization of virus infected cells showed that the HSV1(F)-Cy3 probe recognized viral genomes specifically. Uninfected cells (a, b) showed no Cy3 labeling in the nuclei (N, indicated with dashed line). Cells infected for 8 h showed replication compartments in the nuclei that were labeled by the HSV1(F)-Cy3 probe (c, d) and egressing particles (inset). 12 h pi, the replication compartments became more prominent and even egressing viral particles were detected by *in situ* hybridization as dotted particles in the cytoplasm of the infected cells (e, f, inset). Vero cells were infected with HSV1(17˙) with an MOI of 10 PFU/cell for 8 or 12 hours, fixed with 95% ethanol and 5% acetic acid at -20°C. Cells were prehybridized for 30 min at 37°C in hybridization buffer in a humidified hybridization chamber. The probe was diluted 1:10 in hybridization buffer and incubated at 95°C for 4 min, followed by over night incubation at 37°C in a humidified chamber. After several washing steps, cells were embedded for microscopy.

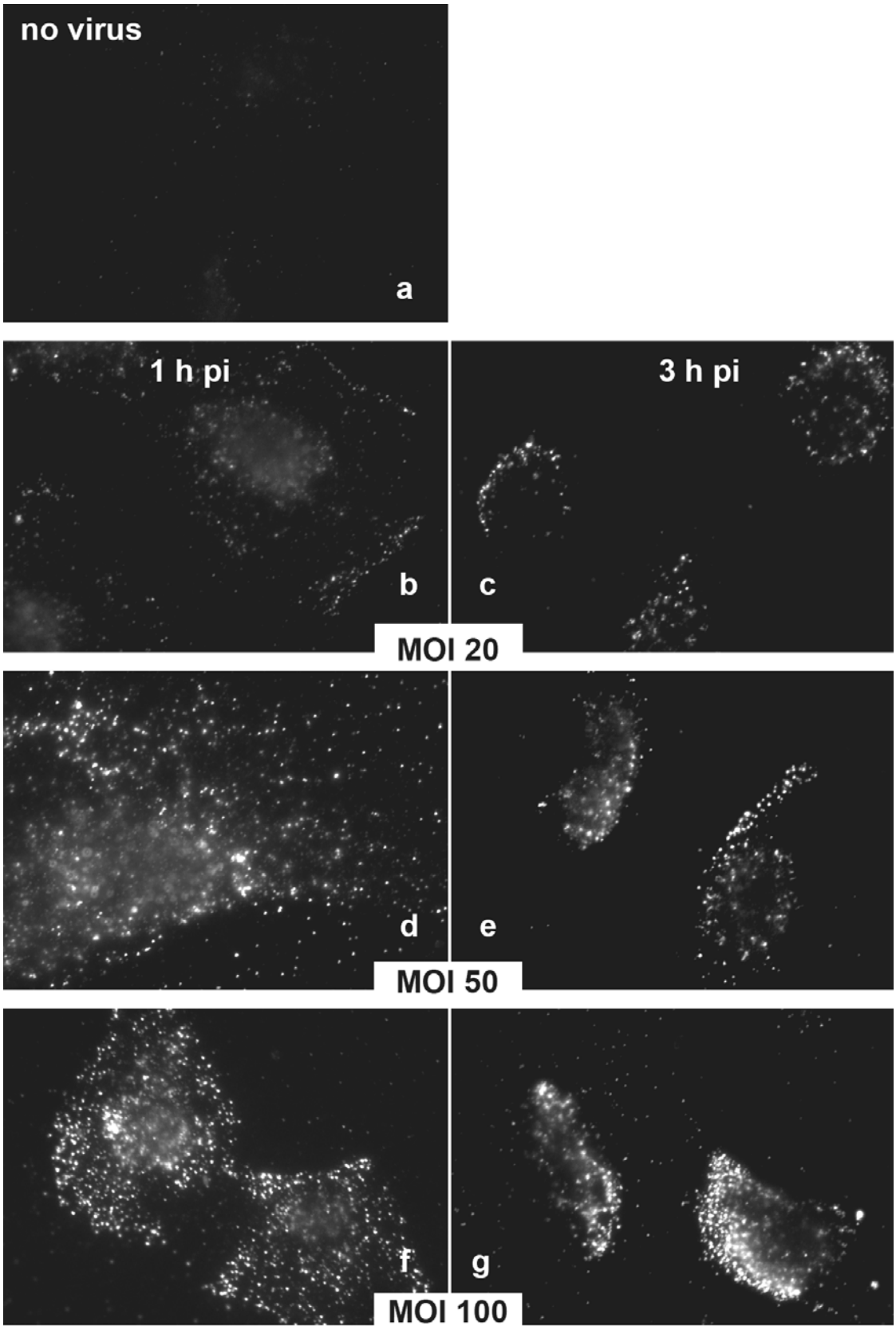

Figure 35: Incoming viral genomes were detected by *in situ* hybridization with the HSV1(F)-Cy3 probe. Cells infected with 20 PFU/cell showed dotted signal throughout the whole cell (b) that accumulated at the nuclear envelope at 3 h pi (c). Increasing the MOI to 50 PFU/cell (d, e) or to 100 PFU/cell (f, g) resulted in an increased labeling of incoming viral genomes. Therefore the particles labeled by the HSV1(F)-Cy3 probe most likely represented incoming viral capsids. Uninfected cells showed very little dotted background labeling derived from the probe (a). Vero cells were infected with HSV1(F) with an MOI of 20, 50 or 100 PFU/cell for 1 or 3 hours, fixed with 95% ethanol and 5% acetic acid at -20°C. Cells were prehybridized for 30 min at 37°C in hybridization buffer in a humidified hybridization chamber. The probe was diluted 1:10 in hybridization buffer and incubated at 95°C for 4 min, followed by over night incubation at 37°C in a humidified chamber. After several washing steps, cells were embedded for microscopy.

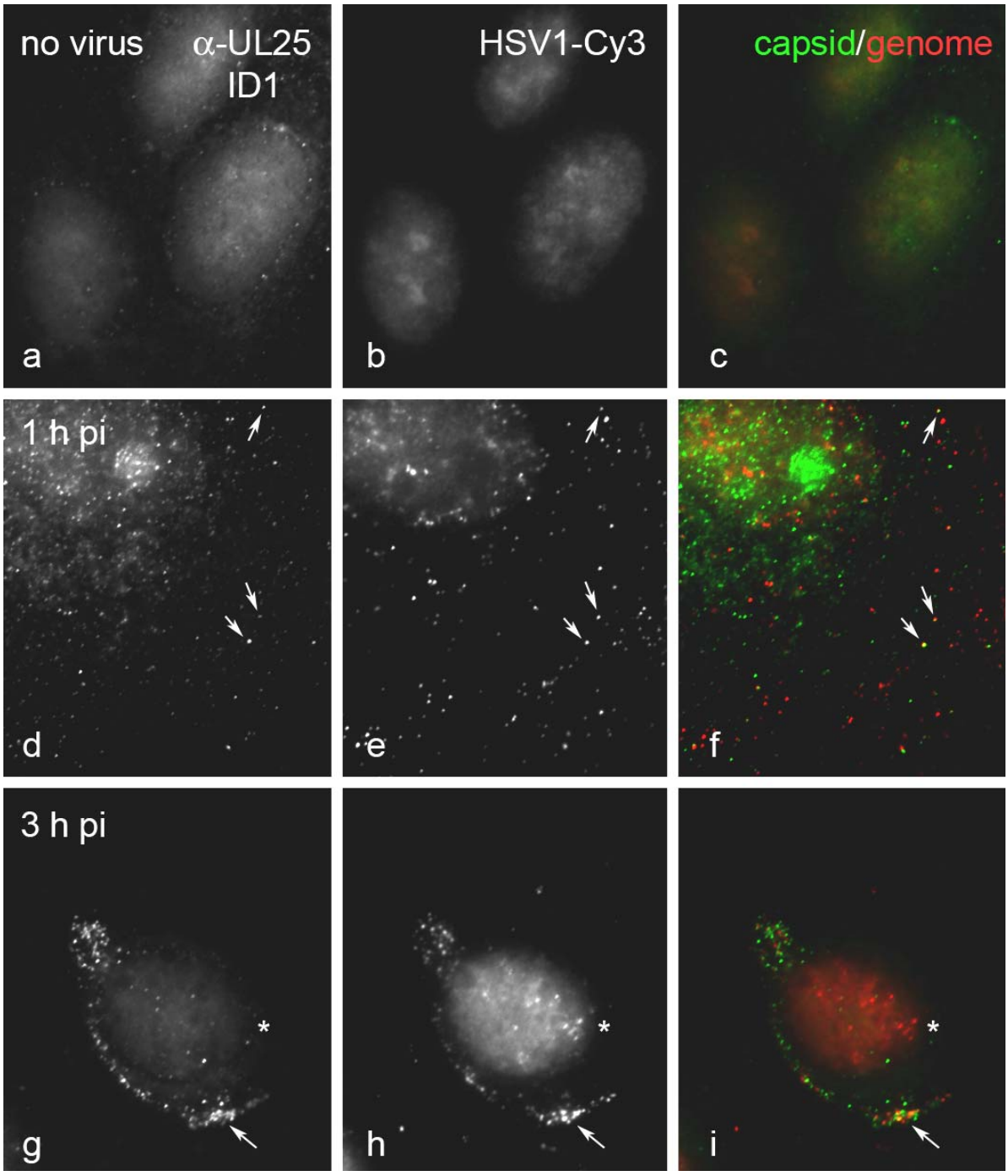

Figure 36: Some incoming viral particles colocalized with viral genomes during virus entry. Uninfected cells showed little background labeling by the UL25-antibody and by the Cy3-probe (a, b). At 1 h pi, viral capsids labeled for UL25 (d) and viral genomes (e) were distributed throughout the cell and some genomes colocalized with capsids (f, arrows). Viral genomes accumulated at the nuclear envelope 3 h pi (g, h), but less capsids labeled for UL25 were located at the nucleus. Some capsids with their genomes were still located in the cytosol (i, arrow). Capsids at the nuclear envelope didn´t show a genome labeling and genomes at the nucleus didn´t have a capsid labeling (i, asterisk). At the nucleus, more DNA signal was visible, suggesting that uncoating might have occured. Vero cells were infected with HSV1(F) with an MOI of 70 PFU/cell for 1 or 3 hours, fixed with 95% ethanol and 5% acetic acid at -20°C. Cells were prehybridized for 30 min at 37°C in hybridization buffer in a humidified hybridization chamber. The probe was diluted 1:10 in hybridization buffer and heated at 95°C for 4 min, followed by over night incubation at 37°C in a humidified chamber. Then cells were labeled for UL25 with the rabbit polyclonal antibody UL25-ID1. After several washing steps, cells were embedded for microscopy.

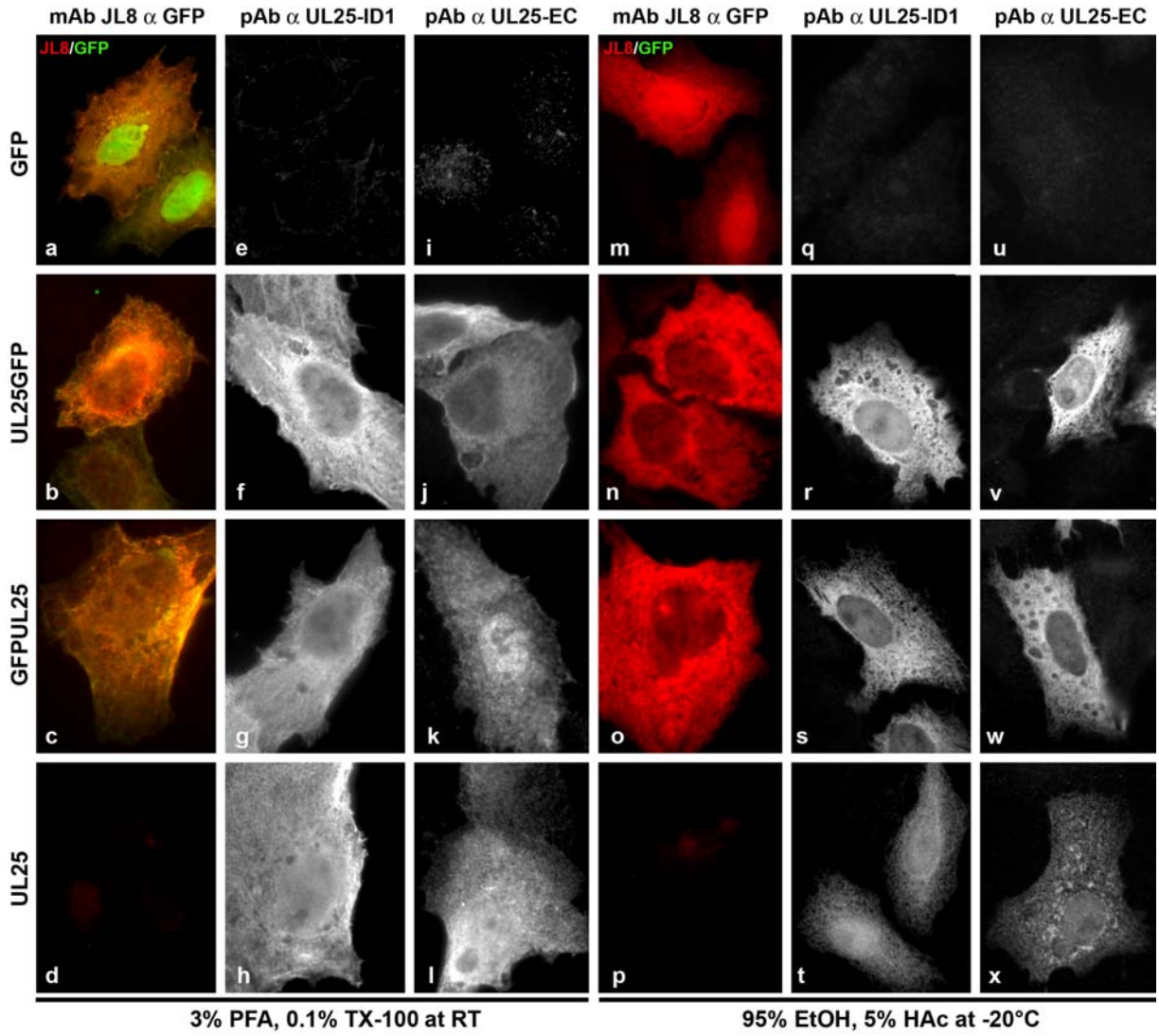

Figure 37: UL25 overexpressing cells were recognized with specific antibodies after the fixation needed for *in situ* hybridization. GFP, UL25GFP, GFPUL25 overexpressing cells could be visualized by GFP fluorescence and labeling with an antibody against GFP (a, b, c) after PFA fixation and TX-100 permeabilization. The UL25-ID1 (f, g, h) or the UL25-EC antibody (j, k, l) recognized cells overexpressing UL25GFP, GFPUL25 or UL25 after PFA fixation and TX-100 permeabilization. When cells were fixed with ethanol-acetic acid, GFP fluorescence was lost but GFP, UL25GFP or GFPUL25 could be visualized with the GFP antibody (m, n, o). The antibodies UL25-ID1 or UL25-EC were able to recognize overexpressed UL25GFP, GFPUL25 or UL25 (r, s, t, v, w, x) but did not crossreact with GFP (q, u) after ethanol-acetic acid fixation. Vero cells overexpressing GFP, UL25GFP, GFPUL25 or UL25 were either fixed with 3% PFA and permeabilzed with 0.1% TX-100 or with 95% ethanol and 5% acetic acid at -20°C. Cells were prehybridized for 30 min at 37°C in hybridization buffer in a humidified hybridization chamber. The probe was diluted 1:10 in hybridization buffer and heated at 95°C for 4 min, followed by over night incubation at 37°C in a humidified chamber. Then cells were labeled for GFP or UL25 with the indicated antibodies. After several washing steps, cells were embedded for microscopy.

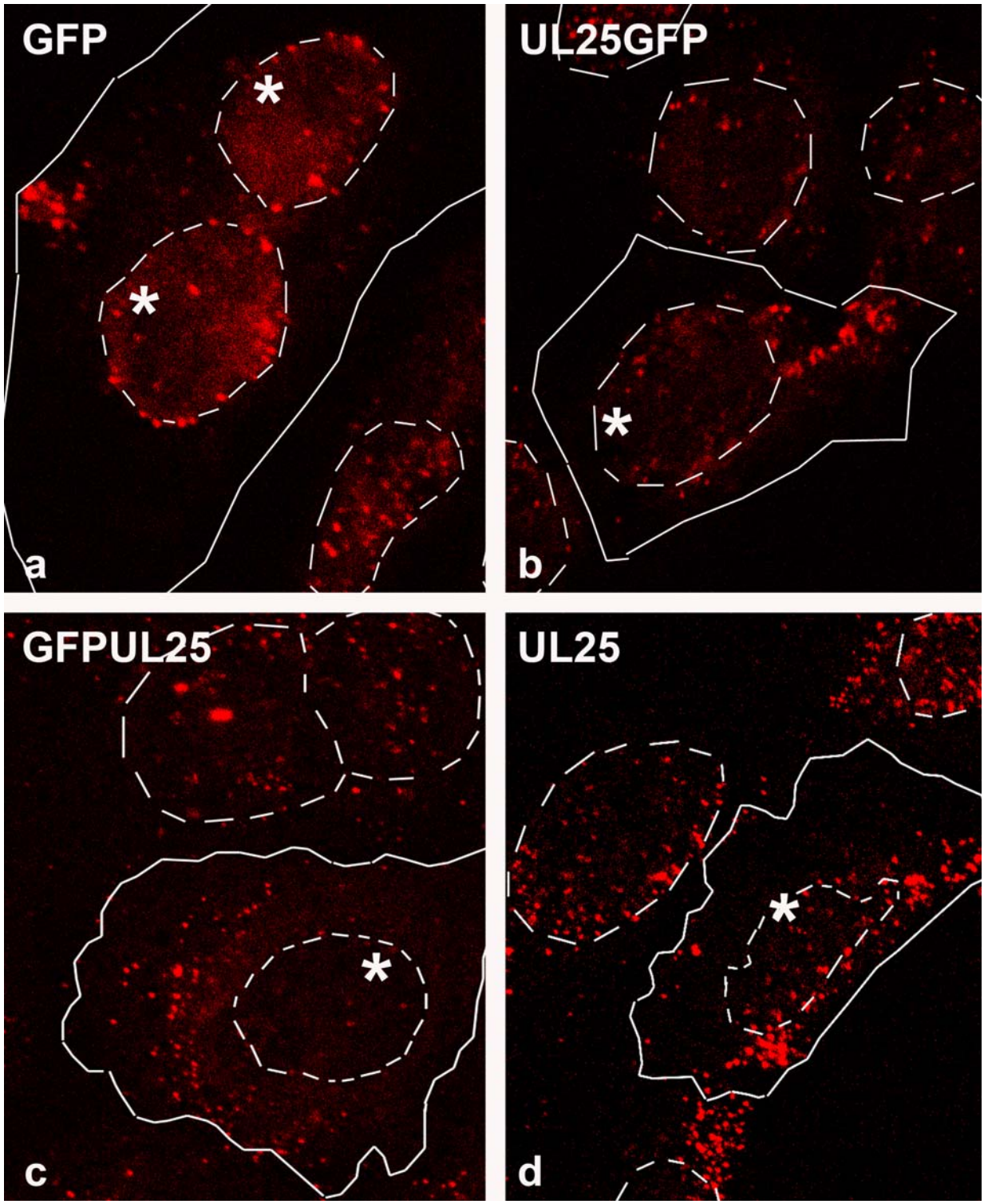

Figure 38: Cells overexpressing UL25 accumulated less genomes in the infected nuclei. Incoming viral genomes were detected with the HSV1(F)-Cy3-DNA probe by *in situ* hybridization in cells with excess GFP (a), UL25GFP (b), GFPUL25 (c) or UL25 (d) indicated by solid lines. Nuclei are labeled with dashed lines. Cells overexpressing GFP and untransfected cells (a-d) showed a punctuated genome labeling within the nucleus at 3 h pi (a). In cells overexpressing UL25GFP, GFPUL25 or UL25, the amount of genomes in the nuclei (asterisks) were reduced compared to GFP-transfected (a) and untransfected cells (a-d). Cells were infected with HSV1(F) at an MOI of 70 PFU/cell and after 3 h pi fixed with ethanol-acetic acid at -20°C. *In situ* hybridization of viral genomes was performed with a Cy3-labeled HSV1(F)-DNA probe followed by an immunolabeling with antibodies against UL25 (pAb UL25-ID1, circled cell) or GFP (mAB JL-8, circled cell). Confocal sections of about 700 nm were generated and slices through the nuclei of infected cells were analysed for the amount of Cy3-labeled HSV1(F) genomes.

4 Discussion

For this thesis, the minor capsid protein UL25 of HSV1 was analyzed during herpesvirus assembly, cell entry and genome uncoating at the nuclear pore. While the functions of UL25 during HSV1 assembly are revealed more and more, possible functions of UL25 during virus entry have only been suggested by the phenotypes of two UL25-ts HSV1 mutants (Addison et al. 1984; cf. chapter 1.4).

Based on overexpression studies I showed that excess UL25 reduced immediate early HSV1 gene expression after virus entry. Since overexpressed HSV1-UL25 did not interfere nuclear targeting of incoming viral capsids (Rode 2003, Diploma thesis), a step between nuclear capsid targeting and synthesis of viral proteins must have been affected (Figure 39).

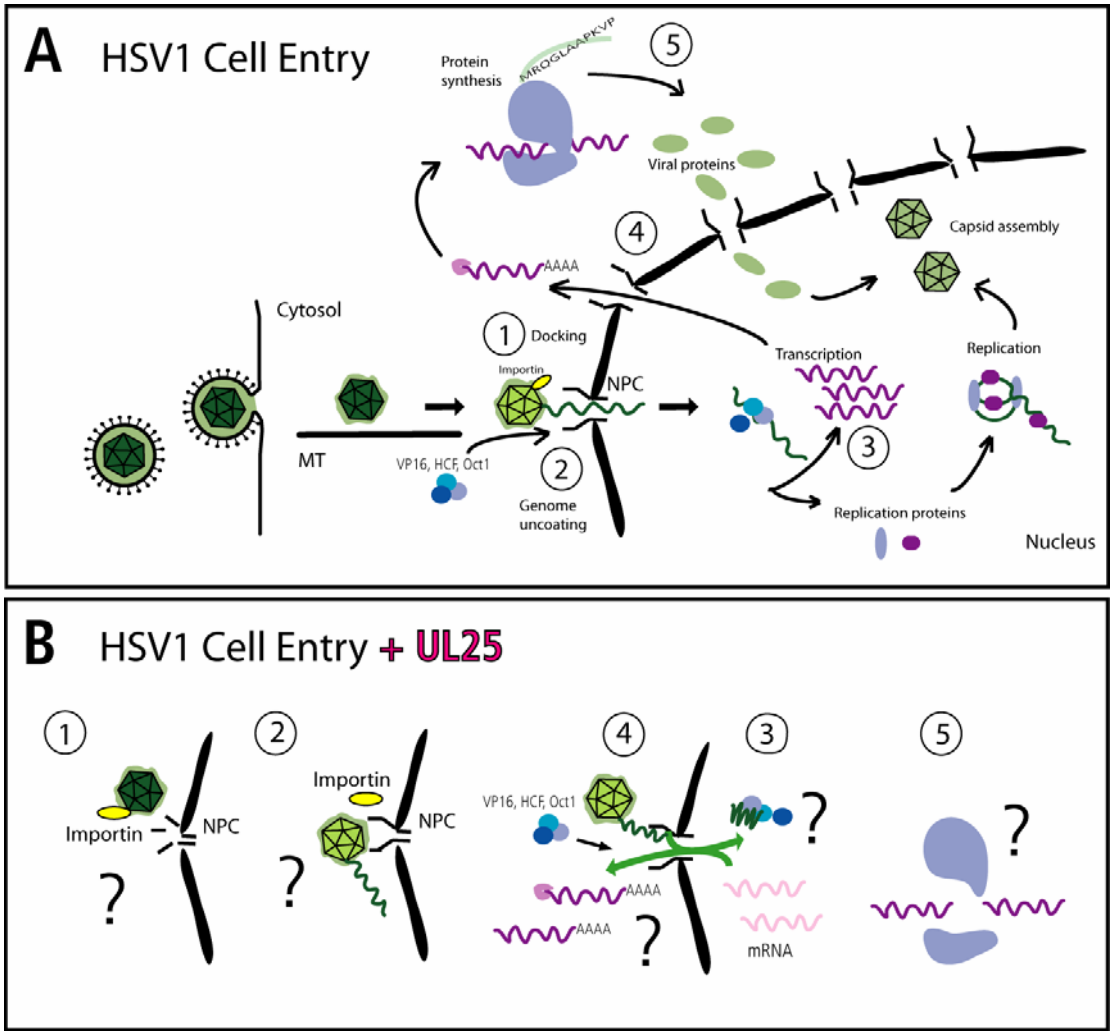

Figure 39: How does overexpressed UL25 prevent viral gene expression? (A) From reaching the nucleus (1) to protein synthesis (5) for subsequent capsid assembly, many steps during viral infection might be impaired by excess UL25 **(B)**. Docking (1) or uncoating at the NPC might be impaired (2), because UL25 might interfere with NPC components or cellular factors involved in the docking process. Viral DNA might not enter the nucleoplasm, because the nuclear pore is blocked with UL25 (2). Alternatively, UL25 may inhibit the RNA polymerase (3), thus preventing transcription and no mRNA could be produced. Further transcription might be working, but mRNA export (4) through the NPC might be blocked. Finally, all previous steps take place, but UL25 could then inhibit the ribosomes (5), which would result in an inhibition of the protein synthesis. In all five scenarios, early viral gene expression would be reduced (Scheme modified from Baines and Weller 2005; Ojala et al. 2000; Rajcani et al. 2004; Roizman and Knipe 2001; Sandri-Goldin 2007; Sodeik et al. 1997).

The first possibly impaired step is the docking of the capsid to the NPC for subsequent uncoating. UL25 might interfere with transport factors like importin β or NPC components involved in the docking process (Figure 39 b; 1). Capsid uncoating at the nuclear pore might be unaffected, but the viral DNA may not reach the nucleoplasm, because the excess UL25 may prevent a certain trigger required for genome release or the nuclear pore could be blocked with UL25 (Figure 39 b; 2). Alternatively, UL25 could inhibit the RNA polymerase and thus prevent mRNA synthesis (Figure 39 b; 3). Furthermore, import of transcription factors or mRNA export through the NPC might be blocked (Figure 39 b; 4). Finally, UL25 could inhibit protein synthesis at the ribosomes (Figure 39 b; 5). In all scenarios, immediate early viral gene expression would be reduced.

In this study, I addressed the function of UL25 during this early phase of HSV1 infection. I showed that the reduction in HSV1 immediate early viral gene expression was significant (Figure 18) and not the result of a mislocalization of importin β (Figure 19), disturbed NPCs (Figure 20), an impaired transcription (Figure 21 to Figure 26, Figure 28) or protein synthesis in general (Figure 27). Since early gene expression of adenovirus and vaccinia virus was not impaired either, the effect was specific for HSV1.

Moreover, reduced gene expression in the presence of excess UL25 was not caused by a defective uncoating of the capsid at the NPC (Figure 30, Figure 31), but *in situ* hybridization data showed that fewer genomes were localized in the nuclei of UL25 expressing cells (Figure 38). Thus, excess UL25 interfered with nuclear import of the viral genome through the NPC. This suggests that capsid-associated UL25 might be involved in translocation of the viral genome into the nucleoplasm, or that some UL25 has to be extracted from the capsids for proper nuclear genome import, and that excess UL25 might impede these functions. Alternatively, overexpressed UL25 may bind herpesviral genomes after release from the capsid, and thereby prevent their translocation into the nucleoplasm.

In summary, my data suggest that the incoming capsid-associated UL25 has to engage in specific host interactions, which are a prerequisite for proper HSV1 genome targeting to the nucleus, or that excess UL25 blocks the function of a host factor which is required for proper HSV1 nuclear genome import.

4.1 Mature Capsids Contained UL25 During Assembly, Egress and Entry

During capsid assembly, the structural protein UL25 retains the packaged viral genome inside the capsid, either by sealing the UL6 portal complex after DNA packaging (Ali et al. 1996; McNab et al. 1998; Ogasawara et al. 2001), and/or by reinforcing the capsid structure possibly as a heterodimer in concert with UL17 or by adding UL25 to the capsids as soon as the DNA packaging has been completed but before the capsids leave the nucleus by budding at the inner nuclear membrane (Klupp et al. 2006; Newcomb et al. 2006; Stow 2001; Thurlow et al. 2005; Trus et al. 2007.

One prediction derived from these hypotheses is, that UL25 should preferentially colocalize with nuclear C-capsids but not with A or B-capsids. Therefore, I analyzed the UL25 expression kinetics as well as the potential colocalization of newly synthesized UL25 with nuclear and cytoplasmic capsids. Consistent with their classification as leaky-late or late genes, VP5 was first detected at 4 h pi, and UL6 as well as UL25 at 6 h pi (Roizman and Campadelli Fiume 2007).

Newly synthesized nuclear and cytoplasmic capsids were labeled by VP5 antibody mAb 5C10 (Döhner et al. 2006; Newcomb et al. 1996; Trus et al. 1992) that recognizes VP5 on mature hexons. The antibodies VP5-LP12 as well as VP5-H1.4 apparently rather labeled free VP5 than capsid-associated VP5, since they revealed a diffuse nuclear signal with few dots, and not cytoplasmic capsids (Figure 12, Figure 14, Figure 15). Thus, these three α-VP5 antibodies recognized different epitopes, which had either a different subcellular localization, or were accessible to a different degree. The diffuse labelling of LP12 and H1.4 most likely represented free VP5, either single molecules or capsomeres, which had not yet been incorporated into capsids. The fact that no capsids in the cytoplasm were recognized by VP5-LP12 and VP5-H1.4 may also indicate that their epitopes were lost during capsid maturation, suggesting that VP5-LP12 and VP5-H1.4 have a stronger affinity to immature capsids (Döhner et al. 2006). In contrast, capsids in the nucleus and in the cytoplasm were labeled with VP5-5C10; therefore those capsids represent mature capsids. The localization of UL25 during assembly and egress was analyzed with α-UL25-ID1 (Koslowski et al. 1997, Figure 13) or α-UL25-EC (Ali et al. 1996, Figure 13). Both antibodies labeled UL25 during assembly and egress in a punctuate pattern most likely representing capsids, whereas soluble UL25 had either not been fixed or was not recognized by these antibodies. Thus the UL25 pattern was more comparable to the VP5-5C10 than to the VP5-LP12 or VP5-H1.4 labeling (Figure 14, Figure 15).

Taken together, these data support previous biochemical studies where UL25 associates in the nucleus with mature capsids and then may provide a signal for nuclear egress. Most of the UL25 colocalized with capsids labeled with an antibody that regcognizes VP5 hexon epitopes on mature capsids and not with VP5-LP12 or VP5-H1.4.

Next I analyzed the subcellular localization of UL25 during HSV1 entry. Many capsid associated proteins and tegument proteins (e.g. VP11/12, VP22) dissociate from incoming capsids during nuclear targeting, while others remain associated until arrival at the nuclear pores (Granzow et al. 2005; Luxton et al. 2005; Sodeik et al. 1997). Incoming capsids were labeled with the VP5-5C10 and the UL25-ID1 antibody. Both proteins colocalized until arrival at the nucleus. Moreover, immuno blot analysis showed that UL25 and VP5 were not degraded during HSV1-entry (Figure 16). Thus, UL25 remained capsid-associated until arrival at the nucleus, and therefore could stabilize the capsid until docking at the nuclear pore. However, then the capsid must be destabilized and release the HSV1 genome and this may require that some UL25 may be extracted from the capsid at the nuclear pore.

4.2 Reduction of HSV1 Gene Expression by Excess UL25

Since PrV-UL25 had been suggested to be a microtubule motor receptor (Kaelin et al. 2000), cells overexpressing HSV1-UL25 were analyzed with regard to their efficiency of capsid transport to the nucleus. Overexpressed UL25 might bind to microtubule motors or microtubules directly and thereby compete with capsid associated UL25 on incoming capsids during nuclear targeting. However, my previous experiments showed that overexpressed HSV1-UL25 did not colocalize with microtubules and that nuclear targeting of incoming viral capsids was not impaired by excess HSV1-UL25 (Rode 2003, Diploma thesis). Moreover, a tight localization of UL25 with microtubules might rather obstruct than stimulate transport.

Thus, it seems unlikely that HSV1-UL25 is involved in nuclear targeting of incoming capsids. To test whether overexpressed UL25 had any effect on later steps of the HSV1 life cycle, I analyzed the expression of immediate early HSV1 proteins (cf. chapter 1.3.6). UL25 overexpressing cells synthesized significantly less of the immediate early HSV1 proteins ICP0 (Figure 17, Figure 18), ICP4, ICP8, ICP22, or ICP27 (not shown). Since nuclear targeting of HSV1 capsids in UL25 overexpressing cells was not affected, further steps after the transport to the nucleus such as viral DNA uncoating at the NPC, viral DNA import into the nucleus, viral transcription, mRNA export into the cytosol or protein synthesis must have been impaired (cf. Figure 39 b).

4.3 No Effect on Importin β and Nuclear Pores

HSV1 capsids need the nuclear transport factor importin β to bind to the nuclear pore complex. The direct interaction partners of the capsid have not been identified, but the nucleoporins Nup358/RanBP2 or Nup214/CAN which are components of the cytoplasmic filaments emanating from the nuclear pores (Ojala et al. 2000; Pante and Aebi 1993) are likely candidates. Since excess UL25 might interfere with the specific docking at the nuclear pore, the subcellular localization of importin β (Figure 19), and the nuclear pore architecture were analyzed (Figure 20). The localization of importin β was not changed in the presence of overexpressed GFP or UL25GFP (Figure 19). UL25 overexpressing cells labeled with the UL25-EC antibody together with the importin β antibody showed less signal for importin β. It seemed not to be a specific inhibition of importin β but only enriched background labeling by the UL25 antibody since also untransfected cells displayed less importin β signal.

The nuclear rim labeling obtained with the mAb414 antibody that recognizes nucleoporins with FG-domains (Aris and Blobel 1989; Davis and Blobel 1987) was very similar in untransfected, GFP, UL25GFP or UL25 transfected cells (Figure 20). Some irregularities within the NPC labeling were detected in all cell populations, and most likely represent a heterogenous amount of NPCs in the nuclear membrane during the different stages in the cell cycle (Maeshima et al. 2006). Cells stably expressing the inner nuclear membrane protein lamin B receptor coupled to a yellow fluorescent protein (Lippincott-Schwartz et al. 1999) did also not show any changes in the localization of the lamin B receptor in the presence of UL25 or GFP-tagged UL25 (data not shown). Thus, the reduced HSV1-immediate early gene expression in the presence of excess UL25 seemed not to be due to a major mislocalization of importin β or a disturbed nuclear pore network.

4.4 Transcription in the Presence of Overexpressed UL25

Upon virus entry, the tegument protein VP16 in a complex with the cellular proteins Oct-1 and HCF is transported into the nucleus and facilitates the induction of HSV1 transcription (Narayanan et al. 2005; Rajcani et al. 2004). A reduction in immediate early viral gene expression could have been the result of mislocalized VP16 in UL25 overexpressing, infected cells. Therefore the degree of nuclear accumulation of VP16 was quantified. VP16 entered the nuclei of GFPUL25 overexpressing cells as efficiently as in untransfected cells.

The translocation of VP16 into the nucleus was not impaired, and VP16 may function as a transcriptional activator irrespectively of overexpressend GFPUL25 (Figure 22, Figure 23). Moreover, the localization of cellular transcription factors was analyzed in the presence of excess UL25 since the transcription factors NFκB and its inhibitor IκB, as well as STAT and NFAT are activated or reduced in HSV1 infection (Goodkin et al. 2003; Scott et al. 2001; Yokota et al. 2001). None of these transcription factors or the inhibitor IκB showed an altered subcellular localization in UL25GFP expressing cells (Figure 23). Thus, it seems unlikely that the function of those factors was impaired by overexpressed UL25.

Additionally, the transactivation of transcription through promoters or responsive elements was analyzed by luciferase based reporter assays. Although high amounts of UL25 repressed luciferase activity driven by the cylin E promoter, EBV-c promoter or a serum responsive element, the repression was not specific for a particular promoter element because the intrinsic luciferase activity of the corresponding luciferase vectors without promoter elements was repressed to a similar degree (Figure 24 to Figure 26).

These results indicated that, in contrast to experiments conducted at 18 to 24 h after transfection of UL25-expressing plasmids, the prolonged overexpression of 30 to 35 h decreased gene expression in general. One could argue that the reduction in HSV1 immediate early gene expression was due to unspecific cytotoxic effects of overexpressed UL25, but later experiments using adenovirus or vaccinia virus showed that transcription and protein expression were not affected per se at UL25 expression levels which repressed HSV1 immediate early gene expression.

UL25 is a minor bona fide capsid protein and remained associated with incoming capsids until arrival at the NPC. It seems unlikely that the few molecules of incoming UL25 would then be released to transactivate or repress transcription. There is no data in the literature suggesting any regulatory functions of UL25 in HSV1 transcription. However, at present a potentially modulatory function cannot be ruled out. UL25 may act as a transcriptional repressor to promote the next step in the infection cycle, the capsid assembly. But to test this hypothesis, the luciferase assays need to be adjusted to shorter expression times, and higher sample numbers for statistical analysis.

4.5 Vaccinia Virus Late, but not Early Gene Expression was Impaired by Excess UL25

Poxviruses, e.g. vaccinia virus (VV), are DNA viruses that exclusively replicate in the cytosol of infected cells (Schramm and Locker 2005). I used VV early gene expression, which is independent of the nucleus to test whether UL25 influenced protein synthesis in general, and thereby reduced HSV1 early gene expression. GFP (Figure 27 a, c) or UL25GFP (Figure 27 e, g) overexpressing Hela cells were infected with VV (Jensen et al. 1996; Schepis et al. 2006), and the expression of the early gene p35/H5R and the late gene p16/A14L were analyzed.

VV replication compartments contained similar amounts of p35, irrespective of the protein ectopically expressed (Figure 27). The expression of the late protein p16 was slightly reduced in UL25GFP overexpressing cells compared to GFP expressing or untransfected cells (Figure 27). During VV assembly, crescents of ER derived cisternae mature into spherical immature viruses (IV) into which the viral DNA is packaged (Sodeik and Krijnse-Locker 2002). The protein A14/p16 is located at the ER-Golgi compartment in perinuclear areas during assembly of VV and is essential for further maturation from the IV to the first infectious form of VV, the intracellular mature virus (IMV, Rodriguez et al. 1998). Overexpressed UL25 might slow down the recruitment of cellular membranes to virus factories at juxtanuclear positions.

Herpesvirus transcription and replication take place in the nucleus. Efficient cellular DNA transcription and DNA replication not only require proteins for chromatin reorganization or DNA polymerization but also an intact nuclear membrane with functional NPCs and a nuclear lamina (Gant and Wilson 1997). The NE is physically connected to the rough endoplasmic reticulum (ER). During nuclear envelope assembly and disassembly, proteins are sequestered into the NE because of their affinity to chromatin and lamins, whereas ER proteins reside in the ER (Ellenberg et al. 1997).

VV replication occurs in ER-enclosed viral factories suggesting an establishment of so called ER-derived mini nuclei that lack components of the nuclear envelope. The mini nuclei disappear upon ER dissociation later in infection to allow further maturation of the replicated genomes (Tolonen et al. 2001). This is the point when UL25 could interfere with further VV maturation. UL25 might associate with the VV DNA due to its DNA binding ability (Ogasawara et al. 2001), and thereby prevent the formation of the IMV that was visualized here by the protein A14L/p16. Since both genomes are very GC rich (poxviruses: ~63%, herpesviruses: ~68%; Roizman and Knipe 2001; Senkevich et al. 1996), UL25 might recognize VV as well as HSV1 DNA. That excess UL25 reduced late VV protein synthesis was an unexpected and interesting finding.

However, early VV gene expression was not affected by UL25, indicating that excess UL25 did not inhibit protein synthesis in general.

4.6 UL25 did not Reduce Adenovirus Mediated Gene Expression

Like herpesvirus capsids, adenovirus capsids are targeted to the nucleus where they release their viral genomes through the nuclear pores into the nucleoplasm for viral DNA transcription and replication (Greber and Fassati 2003).

To test whether the excess UL25 decreased adenoviral early gene expression, we infected GFP or UL25GFP overexpressing Hela cells with adenovirus. The adenovirus mediated transgene expression was not reduced irrespective of the overexpressed protein (Figure 28). This indicated that the cell entry of adenovirus, uncoating at the NPC, genome release, nuclear transcription and protein synthesis at the ribosomes were functional in UL25 overexpressing cells. Therefore I concluded that overexpressed UL25 rather influences herpesvirus infection than infection with other DNA viruses which replicate in the nucleus.

4.7 HSV1 Genome Uncoating in the Presence of Excess UL25

The correct nuclear import of the viral genome is mandatory for infection. An impaired DNA release from the capsid at the NPC would result in reduced early viral gene expression in UL25 overexpressing cells. In electron microscopy images, DNA containing capsids can be easily distinguished from empty capsids by their electron-dense core (Sodeik et al. 1997). To include only cells that express UL25 for electron microscopy, I established a protocol for FACS based enrichment of transfected cells prior to processing for electron microscopy (Figure 29).

Ultrathin sections were analyzed for the amount of capsids localized at the nuclear membrane, at the NPC or in the cytosol (Figure 30). In GFP and GFPUL25 overexpressing cells, most capsids were found at the NPC and appeared empty, whereas the cytosolic capsids still contained their genome (Figure 31). In UL25GFP overexpressing cells, the total number of empty capsids at the nuclear envelope was reduced, and instead the cytosol contained more filled capsids (Figure 31 a). This was the first experimental difference between cells overexpressing GFPUL25 or UL25GFP. In all other experiments, GFPUL25 and UL25GFP showed similar phenotypes (cf. Figure 18, Figure 38). According to the electron microscopy data, the nuclear targeting efficiency of capsids was reduced in UL25GFP overexpressing cells. However, when the nuclear targeting of capsids was analyzed by immunofluorescence microscopy, capsids reached the nucleus as efficiently in GFP or UL25GFP overexpressing cells (Figure 9).

A major difference between those two experiments was the MOI used for HSV1 infection. For immunofluorescence microscopy, cells were infected with an MOI of 70 to 100, whereas for the electron microscopy studies, the cells were infected at an MOI of 500 PFU/cell. Even with this high MOI, the number of capsids present in one image was only about 1 to 5 capsids per image; therefore the quantification required the analysis of many sections. Another discrepancy between those two experiments was the treatment of the cells after the infection. For immunofluorescence microscopy, adherent cells were washed, fixed, permeabilized and subsequently labeled with antibodies.

For electron microscopy analysis, the cells were first trypsinized, lightly fixed in suspension, sorted by FACS, fixed again, pelleted several times by centrifugation and then processed for electron microscopy. Thus, cells processed for electron microscopy underwent more handling steps than cells for immunofluorescence microscopy.

Proteins with C-terminal fused tags often display properties and localizations of the untagged protein, whereas N-terminal fusion proteins are often non-functional (Palmer and Freeman 2004). This may explain why GFP and GFPUL25 show similar results in the electron microscopy quantification (Figure 31 a). GFPUL25 might not compete as well as the untagged UL25 or UL25GFP for potential viral or cellular interaction partners. However, this hypothesis was not supported by the immunofluorescence microscopy data, where all three GFPUL25, UL25GFP and UL25 reduced immediate early gene expression to a similar extent (Figure 18). To analyze genome uncoating at the NPC, also the number of empty capsids located either at the nuclear membrane or at the NPC was determined (Figure 31 b). All populations had a similar number of capsids.

The uncoating of the genomes was not impaired by excess UL25. So, if the HSV1 genome was uncoated, why was there less expression of immediate early HSV1 proteins?

4.8 Less Genomes Accumulated in the Nucleoplasm in the Presence of UL25

Electron microscopy of UL25 overexpressing, HSV1 infected cells showed that uncoating at the NPC was not affected. Empty capsids were found at the NPC indicating that genome uncoating took place. However, since immediate early HSV1 gene expression was not blocked completely but rather delayed (Figure 17, Figure 18), less viral genomes might have reached the nucleoplasm. To address whether or not the viral genome had reached the nucleoplasm in UL25 overexpressing cells, I had to establish a protocol which combined viral genome detection by *in situ* hybridization with the detection of the overexpressed protein. The *in situ* probe was synthesized from HSV1(F)-DNA according to Everett & Murray (2005) and specifically recognized newly synthesized (Figure 34) as well as incoming genomes (Figure 35) in the replication compartments and in the cytosol.

Due to the harsh fixation of the cells, GFP was denatured and no longer fluorescent. I tested several antibodies to identify those which detected the overepressed proteins under these conditions (Figure 36). The cytoplasm still contained UL25-positve capsids, but not every capsid colocalized with Cy3-labeled genomes. At the nucleus, there were more genomes detected than capsids. Nevertheless, incoming genomes and UL25 labeled capsids occasionally colocalized. Moreover, both UL25 antibodies and the GFP antibody recognized their epitopes after PFA and *in situ* fixation, therefore the *in situ* hybridization of incoming viral genomes could be combined in UL25 overexpressing cells (Figure 37).

When the genomes were *in situ* hybridized in infected UL25-overexpressing cells, preliminary data revealed that fewer genomes accumulated in the nuclei of UL25 overexpressig cells (Figure 38). These results suggested that genome translocation through the NPC channel was impaired by an excess of UL25.

During adenovirus (Ad) infection, a stepwise disassembly of the Ad capsid by an adenovirus encoded protease occurs (Greber et al. 1996; Greber et al. 1993). Then the Ad capsid interacts with the nuclear pore component CAN/Nup214, a cytoplasmic filament, and the Ad genome is pulled out of the capsid by the host protein histone H1 (Greber et al. 1997; Trotman et al. 2001). Since herpesviruses and adenoviruses both use microtubules and the microtubule motor dynein for nuclear targeting (Mabit et al. 2002; Sodeik et al. 1997), herpesviruses might exploit a similar mechanism for DNA release at the nucleus. Moreover, the phenotype of a temperature-sensitive HSV1 mutant which has mutations in the UL36 open reading frame suggested that the large tegument protein VP1-3 might be involved in genome uncoating at the NPC. At the non-permissive temperature, C-capsids accumulated at the NPC and failed to uncoat their genome (Batterson et al. 1983). Furthermore, it was shown that VP1-3 remained associated with incoming viral capsids during nuclear targeting (Schipke & Sodeik, personal communication). Finally, the C-terminus of VP1-3 interacts with UL25 (Coller 2007). Since overexpressed UL25 reduced immediate early gene expression presumably by disturbing viral genome translocation through the NPC channel, it is conceivable that a putative function of VP1-3 during nuclear import of the viral genome was masked by the overexpressed UL25. In such a scenario, the incoming HSV1 genomes may be released into the cytosol rather than into the nucleoplasm. Alternatively, excess UL25 could interfere with DNA translocation through the nucleus by binding to the viral genome (Ogasawara et al. 2001), and thus blocking interaction sites for cellular factors, such as importins, which may be involved in genome translocation (Figure 40).

Uncoating of herpesvirus genomes exclusively takes place at the NPC of infected cells (Batterson et al. 1983; Ojala et al. 2000, Sodeik et al. 1997) and was not disturbed by overexpressed UL25 (Figure 31). Thus, a step between uncoating at the NPC and genome translocation through the NPC channel might have been blocked by the excess UL25. In turn that would mean that endogenous UL25 might trigger a certain process or has to interact with a cellular factor which is required for correct genome translocation into the nucleus.

In summary, the *in situ* hybridization of viral genomes in the presence of excess UL25 suggested a mechanism that may explain the reduction of immediate early HSV1 gene expression in the presence of excess UL25. In the future, this assay can also be used to set up *in situ* uncoating assay. To monitor uncoating of the viral genome, this method will require further optimization of the *in situ* hybridization in such a way that incoming genomes will be only detected after uncoating and not during nuclear targeting. Such an assay would provide a powerful tool to further analyze genome uncoating of HSV1 at the NPC, and may contribute to the identification of host and viral factors involved in HSV1 uncoating.

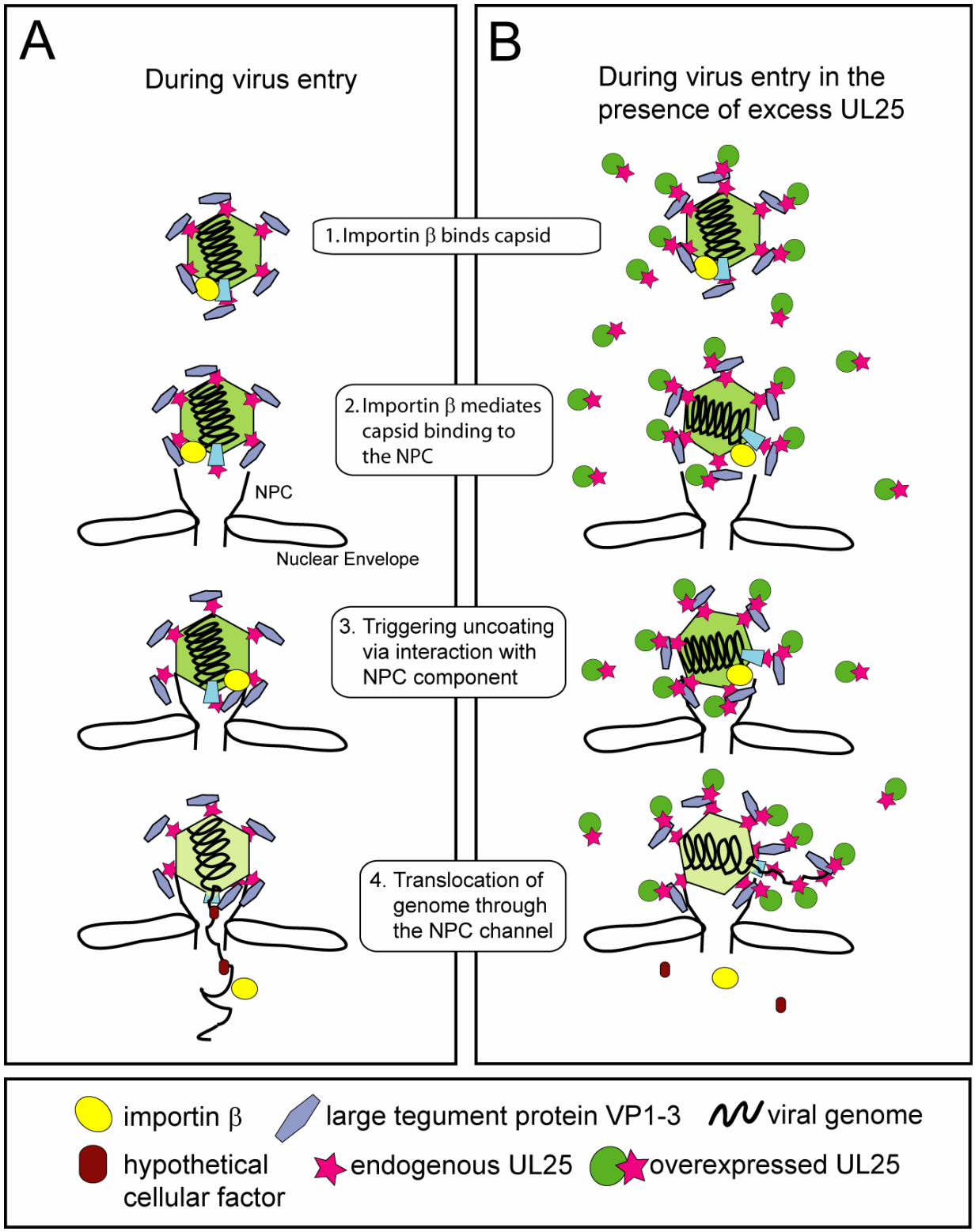

Figure 40: Hypothetical model of genome translocation through the NPC channel: In untransfected cells (A), Importin β binds (1) and shuttles the capsid to the NPC (2). It docks at the NPC with one vertex, presumably the UL6 portal complex, since the viral genome is packaged through it. A certain trigger at the NPC (3), maybe mediated through an interaction of VP1-3 or by an unknown cellular factor or NPC protein, leads to DNA injection through the NPC (4). In UL25-overexpressing cells (B), the shuttling from the capsid via importins may be functional, since nuclear targeting of incoming capsids is not impaired by overexpressed UL25 (1-2). Uncoating of capsids at the NPC is not impaired in UL25 overexpressing cells, but still gene expression is not detectable. In this scenario, excess UL25 may somehow interfere with proper binding at the NPC, in such a way that the wrong vertex binds to the NPC. The UL6 portal complex might not point in the direction of the NPC channel but into the cytosol. Nevertheless, the putative trigger function of VP1-3 or a cellular factor might still lead to uncoating (3), but the genome is translocated into the cytosol instead of into the nucleus (4). Scheme derived from Batterson et al. 1983; Newcomb et al. 2007; Ojala et al. 2000 and Schipke and Sodeik, personal communication.

5 Outlook

5.1 Further Analysis of UL25 During the Viral Life Cycle of HSV1

The minor capsid-associated protein UL25 stabilizes the packaged viral genome inside the capsid during capsid assembly and remains associated with the capsid during egress and cell entry. The latter would be consistent with the hypothesis, that genome uncoating, which requires first capsid destabilization, takes place exclusively at the nuclear pore. Thus it seems reasonable to assume that uncoating of the viral genome occurs at the the same time as UL25 has to detach from the incoming capsid to allow capsid destabilization. This hypothetical scenario can now be addressed further by combining immunolabeling with the *in situ* hybridization of the incoming genomes. It may even be possible to develop this assay further, and to modify it in such a way that only genomes released from HSV1 capsids will be detected, but not those genomes which are localized in incoming, cytoplasmic capsids.

It was recently suggested that UL25 is added to C-capsids in order to provide a signal for nuclear egress. Since UL25 was also found on B-capsids, although to a lesser extent, the subnuclear localization of UL25 on the several capsid types should be further analyzed using immunofluorescence and immunoelectron microscopy. For this aim, antibodies specific for A, B (e.g. against the scaffold protein VP22a) and C-capsids could be used.

Overexpressed UL25 reduced immediate HSV1 early gene expression. This effect could be further validated and characterized using FACS for a single cell analysis correlating GFPUL25 expression with HSV1 immediate early gene expression by using a mutant virus expressing a reporter gene such as RFP. Such a set-up would allow a quantitative screen of several UL25 constructs to determine which protein domain of UL25 interferes with the HSV1 nuclear import, and also if any positively charged protein could prevent HSV1 immediate early gene expression.

The luciferase reporter assays suggested that excess UL25 induced a general reduction of transcription. These experiments should be further quantified by increasing the data set. Moreover, potential effects on HSV1 specific promoter elements and HSV1-VP16 mediated transactivation need to be determined, to test whether UL25 interferes specifically with HSV1 transcription.

The electron microscopy analysis using a high MOI revealed a difference in the subcellular localization of incoming capsids after UL25GFP or GFPUL25 overexpression, which was not detected in immunofluorescence microscopy experiments using a low MOI. Thus, the electron microscopy study may be extended using a bicistronic pIRES vector that contains GFP and authentic UL25. Due to an internal ribosomal binding site both proteins will be translated from a single RNA transcript, but GFP could still be used as a marker for FACS sorting, and the effect of untagged UL25 on the early steps of the HSV1 life cycle could then also be analyzed at the ultrastuctural level.

5.2 Perspectives

When an overexpressed viral protein interferes with a specific function during the life cycle of this virus, it is likely that the endogenous protein might fulfill a crucial function. My experiments with excess UL25 suggest that the endogenous UL25 has additional functions during the ill-characterized step of HSV1-DNA import into the nucleus. Since HSV1 and other members of the *Herpesviridae* cause several severe human diseases, elucidating the molecular details of nuclear import of the incoming viral genomes could provide a basis for identifying new drug targets for the treatment of herpesviruses.

Recent candidate proteins for developing HSV1 pharmaceuticals are the packaging proteins UL6 and UL15. The thiourea compound WAY-150138 inhibits viral replication by antagonizing DNA encapsidation by interfering with the packaging proteins UL6 and UL15 during the assembly process (Newcomb and Brown 2002; van Zeijl et al. 2000). A novel thiazole urea compound BAY 57-1293 targets the HSV1 helicase-primase complex (Betz et al. 2002; Crumpacker and Schaffer 2002; Kleymann et al. 2002). This complex is composed of UL5, UL8 and UL52 which act together to unwind double-stranded viral DNA and generate primers for DNA synthesis by UL30 (Chattopadhyay et al. 2006; Zhu and Weller 1992). BAY 57-1293 inhibits the helicase-primase complex by enhancing the binding of UL5 and UL52 to the DNA (Crumpacker and Schaffer 2002; Crute et al. 2002; Kleymann et al. 2002).

Since UL25 is also involved during packaging and capsid stabilization, compounds against the UL25 function could be developed or recombinant UL25 could be used as an inhibitory peptide, because those compounds represent a novel promising therapeutic agent against virus infections (Munch et al. 2007). Moreover, my data suggest that it may also be possible to develop new drugs which in addition to assembly also target essential steps of virus entry.

6 References

Adams DJ. 2005. http://www.med.umich.edu/flowcytometry/training/lessons/lesson1/index.htm.

Addison C, Rixon FJ, Palfreyman JW, O'Hara M, Preston VG. 1984. Characterisation of a herpes simplex virus type 1 mutant which has a temperature-sensitive defect in penetration of cells and assembly of capsids. Virology 138(2):246-59.

Ali MA, Forghani B, Cantin EM. 1996. Characterization of an essential HSV-1 protein encoded by the UL25 gene reported to be involved in virus penetration and capsid assembly. Virology 216(1):278-83.

Aris JP, Blobel G. 1989. Yeast nuclear envelope proteins cross react with an antibody against mammalian pore complex proteins. J Cell Biol 108(6):2059-67.

Baines JD, Weller SK. 2005. Cleavage and Packaging of Herpes Simplex Viral 1 DNA. In: Catalano CE, editor. Viral Genome Packaging Machines: Genetics, Structures and Mechanism. New York: Landes Biosciences. p 135-150.

Baines JD, Wills E, Jacob RJ, Pennington J, Roizman B. 2007. Glycoprotein M of herpes simplex virus 1 is incorporated into virions during budding at the inner nuclear membrane. J Virol 81(2):800-12.

Baker ML, Jiang W, Rixon FJ, Chiu W. 2005. Common ancestry of herpesviruses and tailed DNA bacteriophages. J Virol 79(23):14967-70.

Batterson W, Furlong D, Roizman B. 1983. Molecular genetics of herpes simplex virus. VIII. further characterization of a temperature-sensitive mutant defective in release of viral DNA and in other stages of the viral reproductive cycle. J Virol 45(1):397-407.

Beard P, Duffy C, Baines J. 2004. Quantification of the DNA cleavage and packaging proteins UL15 and UL28 in A and B capsids of HSV1. J Virol 78(3):1367-74.

Beard PM, Taus NS, Baines JD. 2002. DNA cleavage and packaging proteins encoded by genes U(L)28, U(L)15, and U(L)33 of herpes simplex virus type 1 form a complex in infected cells. J Virol 76(10):4785-91.

Betz UA, Fischer R, Kleymann G, Hendrix M, Rubsamen-Waigmann H. 2002. Potent in vivo antiviral activity of the herpes simplex virus primase-helicase inhibitor BAY 57-1293. Antimicrob Agents Chemother 46(6):1766-72.

Bjerke SL, Roller RJ. 2006. Roles for herpes simplex virus type 1 UL34 and US3 proteins in disrupting the nuclear lamina during herpes simplex virus type 1 egress. Virology 347(2):261-76.

Bloom DC. 2004. HSV LAT and neuronal survival. Int Rev Immunol 23(1-2):187-98.

Booy FP, Newcomb WW, Trus BL, Brown JC, Baker TS, Steven AC. 1991. Liquid-crystalline, phage-like packing of encapsidated DNA in herpes simplex virus. Cell 64(5):1007-15.

Bowman BR, Welschhans RL, Jayaram H, Stow ND, Preston VG, Quiocho FA. 2006. Structural characterization of the UL25 DNA-packaging protein from herpes simplex virus type 1. J Virol 80(5):2309-17.

Burnette WN. 1981. "Western blotting": electrophoretic transfer of proteins from sodium dodecyl sulfate-polyacrylamide gels to unmodified nitrocellulose and radiographic detection with antibody and radioiodinated protein A. Anal Biochem 112(2):195-203.

Campadelli-Fiume G. 2007. The egress of alphaherpesviruses from the cell. In: Arvin A, Campadelli Fiume G, Mocarski E, Moore PS, Roizman B, Whitley R, Yamanishi K, editors. Human Herpesviruses, Biology, Therapy and Immunoprophylaxis. New York: Cambridge University Press: pp 151-162

Campadelli-Fiume G, Amasio M, Avitabile E, Cerretani A, Forghieri C, Gianni T, Menotti L. 2007. The multipartite system that mediates entry of herpes simplex virus into the cell. Rev Med Virol. 17(5):313-26. Review.

Campadelli-Fiume G, Roizman B. 2006. The Egress of Herpesvirus from Cells: the unanswered Questions. Journal of Virology 80(13):6716-6719.

Cardone G, Winkler DC, Trus BL, Cheng N, Heuser JE, Newcomb WW, Brown JC, Steven AC. 2007. Visualization of the herpes simplex virus portal in situ by cryo-electron tomography. Virology 361(2):426-34.

Caroll M, Ward, E.S., Ravetch, J., Kelsoe, G., and Fearon, D. 2001. Failure of Host Defense Mechanisms. C.A. Janeway PT, M. Walport, and M. Shlomchik, editor. New York: Garland Publishing. pp 424-469

Casjens S, Wyckoff E, Hayden M, Sampson L, Eppler K, Randall S, Moreno ET, Serwer P. 1992. Bacteriophage P22 portal protein is part of the gauge that regulates packing density of intravirion DNA. J Mol Biol 224(4):1055-74.

Catalano CE. 2005. Viral Genome Packaging Machines: Genetics, Structure, and Mechanisms. Catalano CE, editor. New York: Landes Biosciences. pp.1-151

Chattopadhyay S, Chen Y, Weller SK. 2006. The two helicases of herpes simplex virus type 1 (HSV-1). Front Biosci 11:2213-23.

Chen DH, Jakana J, McNab D, Mitchell J, Zhou ZH, Dougherty M, Chiu W, Rixon FJ. 2001. The pattern of tegument-capsid interaction in the herpes simplex virus type 1 virion is not influenced by the small hexon-associated protein VP26. J Virol 75(23):11863-7.

Cleator MC, Klapper PE. 2004. The Herpesviridae. Principles and Practice of Clinical Virology, 5th Edition: John Wiley & Sons Ltd.

Clement C, Tiwari V, Scanlan PM, Valyi-Nagy T, Yue BY, Shukla D. 2006. A novel role for phagocytosis-like uptake in herpes simplex virus entry. J Cell Biol 174(7):1009-21.

Cohen GH, Ponce de Leon M, Diggelmann H, Lawrence WC, Vernon SK, Eisenberg RJ. 1980. Structural analysis of the capsid polypeptides of herpes simplex virus types 1 and 2. J Virol 34(2):521-31.

Coller KE. 2007. The capsid and tegument of the alpha herpesviruses are linked by an interaction between the UL25 and VP1/2 proteins. J Virol 81(21):11790-7

Crumpacker CS, Schaffer PA. 2002. New anti-HSV therapeutics target the helicase-primase complex. Nat Med 8(4):327-8.

Crute JJ, Grygon CA, Hargrave KD, Simoneau B, Faucher AM, Bolger G, Kibler P, Liuzzi M, Cordingley MG. 2002. Herpes simplex virus helicase-primase inhibitors are active in animal models of human disease. Nat Med 8(4):386-91.

Cunningham C, Davison AJ. 1993. A cosmid-based system for constructing mutants of herpes simplex virus type 1. Virology 197(1):116-24.

Dargan DJ, Subak-Sharpe JH. 1997. The effect of herpes simplex virus type 1 L-particles on virus entry, replication, and the infectivity of naked herpesvirus DNA. Virology 239(2):378-88.

Darlington RW, Moss LH, 3rd. 1968. Herpesvirus envelopment. J Virol 2(1):48-55.

Davis LI, Blobel G. 1987. Nuclear pore complex contains a family of glycoproteins that includes p62: glycosylation through a previously unidentified cellular pathway. Proc Natl Acad Sci U S A 84(21):7552-6.

Davison AJ, Eberle R, Ehlers B, Hayward GS, McGeoch DJ, Minson A, Pellett PE, Roizman B, Studdert MJ, Thiry E. A planned order for herpesviruses; 2005; Contribution at the International Herpesvirus Workshop 2005, Turku, Finland.

De Clercq E. 2007. Acyclic nucleoside phosphonates: past, present and future. Bridging chemistry to HIV, HBV, HCV, HPV, adeno-, herpes- and poxvirus infections: the phosphonate bridge. Biochem Pharmacol 73(7):911-22.

Decman V, Freeman ML, Kinchington PR, Hendricks RL. 2005. Immune control of HSV-1 latency. Viral Immunol 18(3):466-73.

Desai P, Sexton GL, McCaffery JM, Person S. 2001. A null mutation in the gene encoding the herpes simplex virus type 1 UL37 polypeptide abrogates virus maturation. J Virol 75(21):10259-71.

Desai PJ. 2000. A null mutation in the UL36 gene of herpes simplex virus type 1 results in accumulation of unenveloped DNA-filled capsids in the cytoplasm of infected cells. J Virol 74(24):11608-18.

Desloges N, Simard C. 2003. Implication of the product of the bovine herpesvirus type 1 UL25 gene in capsid assembly. J Gen Virol 84(Pt 9):2485-90.

Dey A, Ellenberg J, Farina A, Coleman AE, Maruyama T, Sciortino S, Lippincott-Schwartz J, Ozato K. 2000. A bromodomain protein, MCAP, associates with mitotic chromosomes and affects G(2)-to-M transition. Mol Cell Biol 20(17):6537-49.

Doerr H. 2002. Medizinische Virologie - Grundlagen, Diagnostik und Therapie virologischer Krankheitsbilder: Thieme: pp 102-107

Döhner K, Nagel CH, Sodeik B. 2005. Viral stop-and-go along microtubules: taking a ride with dynein and kinesins. Trends Microbiol 13(7):320-7.

Döhner K, Radtke K, Schmidt S, Sodeik B. 2006. Eclipse phase of herpes simplex virus type 1 infection: Efficient dynein-mediated capsid transport without the small capsid protein VP26. J Virol 80(16):8211-24.

Döhner K, Wolfstein A, Prank U, Echeverri C, Dujardin D, Vallee R, Sodeik B. 2002. Function of dynein and dynactin in herpes simplex virus capsid transport. Mol Biol Cell 13(8):2795-809.

Downing KH. 2000. Structural basis for the interaction of tubulin with proteins and drugs that affect microtubule dynamics. Annu Rev Cell Dev Biol 16:89-111.

Duda RL, Hendrix RW, Huang WM, Conway JF. 2006. Shared architecture of bacteriophage SPO1 and herpesvirus capsids. Curr Biol 16(1):R11-3.

Duffy C, Baines J.D. 2006. Nucleocapsid Assembly and Envelopment of Herpes Simplex Virus. Sandri-Goldin RM, editor. Norfolk, UK: Caister Academic Press. pp. 175-204

Ellenberg J, Siggia ED, Moreira JE, Smith CL, Presley JF, Worman HJ, Lippincott-Schwartz J. 1997. Nuclear membrane dynamics and reassembly in living cells: targeting of an inner nuclear membrane protein in interphase and mitosis. J Cell Biol 138(6):1193-206.

Enquist LW, Husak PJ, Banfield BW, Smith GA. 1998. Infection and spread of alphaherpesviruses in the nervous system. Adv Virus Res 51:237-347.

Everett RD, Murray J. 2005. ND10 components relocate to sites associated with herpes simplex virus type 1 nucleoprotein complexes during virus infection. J Virol 79(8):5078-89.

Everett RD, Orr A, Elliott M. 1991. High level expression and purification of herpes simplex virus type 1 immediate early polypeptide Vmw110. Nucleic Acids Res 19(22):6155-61.

Everett RD, Sourvinos G, Leiper C, Clements JB, Orr A. 2004. Formation of nuclear foci of the herpes simplex virus type 1 regulatory protein ICP4 at early times of infection: localization, dynamics, recruitment of ICP27, and evidence for the de novo induction of ND10-like complexes. J Virol 78(4):1903-17.

Everett RD, Sourvinos G, Orr A. 2003. Recruitment of herpes simplex virus type 1 transcriptional regulatory protein ICP4 into foci juxtaposed to ND10 in live, infected cells. J Virol 77(6):3680-9.

Farley CA, Banfield WG, Kasnic G, Jr., Foster WS. 1972. Oyster herpes-type virus. Science 178(62):759-60.

Farnsworth A, Wisner TW, Webb M, Roller R, Cohen G, Eisenberg R, Johnson DC. 2007. Herpes simplex virus glycoproteins gB and gH function in fusion between the virion envelope and the outer nuclear membrane. Proc Natl Acad Sci U S A 104(24):10187-92.

Feis M, Catalano, CE. 2005. Bacteriophage Lambda Terminase and the Mechanism of Viral DNA Packaging. In: Catalano CE, editor. Viral Genome Packaging Machines: Genetics, Structures, and Mechanisms. New York: Landes Biosciences. pp 5-39.

Feldman L, Blankenship ML, Ben-Porat T. 1981. Isolation and characterization of a temperature-sensitive uncoating mutant of pseudorabies virus. J Gen Virol 54(Pt 2):333-42.

Fuchs W, Klupp BG, Granzow H, Osterrieder N, Mettenleiter TC. 2002. The interacting UL31 and UL34 gene products of pseudorabies virus are involved in egress from the host-cell nucleus and represent components of primary enveloped but not mature virions. J Virol 76(1):364-78.

Gant TM, Wilson KL. 1997. Nuclear assembly. Annu Rev Cell Dev Biol 13:669-695.

Gao M, Matusick-Kumar L, Hurlburt W, DiTusa SF, Newcomb WW, Brown JC, McCann PJ, 3rd, Deckman I, Colonno RJ. 1994. The protease of herpes simplex virus type 1 is essential for functional capsid formation and viral growth. J Virol 68(6):3702-12.

Geng Y, Eaton EN, Picon M, Roberts JM, Lundberg AS, Gifford A, Sardet C, Weinberg RA. 1996. Regulation of cyclin E transcription by E2Fs and retinoblastoma protein. Oncogene 12(6):1173-80.

Gianni T, Campadelli-Fiume G, Menotti L. 2004. Entry of herpes simplex virus mediated by chimeric forms of nectin1 retargeted to endosomes or to lipid rafts occurs through acidic endosomes. J Virol 78(22):12268-76.

Gianni T, Fato R, Bergamini C, Lenaz G, Campadelli-Fiume G. 2006a. Hydrophobic alpha-helices 1 and 2 of herpes simplex virus gH interact with lipids, and their mimetic peptides enhance virus infection and fusion. J Virol 80(16):8190-8.

Gianni T, Forghieri C, Campadelli-Fiume G. 2006b. The herpesvirus glycoproteins B and H.L are sequentially recruited to the receptor-bound gD to effect membrane fusion at virus entry. Proc Natl Acad Sci U S A 103(39):14572-7.

Gianni T, Martelli PL, Casadio R, Campadelli-Fiume G. 2005a. The ectodomain of herpes simplex virus glycoprotein H contains a membrane alpha-helix with attributes of an internal fusion peptide, positionally conserved in the herpesviridae family. J Virol 79(5):2931-40.

Gianni T, Menotti L, Campadelli-Fiume G. 2005b. A heptad repeat in herpes simplex virus 1 gH, located downstream of the alpha-helix with attributes of a fusion peptide, is critical for virus entry and fusion. J Virol 79(11):7042-9.

Goodkin ML, Ting AT, Blaho JA. 2003. NF-kappaB is required for apoptosis prevention during herpes simplex virus type 1 infection. J Virol 77(13):7261-80.

Grant SG, Jessee J, Bloom FR, Hanahan D. 1990. Differential plasmid rescue from transgenic mouse DNAs into Escherichia coli methylation-restriction mutants. Proc Natl Acad Sci U S A 87(12):4645-9.

Granzow H, Klupp BG, Mettenleiter TC. 2004. The pseudorabies virus US3 protein is a component of primary and of mature virions. J Virol 78(3):1314-23.

Granzow H, Klupp BG, Mettenleiter TC. 2005. Entry of pseudorabies virus: an immunogold-labeling study. J Virol 79(5):3200-5.

Greaves RF, O'Hare P. 1990. Structural requirements in the herpes simplex virus type 1 transactivator Vmw65 for interaction with the cellular octamer-binding protein and target TAATGARAT sequences. J Virol 64(6):2716-24.

Greber UF, Fassati A. 2003. Nuclear import of viral DNA genomes. Traffic 4(3):136-43.

Greber UF, Suomalainen M, Stidwill RP, Boucke K, Ebersold MW, Helenius A. 1997. The role of the nuclear pore complex in adenovirus DNA entry. Embo J 16(19):5998-6007.

Greber UF, Webster P, Weber J, Helenius A. 1996. The role of the adenovirus protease on virus entry into cells. Embo J 15(8):1766-77.

Greber UF, Willetts M, Webster P, Helenius A. 1993. Stepwise dismantling of adenovirus 2 during entry into cells. Cell 75(3):477-86.

Grünewald K, Desai P, Winkler DC, Heymann JB, Belnap DM, Baumeister W, Steven AC. 2003. Three-dimensional structure of herpes simplex virus from cryo-electron tomography. Science 302(5649):1396-8.

Guo P, Lee TJ. 2007. Viral nanomotors for packaging of dsDNA and dsRNA. Mol Microbiol 64(4):886-903.

Haines H, Baerwald RJ. 1976. Nuclear membrane changes in herpes simplex virus-infected BHK-21 cells as seen by freeze-fracture. J Virol 17(3):1038-42.

Hanz S, Perlson E, Willis D, Zheng JQ, Massarwa R, Huerta JJ, Koltzenburg M, Kohler M, van-Minnen J, Twiss JL and others. 2003. Axoplasmic importins enable retrograde injury signaling in lesioned nerve. Neuron 40(6):1095-104.

Harel A, Forbes DJ. 2001. Welcome to the nucleus: CAN I take your coat? Nat Cell Biol 3(12):E267-9.

Harley CA, Dasgupta A, Wilson DW. 2001. Characterization of herpes simplex virus-containing organelles by subcellular fractionation: role for organelle acidification in assembly of infectious particles. J Virol 75(3):1236-51.

Heymann JB, Cheng N, Newcomb WW, Trus BL, Brown JC, Steven AC. 2003. Dynamics of herpes simplex virus capsid maturation visualized by time-lapse cryo-electron microscopy. Nat Struct Biol 10(5):334-41.

Homa FL, Brown JC. 1997. Capsid assembly and DNA packaging in herpes simplex virus. Rev Med Virol 7(2):107-122.

Huang CJ, Wagner EK. 1994. The herpes simplex virus type 1 major capsid protein (VP5-UL19) promoter contains two cis-acting elements influencing late expression. J Virol 68(9):5738-47.

Jensen ON, Houthaeve T, Shevchenko A, Cudmore S, Ashford T, Mann M, Griffiths G, Krijnse Locker J. 1996. Identification of the major membrane and core proteins of vaccinia virus by two-dimensional electrophoresis. J Virol 70(11):7485-97.

Jerome KR, Ashley RL. 2003. Herpes simplex viruses and herpes B virus. In: Murray PR, Baron EJ, Jorgensen JH, Pfaller MA, Yolken RH, editors. Manual of Clinical Microbiology, 8th edition. Washington, DC: ASM Press. p 1291-1303.

Johnson DC, Spear PG. 1982. Monensin inhibits the processing of herpes simplex virus glycoproteins, their transport to the cell surface, and the egress of virions from infected cells. J Virol 43(3):1102-12.

Kaelin K, Dezelee S, Masse MJ, Bras F, Flamand A. 2000. The UL25 protein of pseudorabies virus associates with capsids and localizes to the nucleus and to microtubules. J Virol 74(1):474-82.

Kann M. 2004. Nucleoprotein transport of HBV capsid particles. Methods Mol Med 95:213-26.

Kann M, Sodeik B, Vlachou A, Gerlich WH, Helenius A. 1999. Phosphorylation-dependent binding of hepatitis B virus core particles to the nuclear pore complex. J Cell Biol 145(1):45-55.

Khanna KM, Bonneau RH, Kinchington PR, Hendricks RL. 2003. Herpes simplex virus-specific memory CD8+ T cells are selectively activated and retained in latently infected sensory ganglia. Immunity 18(5):593-603.

Khanna KM, Lepisto AJ, Decman V, Hendricks RL. 2004. Immune control of herpes simplex virus during latency. Curr Opin Immunol 16(4):463-9.

King J, Botstein D, Casjens S, Earnshaw W, Harrison S, Lenk E. 1976. Structure and assembly of the capsid of bacteriophage P22. Philos Trans R Soc Lond B Biol Sci 276(943):37-49.

King J, Lenk EV, Botstein D. 1973. Mechanism of head assembly and DNA encapsulation in Salmonella phage P22. II. Morphogenetic pathway. J Mol Biol 80(4):697-731.

Kleymann G, Fischer R, Betz UA, Hendrix M, Bender W, Schneider U, Handke G, Eckenberg P, Hewlett G, Pevzner V and others. 2002. New helicase-primase inhibitors as drug candidates for the treatment of herpes simplex disease. Nat Med 8(4):392-8.

Klupp BG, Granzow H, Keil GM, Mettenleiter TC. 2006. The capsid-associated UL25 protein of the alphaherpesvirus pseudorabies virus is nonessential for cleavage and encapsidation of genomic DNA but is required for nuclear egress of capsids. J Virol 80(13):6235-46.

Klupp BG, Granzow H, Mettenleiter TC. 2001. Effect of the pseudorabies virus US3 protein on nuclear membrane localization of the UL34 protein and virus egress from the nucleus. J Gen Virol 82(Pt 10):2363-71.

Koslowski KM, Shaver PR, Wang XY, Tenney DJ, Pederson NE. 1997. The pseudorabies virus UL28 protein enters the nucleus after coexpression with the herpes simplex virus UL15 protein. J Virol 71(12):9118-23.

Kouklis PD, Merdes A, Papamarcaki T, Georgatos SD. 1993. Transient arrest of 3T3 cells in mitosis and inhibition of nuclear lamin reassembly around chromatin induced by anti-vimentin antibodies. Eur J Cell Biol 62(2):224-36.

Kovacs GR, Moss B. 1996. The vaccinia virus H5R gene encodes late gene transcription factor 4: purification, cloning, and overexpression. J Virol 70(10):6796-802.

Koyama AH, Uchida T. 1987. The mode of entry of herpes simplex virus type 1 into Vero cells. Microbiol Immunol 31(2):123-30.

Kozak M. 1986. Point mutations define a sequence flanking the AUG initiator codon that modulates translation by eukaryotic ribosomes. Cell 44(2):283-92.

La Boissiere S, Hughes T, O'Hare P. 1999. HCF-dependent nuclear import of VP16. Embo J 18(2):480-9.

Laemmli UK. 1970. Cleavage of structural proteins during the assembly of the head of bacteriophage T4. Nature 227(259):680-5.

Lamberti C, Weller SK. 1998. The herpes simplex virus type 1 cleavage/packaging protein, UL32, is involved in efficient localization of capsids to replication compartments. J Virol 72(3):2463-73.

Lenk E, Casjens S, Weeks J, King J. 1975. Intracellular visualization of precursor capsids in phage P22 mutant infected cells. Virology 68(1):182-99.

Lessard JL. 1988. Two monoclonal antibodies to actin: one muscle selective and one generally reactive. Cell Motil Cytoskeleton 10(3):349-62.

Leuzinger H, Ziegler U, Schraner EM, Fraefel C, Glauser DL, Heid I, Ackermann M, Mueller M, Wild P. 2005. Herpes simplex virus 1 envelopment follows two diverse pathways. J Virol 79(20):13047-59.

Lippincott-Schwartz J, Presley JF, Zaal KJ, Hirschberg K, Miller CD, Ellenberg J. 1999. Monitoring the dynamics and mobility of membrane proteins tagged with green fluorescent protein. Methods Cell Biol 58:261-81.

Luxton GW, Haverlock S, Coller KE, Antinone SE, Pincetic A, Smith GA. 2005. Targeting of herpesvirus capsid transport in axons is coupled to association with specific sets of tegument proteins. Proc Natl Acad Sci U S A 102(16):5832-7.

Luxton GW, Lee JI, Haverlock-Moyns S, Schober JM, Smith GA. 2006. The pseudorabies virus VP1/2 tegument protein is required for intracellular capsid transport. J Virol 80(1):201-9.

Lycke E, Hamark B, Johansson M, Krotochwil A, Lycke J, Svennerholm B. 1988. Herpes simplex virus infection of the human sensory neuron. An electron microscopy study. Arch Virol 101(1-2):87-104.

Mabit H, Nakano MY, Prank U, Saam B, Döhner K, Sodeik B, Greber UF. 2002. Intact microtubules support adenovirus and herpes simplex virus infections. J Virol 76(19):9962-71.

MacLean AR. 1998. Preparation of HSV-DNA and Production of Infectious Virus. In: Brown SM, MacLean AR, editors. Herpes Simplex Virus Protocols. Totowa, New Jersey: Humana Press Inc. p 19-25.

Maeshima K, Yahata K, Sasaki Y, Nakatomi R, Tachibana T, Hashikawa T, Imamoto F, Imamoto N. 2006. Cell-cycle-dependent dynamics of nuclear pores: pore-free islands and lamins. J Cell Sci 119(Pt 21):4442-51.

McGeoch DJ, Dalrymple MA, Davison AJ, Dolan A, Frame MC, McNab D, Perry LJ, Scott JE, Taylor P. 1988. The complete DNA sequence of the long unique region in the genome of herpes simplex virus type 1. J Gen Virol 69(Pt 7):1531-74.

McGeoch DJ, Dolan A, Donald S, Brauer DH. 1986. Complete DNA sequence of the short repeat region in the genome of herpes simplex virus type 1. Nucleic Acids Res 14(4):1727-45.

McGeoch DJ, Gatherer D. 2005. Integrating reptilian herpesviruses into the family herpesviridae. J Virol 79(2):725-31.

McGeoch DJ, Rixon FJ, Davison AJ. 2006. Topics in herpesvirus genomics and evolution. Virus Res 117(1):90-104.

McNab AR, Desai P, Person S, Roof LL, Thomsen DR, Newcomb WW, Brown JC, Homa FL. 1998. The product of the herpes simplex virus type 1 UL25 gene is required for encapsidation but not for cleavage of replicated viral DNA. J Virol 72(2):1060-70.

Meitinger C, Strobl LJ, Marschall G, Bornkamm GW, Zimber-Strobl U. 1994. Crucial sequences within the Epstein-Barr virus TP1 promoter for EBNA2-mediated transactivation and interaction of EBNA2 with its responsive element. J Virol 68(11):7497-506.

Mettenleiter TC. 2002. Herpesvirus assembly and egress. J Virol 76(4):1537-47.

Mettenleiter TC. 2004. Budding events in herpesvirus morphogenesis. Virus Res 106(2):167-80.

Mettenleiter TC. 2006. Intriguing interplay between viral proteins during herpesvirus assembly or: the herpesvirus assembly puzzle. Vet Microbiol 113(3-4):163-9.

Mettenleiter TC, Klupp BG, Granzow H. 2006. Herpesvirus assembly: a tale of two membranes. Curr Opin Microbiol 9(4):423-9.

Mettenleiter TC, Minson T. 2006. Egress of alphaherpesviruses. J Virol 80(3):1610-1; author reply 1611-2.

Milne RS, Nicola AV, Whitbeck JC, Eisenberg RJ, Cohen GH. 2005. Glycoprotein D receptor-dependent, low-pH-independent endocytic entry of herpes simplex virus type 1. J Virol 79(11):6655-63.

Morrison EE, Stevenson AJ, Wang YF, Meredith DM. 1998. Differences in the intracellular localization and fate of herpes simplex virus tegument proteins early in the infection of Vero cells. J Gen Virol 79(Pt 10):2517-28.

Mou F, Forest T, Baines JD. 2007. US3 of herpes simplex virus type 1 encodes a promiscuous protein kinase that phosphorylates and alters localization of lamin A/C in infected cells. J Virol 81(12):6459-70.

Müller M. 2000, Internship report at the Institute of Virology, Hannover Medical School. Subzelluläre Lokalisation von transient überexprimiertem GFPUL25.

Munch J, Standker L, Adermann K, Schulz A, Schindler M, Chinnadurai R, Pohlmann S, Chaipan C, Biet T, Peters T and others. 2007. Discovery and optimization of a natural HIV-1 entry inhibitor targeting the gp41 fusion peptide. Cell 129(2):263-75.

Murialdo H. 1991. Bacteriophage lambda DNA maturation and packaging. Annu Rev Biochem 60:125-53.

Nagel CH, Döhner K, Fathollahy M, Strive T, Borst EM, Messerle M, Sodeik B. Nuclear egress and envelopment of Herpes Simplex Virus capsids analyzed with dual-color fluorescence HSV1(17+)-GFPVP26-gDRFP. Journal of Virology, accepted.

Naldinho-Souto R, Browne H, Minson T. 2006. Herpes simplex virus tegument protein VP16 is a component of primary enveloped virions. J Virol 80(5):2582-4.

Narayanan A, Nogueira ML, Ruyechan WT, Kristie TM. 2005. Combinatorial transcription of herpes simplex virus and varicella zoster virus immediate early genes is strictly determined by the cellular coactivator HCF-1. J Biol Chem 280(2):1369-75.

Newcomb WW, Booy FP, Brown JC. 2007. Uncoating the herpes simplex virus genome. J Mol Biol 370(4):633-42.

Newcomb WW, Brown JC. 2002. Inhibition of herpes simplex virus replication by WAY-150138: assembly of capsids depleted of the portal and terminase proteins involved in DNA encapsidation. J Virol 76(19):10084-8.

Newcomb WW, Homa FL, Brown JC. 2005. Involvement of the portal at an early step in herpes simplex virus capsid assembly. J Virol 79(16):10540-6.

Newcomb WW, Homa FL, Brown JC. 2006. Herpes simplex virus capsid structure: DNA packaging protein UL25 is located on the external surface of the capsid near the vertices. J Virol 80(13):6286-94.

Newcomb WW, Homa FL, Thomsen DR, Booy FP, Trus BL, Steven AC, Spencer JV, Brown JC. 1996. Assembly of the herpes simplex virus capsid: characterization of intermediates observed during cell-free capsid formation. J Mol Biol 263(3):432-46.

Newcomb WW, Homa FL, Thomsen DR, Trus BL, Cheng N, Steven A, Booy F, Brown JC. 1999. Assembly of the herpes simplex virus procapsid from purified components and identification of small complexes containing the major capsid and scaffolding proteins. J Virol 73(5):4239-50.

Newcomb WW, Homa FL, Thomsen DR, Ye Z, Brown JC. 1994. Cell-free assembly of the herpes simplex virus capsid. J Virol 68(9):6059-63.

Newcomb WW, Juhas RM, Thomsen DR, Homa FL, Burch AD, Weller SK, Brown JC. 2001. The UL6 gene product forms the portal for entry of DNA into the herpes simplex virus capsid. J Virol 75(22):10923-32.

Nicola AV, Hou J, Major EO, Straus SE. 2005. Herpes simplex virus type 1 enters human epidermal keratinocytes, but not neurons, via a pH-dependent endocytic pathway. J Virol 79(12):7609-16.

Nicola AV, McEvoy AM, Straus SE. 2003. Roles for endocytosis and low pH in herpes simplex virus entry into HeLa and Chinese hamster ovary cells. J Virol 77(9):5324-32.

Nicola AV, Straus SE. 2004. Cellular and viral requirements for rapid endocytic entry of herpes simplex virus. J Virol 78(14):7508-17.

Nikolov DB, Burley SK. 1997. RNA polymerase II transcription initiation: a structural view. Proc Natl Acad Sci U S A 94(1):15-22.

Noble S, Faulds D. 1998. Ganciclovir. An update of its use in the prevention of cytomegalovirus infection and disease in transplant recipients. Drugs 56(1):115-46.

Obrig TG, Culp WJ, McKeehan WL, Hardesty B. 1971. The mechanism by which cycloheximide and related glutarimide antibiotics inhibit peptide synthesis on reticulocyte ribosomes. J Biol Chem 246(1):174-81.

Ogasawara M, Suzutani T, Yoshida I, Azuma M. 2001. Role of the UL25 gene product in packaging DNA into the herpes simplex virus capsid: location of UL25 product in the capsid and demonstration that it binds DNA. J Virol 75(3):1427-36.

Ojala PM, Sodeik B, Ebersold MW, Kutay U, Helenius A. 2000. Herpes simplex virus type 1 entry into host cells: reconstitution of capsid binding and uncoating at the nuclear pore complex in vitro. Mol Cell Biol 20(13):4922-31.

Ottinger M. 2005. Functional Characterisation of Gamma 2-Herpesviral orf73 Proteins and their Interaction with the Cellular Proteins BRD2 and BRD 4 [PhD thesis]. Hannover: Universtity of Veterinary Medicine, Foundation.

Palmer E, Freeman T. 2004. Investigation into the use of C- and N-terminal GFP fusion proteins for subcellular localization studies using reverse transfection microarrays. Comparative and Functional Genomics 5:342-353.

Pante N, Aebi U. 1993. The nuclear pore complex. J Cell Biol 122(5):977-84.

Pante N, Kann M. 2002. Nuclear pore complex is able to transport macromolecules with diameters of about 39 nm. Mol Biol Cell 13(2):425-34.

Parker RF, Bronson LH, Green RH. 1941. Further studies of the infectious unit of vaccinia. J Exp Med 74:263-281.

Parry C, Bell S, Minson T, Browne H. 2005. Herpes simplex virus type 1 glycoprotein H binds to alphavbeta3 integrins. J Gen Virol 86(Pt1):7-10.

Perez A, Li QX, Perez-Romero P, Delassus G, Lopez SR, Sutter S, McLaren N, Fuller AO. 2005. A new class of receptor for herpes simplex virus has heptad repeat motifs that are common to membrane fusion proteins. J Virol 79(12):7419-30.

Perez-Romero P, Fuller AO. 2005. The C terminus of the B5 receptor for herpes simplex virus contains a functional region important for infection. J Virol 79(12):7431-7.

Perucchetti R, Parris W, Becker A, Gold M. 1988. Late stages in bacteriophage lambda head morphogenesis: in vitro studies on the action of the bacteriophage lambda D-gene and W-gene products. Virology 165(1):103-14.

Phelan A, Dunlop J, Patel AH, Stow ND, Clements JB. 1997. Nuclear sites of herpes simplex virus type 1 DNA replication and transcription colocalize at early times postinfection and are largely distinct from RNA processing factors. J Virol 71(2):1124-32.

Popov S, Rexach M, Ratner L, Blobel G, Bukrinsky M. 1998a. Viral protein R regulates docking of the HIV-1 preintegration complex to the nuclear pore complex. J Biol Chem 273(21):13347-52.

Popov S, Rexach M, Zybarth G, Reiling N, Lee MA, Ratner L, Lane CM, Moore MS, Blobel G, Bukrinsky M. 1998b. Viral protein R regulates nuclear import of the HIV-1 pre-integration complex. Embo J 17(4):909-17.

Preston CM. 2000. Repression of viral transcription during herpes simplex virus latency. J Gen Virol 81(Pt 1):1-19.

Prevelige PE, Jr., King J. 1993. Assembly of bacteriophage P22: a model for ds-DNA virus assembly. Prog Med Virol 40:206-21.

Rabe B, Vlachou A, Pante N, Helenius A, Kann M. 2003. Nuclear import of hepatitis B virus capsids and release of the viral genome. Proc Natl Acad Sci U S A 100(17):9849-54.

Rabut G, Doye V, Ellenberg J. 2004. Mapping the dynamic organization of the nuclear pore complex inside single living cells. Nat Cell Biol 6(11):1114-21.

Radtke K, Döhner K, Sodeik B. 2006. Viral interactions with the cytoskeleton: a hitchhiker's guide to the cell. Cell Microbiol 8(3):387-400.

Rajcani J, Andrea V, Ingeborg R. 2004. Peculiarities of herpes simplex virus (HSV) transcription: an overview. Virus Genes 28(3):293-310.

Reske A, Pollara G, Krummenacher C, Chain BM, Katz DR. 2007. Understanding HSV-1 entry glycoproteins. Rev Med Virol 17(3):205-15.

Reynolds AE, Liang L, Baines JD. 2004. Conformational changes in the nuclear lamina induced by herpes simplex virus type 1 require genes UL31 and UL34. J Virol 78(11):5564-75.

Reynolds AE, Ryckman BJ, Baines JD, Zhou Y, Liang L, Roller RJ. 2001. UL31 and UL34 proteins of herpes simplex virus type 1 form a complex that accumulates at the nuclear rim and is required for envelopment of nucleocapsids. J Virol 75(18):8803-17.

Reynolds AE, Wills EG, Roller RJ, Ryckman BJ, Baines JD. 2002. Ultrastructural localization of the herpes simplex virus type 1 UL31, UL34, and US3 proteins suggests specific roles in primary envelopment and egress of nucleocapsids. J Virol 76(17):8939-52.

Reynolds ES. 1963. The use of lead citrate at high pH as an electron-opaque stain in electron microscopy. J Cell Biol 17:208-12.

Rode K. 2002, Internship report of the Institut of Virology at Hannover Medical School. Das UL25-Protein des Herpes Simplex Virus Typ 1 - Subzelluläre Lokalisation und Auswirkungen auf den Kapsidtransport des HSV1.

Rode K. 2003, Diploma thesis. Die Rolle der Herpes-Simplex-Virus Proteine UL25 und VP1/3 (UL36) beim Viruseintritt in die Zelle [Diplomarbeit]: Gottfried Wilhelm Leibniz Universität Hannover.

Rodriguez JR, Risco C, Carrascosa JL, Esteban M, Rodriguez D. 1998. Vaccinia virus 15-kilodalton (A14L) protein is essential for assembly and attachment of viral crescents to virosomes. J Virol 72(2):1287-96.

Roeder RG. 1996. The role of general initiation factors in transcription by RNA polymerase II. Trends Biochem Sci 21(9):327-35.

Roizman B, Campadelli Fiume G. 2007. Alphaherpes viral genes and their function. In: Arvin A, Campadelli Fiume G, Mocarski E, Moore PS, Roizman B, Whitley R, Yamanishi K, editors. Human Herpesviruses, Biology, Therapy and Immunoprophylaxis. New York: Cambridge University Press.

Roizman B, Knipe DM. 2001. Herpes Simplex Viruses and Their Replication. In: Knipe DM, Howley PM, editors. Fundamental Virology. Fourth Edition ed. Philadelphia: Lippincott Williams & Wilkins. p 1123-1183.

Roizman B, Taddeo B. 2007. The strategy of herpes simplex virus replication and takeover of the host cell. In: Arvin A, Campadelli Fiume G, Mocarski E, Moore PS, Roizman B, Whitley R, Yamanishi K, editors. Human Herpesviruses, Biology, Therapy and Immunoprophylaxis. New York: Cambridge University Press.

Ryckman BJ, Roller RJ. 2004. Herpes simplex virus type 1 primary envelopment: UL34 protein modification and the US3-UL34 catalytic relationship. J Virol 78(1):399-412.

Salmons T, Kuhn A, Wylie F, Schleich S, Rodriguez JR, Rodriguez D, Esteban M, Griffiths G, Locker JK. 1997. Vaccinia virus membrane proteins p8 and p16 are cotranslationally inserted into the rough endoplasmic reticulum and retained in the intermediate compartment. J Virol 71(10):7404-20.

Sambrook J, Fritsch EF, Maniatis T. 1989. Expression of cloned genes in cultured mammalian cells. In: Nolan C, editor. Molecular cloning: a laboratory manual. Second edition ed. New York: Cold Spring Harbour Laboratory Press.

Sancho MC, Schleich S, Griffiths G, Krijnse-Locker J. 2002. The block in assembly of modified vaccinia virus Ankara in HeLa cells reveals new insights into vaccinia virus morphogenesis. J Virol 76(16):8318-34.

Sandri-Goldin RM. 2007. Initiation of transcription and RNA synthesis, processing, and transport in HSV and VZV infected cells. In: Arvin A, Campadelli Fiume G, Mocarski E, Moore PS, Roizman B, Whitley R, Yamanishi K, editors. Human Herpesviruses, Biology, Therapy and Immunoprophylaxis. New York: Cambridge University Press: pp 128-137

Schepis A, Schramm B, de Haan CA, Locker JK. 2006. Vaccinia virus-induced microtubule-dependent cellular rearrangements. Traffic 7(3):308-23.

Schiedner G, Hertel S, Kochanek S. 2000. Efficient transformation of primary human amniocytes by E1 functions of Ad5: generation of new cell lines for adenoviral vector production. Hum Gene Ther 11(15):2105-16.

Schramm B, Locker JK. 2005. Cytoplasmic organization of POXvirus DNA replication. Traffic 6(10):839-46.

Scott ES, Malcomber S, O'Hare P. 2001. Nuclear translocation and activation of the transcription factor NFAT is blocked by herpes simplex virus infection. J Virol 75(20):9955-65.

Senkevich TG, Bugert JJ, Sisler JR, Koonin EV, Darai G, Moss B. 1996. Genome sequence of a human tumorigenic poxvirus: prediction of specific host response-evasion genes. Science 273(5276):813-6.

Shahin V, Hafezi W, Oberleithner H, Ludwig Y, Windoffer B, Schillers H, Kuhn JE. 2006. The genome of HSV-1 translocates through the nuclear pore as a condensed rod-like structure. J Cell Sci 119(Pt 1):23-30.

Sheaffer AK, Newcomb WW, Brown JC, Gao M, Weller SK, Tenney DJ. 2000. Evidence for controlled incorporation of herpes simplex virus type 1 UL26 protease into capsids. J Virol 74(15):6838-48.

Sheaffer AK, Newcomb WW, Gao M, Yu D, Weller SK, Brown JC, Tenney DJ. 2001. Herpes simplex virus DNA cleavage and packaging proteins associate with the procapsid prior to its maturation. J Virol 75(2):687-98.

Sherman MP, Greene WC. 2002. Slipping through the door: HIV entry into the nucleus. Microbes Infect 4(1):67-73.

Shukla D, Spear PG. 2001. Herpesviruses and heparan sulfate: an intimate relationship in aid of viral entry. J Clin Invest 108(4):503-10.

Singer GP, Newcomb WW, Thomsen DR, Homa FL, Brown JC. 2005. Identification of a region in the herpes simplex virus scaffolding protein required for interaction with the portal. J Virol 79(1):132-9.

Skepper JN, Whiteley A, Browne H, Minson A. 2001. Herpes simplex virus nucleocapsids mature to progeny virions by an envelopment --> deenvelopment --> reenvelopment pathway. J Virol 75(12):5697-702.

Sodeik B, Ebersold MW, Helenius A. 1997. Microtubule-mediated transport of incoming herpes simplex virus 1 capsids to the nucleus. J Cell Biol 136(5):1007-21.

Sodeik B, Krijnse-Locker J. 2002. Assembly of vaccinia virus revisited: de novo membrane synthesis or acquisition from the host? Trends Microbiol 10(1):15-24.

Spear PG. 2004. Herpes simplex virus: receptors and ligands for cell entry. Cell Microbiol 6(5):401-10.

Spear PG, Eisenberg RJ, Cohen GH. 2000. Three classes of cell surface receptors for alphaherpesvirus entry. Virology 275(1):1-8.

Spear PG, Longnecker R. 2003. Herpesvirus entry: an update. J Virol 77(19):10179-85.

Spear PG, Manoj S, Yoon M, Jogger CR, Zago A, Myscofski D. 2006. Different receptors binding to distinct interfaces on herpes simplex virus gD can trigger events leading to cell fusion and viral entry. Virology 344(1):17-24.

Spruance SL, Stewart JC, Rowe NH, McKeough MB, Wenerstrom G, Freeman DJ. 1990. Treatment of recurrent herpes simplex labialis with oral acyclovir. J Infect Dis 161(2):185-90.

Steiner I. 1996. Human herpes viruses latent infection in the nervous system. Immunol Rev 152:157-73.

Stow ND. 2001. Packaging of genomic and amplicon DNA by the herpes simplex virus type 1 UL25-null mutant KUL25NS. J Virol 75(22):10755-65.

Strang BL, Stow ND. 2005. Circularization of the herpes simplex virus type 1 genome upon lytic infection. J Virol 79(19):12487-94.

Strunze S, Trotman LC, Boucke K, Greber UF. 2005. Nuclear targeting of adenovirus type 2 requires CRM1-mediated nuclear export. Mol Biol Cell 16(6):2999-3009.

Subramanian RP, Geraghty RJ. 2007. Herpes simplex virus type 1 mediates fusion through a hemifusion intermediate by sequential activity of glycoproteins D, H, L, and B. Proc Natl Acad Sci U S A 104(8):2903-8.

Taus NS, Salmon B, Baines JD. 1998. The herpes simplex virus 1 UL 17 gene is required for localization of capsids and major and minor capsid proteins to intranuclear sites where viral DNA is cleaved and packaged. Virology 252(1):115-25.

Thurlow JK, Murphy M, Stow ND, Preston VG. 2006. Herpes simplex virus type 1 DNA-packaging protein UL17 is required for efficient binding of UL25 to capsids. J Virol 80(5):2118-26.

Thurlow JK, Rixon FJ, Murphy M, Targett-Adams P, Hughes M, Preston VG. 2005. The herpes simplex virus type 1 DNA packaging protein UL17 is a virion protein that is present in both the capsid and the tegument compartments. J Virol 79(1):150-8.

Tiwari V, Clement C, Xu D, Valyi-Nagy T, Yue BY, Liu J, Shukla D. 2006. Role for 3-O-sulfated heparan sulfate as the receptor for herpes simplex virus type 1 entry into primary human corneal fibroblasts. J Virol 80(18):8970-80.

Tolonen N, Doglio L, Schleich S, Krijnse Locker J. 2001. Vaccinia virus DNA replication occurs in endoplasmic reticulum-enclosed cytoplasmic mini-nuclei. Mol Biol Cell 12(7):2031-46.

Torrisi MR, Di Lazzaro C, Pavan A, Pereira L, Campadelli-Fiume G. 1992. Herpes simplex virus envelopment and maturation studied by fracture label. J Virol 66(1):554-61.

Trotman LC, Mosberger N, Fornerod M, Stidwill RP, Greber UF. 2001. Import of adenovirus DNA involves the nuclear pore complex receptor CAN/Nup214 and histone H1. Nat Cell Biol 3(12):1092-100.

Trus BL, Booy FP, Newcomb WW, Brown JC, Homa FL, Thomsen DR, Steven AC. 1996. The herpes simplex virus procapsid: structure, conformational changes upon maturation, and roles of the triplex proteins VP19c and VP23 in assembly. J Mol Biol 263(3):447-62.

Trus BL, Cheng N, Newcomb WW, Homa FL, Brown JC, Steven AC. 2004. Structure and polymorphism of the UL6 portal protein of herpes simplex virus type 1. J Virol 78(22):12668-71.

Trus BL, Newcomb WW, Booy FP, Brown JC, Steven AC. 1992. Distinct monoclonal antibodies separately label the hexons or the pentons of herpes simplex virus capsid. Proc Natl Acad Sci U S A 89(23):11508-12.

Trus BL, Newcomb WW, Cheng N, Cardone G, Marekov L, Homa FL, Brown JC, Steven AC. 2007. Allosteric signaling and a nuclear exit strategy: binding of UL25/UL17 heterodimers to DNA-Filled HSV-1 capsids. Mol Cell 26(4):479-89.

Turcotte S, Letellier J, Lippe R. 2005. Herpes simplex virus type 1 capsids transit by the trans-Golgi network, where viral glycoproteins accumulate independently of capsid egress. J Virol 79(14):8847-60.

van Zeijl M, Fairhurst J, Jones TR, Vernon SK, Morin J, LaRocque J, Feld B, O'Hara B, Bloom JD, Johann SV. 2000. Novel class of thiourea compounds that inhibit herpes simplex virus type 1 DNA cleavage and encapsidation: resistance maps to the UL6 gene. J Virol 74(19):9054-61.

Vihinen-Ranta M, Wang D, Weichert WS, Parrish CR. 2002. The VP1 N-terminal sequence of canine parvovirus affects nuclear transport of capsids and efficient cell infection. J Virol 76(4):1884-91.

Vihinen-Ranta M, Yuan W, Parrish CR. 2000. Cytoplasmic trafficking of the canine parvovirus capsid and its role in infection and nuclear transport. J Virol 74(10):4853-9.

Vittone V, Diefenbach E, Triffett D, Douglas MW, Cunningham AL, Diefenbach RJ. 2005. Determination of interactions between tegument proteins of herpes simplex virus type 1. J Virol 79(15):9566-71.

Vrabec JT, Alford RL. 2004. Quantitative analysis of herpes simplex virus in cranial nerve ganglia. J Neurovirol 10(4):216-22.

Weinheimer SP, Boyd BA, Durham SK, Resnick JL, O'Boyle DR, 2nd. 1992. Deletion of the VP16 open reading frame of herpes simplex virus type 1. J Virol 66(1):258-69.

Weir JP. 2001. Regulation of herpes simplex virus gene expression. Gene 271(2):117-30.

White CA, Stow ND, Patel AH, Hughes M, Preston VG. 2003. Herpes simplex virus type 1 portal protein UL6 interacts with the putative terminase subunits UL15 and UL28. J Virol 77(11):6351-8.

Wild P, Engels M, Senn C, Tobler K, Ziegler U, Schraner EM, Loepfe E, Ackermann M, Mueller M, Walther P. 2005. Impairment of nuclear pores in bovine herpesvirus 1-infected MDBK cells. J Virol 79(2):1071-83.

Wilkinson DE, Weller SK. 2003. The role of DNA recombination in herpes simplex virus DNA replication. IUBMB Life 55(8):451-8.

Wills E, Scholtes L, Baines JD. 2006. Herpes simplex virus 1 DNA packaging proteins encoded by UL6, UL15, UL17, UL28, and UL33 are located on the external surface of the viral capsid. J Virol 80(21):10894-9.

Wingfield PT, Stahl SJ, Thomsen DR, Homa FL, Booy FP, Trus BL, Steven AC. 1997. Hexon-only binding of VP26 reflects differences between the hexon and penton conformations of VP5, the major capsid protein of herpes simplex virus. J Virol 71(12):8955-61.

Wittels M, Spear PG. 1991. Penetration of cells by herpes simplex virus does not require a low pH-dependent endocytic pathway. Virus Res 18(2-3):271-90.

Wolfstein A, Nagel CH, Radtke K, Dohner K, Allan V, Sodeik B. 2006. The inner tegument promotes Herpes Simplex Virus transport along microtubules in vitro. Traffic 7:1-11.

Yang K, Homa F, Baines JD. 2007. Putative terminase subunits of herpes simplex virus 1 form a complex in the cytoplasm and interact with portal protein in the nucleus. J Virol 81(12):6419-33.

Yao XD, Matecic M, Elias P. 1997. Direct repeats of the herpes simplex virus a sequence promote nonconservative homologous recombination that is not dependent on XPF/ERCC4. J Virol 71(9):6842-9.

Yoakum GH. 1993. Mapping a putative pyruvoyl decarboxylase active site to human cytomegalovirus open reading frame UL77. Biochem Biophys Res Commun 194(3):1207-15.

Yokota A, Narazaki M, Shima Y, Murata N, Tanaka T, Suemura M, Yoshizaki K, Fujiwara H, Tsuyuguchi I, Kishimoto T. 2001. Preferential and persistent activation of the STAT1 pathway in rheumatoid synovial fluid cells. J Rheumatol 28(9):1952-9.

Yu D, Weller SK. 1998. Herpes simplex virus type 1 cleavage and packaging proteins UL15 and UL28 are associated with B but not C capsids during packaging. J Virol 72(9):7428-39.

Zhang Y, Sirko DA, McKnight JL. 1991. Role of herpes simplex virus type 1 UL46 and UL47 in alpha TIF-mediated transcriptional induction: characterization of three viral deletion mutants. J Virol 65(2):829-41.

Zhou ZH, Chen DH, Jakana J, Rixon FJ, Chiu W. 1999. Visualization of tegument-capsid interactions and DNA in intact herpes simplex virus type 1 virions. J Virol 73(4):3210-8.

Zhou ZH, Dougherty M, Jakana J, He J, Rixon FJ, Chiu W. 2000. Seeing the herpesvirus capsid at 8.5 A. Science 288(5467):877-80.

Zhu LA, Weller SK. 1992. The UL5 gene of herpes simplex virus type 1: isolation of a lacZ insertion mutant and association of the UL5 gene product with other members of the helicase-primase complex. J Virol 66(1):458-68.

7 Appendix

Poster presentations:

Herpes Simplex Virus Type 1 early gene expression is inhibited by an excess of the DNA packaging minor capsid protein UL25
Kathrin Rode, Katinka Döhner, Tanja Strive, Rudi Bauerfeind & Beate Sodeik
EMBO Research Conference on Interface of Cell Biology and Cellular Microbiology; Macromolecular Complexes in Microbial Pathogenesis, Membrane Trafficking and Cell Signaling
Sep. 23rd – 28th 2006, San Feliu de Guixols, Spain

Overexpression of HSV1-UL25 reduces early HSV1 gene expression
Kathrin Rode, Katinka Döhner, Tanja Strive & Beate Sodeik
2nd Workshop on the "Cell Biology of Virus Infections" of the German Society of Virology
Sep. 15th – 19th 2003, Zeilitzheim

Oral presentations:

Transiently expressed HSV1-UL25 blocks early viral gene expression
Kathrin Rode, Katinka Döhner, Tanja Strive, Rudi Bauerfeind & Beate Sodeik
4th Workshop on the "Cell Biology of Virus Infections" of the German Society of Virology
Sep. 26th – 28th 2005, Deidesheim

Transiently expressed HSV1-UL25 blocks early viral gene expression
Kathrin Rode, Katinka Döhner, Tanja Strive, Rudi Bauerfeind & Beate Sodeik
International Herpesvirus Workshop,
Jul. 30th – Aug. 5th 2005, Turku, Finland

Transiently expressed HSV1-UL25 blocks early viral gene expression
Kathrin Rode, Katinka Döhner, Tanja Strive & Beate Sodeik
Annual Meeting of the German Society of Virology
Mar. 16th – 19th 2005, Hannover

Overexpression of HSV1-UL25 reduces early HSV1 gene expression
Kathrin Rode, Katinka Döhner, Tanja Strive & Beate Sodeik
3rd Workshop on the "Cell Biology of Virus Infections" of the German Society of Virology
Sep. 13th – 15th 2004, Zeilitzheim

Lebenslauf

KATHRIN RODE

- Diplom-Biochemikerin
- Geburtsdatum: 3. März 1979
- Geburtsort: Hameln
- Familienstand: ledig

UNIVERSITÄRE AUSBILDUNG

■ 19. Dez. 2007	Disputation
■ Nov. 2003 – Okt. 2007	Anfertigung der Doktorarbeit am Institut für Virologie der Medizinischen Hochschule Hannover (MHH) unter der Leitung von Prof. Dr. Beate Sodeik „The Role of the UL25 protein of Herpes Simplex Virus 1 During Assembly, Cell Entry and Nuclear Import of the Viral Genome"
■ Okt. 2006	Forschungsaufenthalt am Technion, Haifa, Israel, im Labor von Dr. Amnon Harel, *Department of Biochemistry*
■ Aug. 2005	Forschungsaufenthalt am Biomedicum Helsinki, Finnland, im Labor von Dr. Päivi Ojala, *Molecular Cancer Biology Program*
■ Apr. 2003 – Okt. 2003	Diplomarbeit am Institut für Virologie, MHH, unter der Leitung von Prof. Dr. Beate Sodeik „Die Rolle der Herpes Simplex Virus Typ 1 Proteine UL25 und UL36 (VP1-3) beim Viruseintritt in die Zelle"
■ Okt. 1998 – Okt. 2003	Diplom-Biochemiestudium an der Universität Hannover Diplom bestanden im Oktober 2003

BERUFSTÄTIGKEITEN

■ Seit Okt. 2007	Wissenschaftliche Mitarbeiterin am Institut für Virologie im Arbeitskreis „Zellbiologie viraler Infektionen" unter der Leitung von Prof. Dr. Beate Sodeik
■ Nov. 2003 – Okt. 2007	Doktorarbeit am Institut für Virologie der MHH im Arbeitskreis von Prof. Dr. Beate Sodeik als Stipendiatin des Landes Niedersachsen (Graduiertenförderung) und als DFG-Stipendiatin im Graduiertenkolleg 745 – Mukosale Wirts-Erreger Interaktionen
■ Okt. 2001 – März 2002	Studentische Hilfskraft am Institut für Biochemie der MHH
■ März 2001 – Okt. 2001	Studentische Hilfskraft am Institut für Zelluläre Chemie der MHH
■ 1998 – 2003	Verschiedene Jobs in der Gastronomie zur Finanzierung des Studiums

SCHULAUSBILDUNG

■ 1992 – 1998	Schiller-Gymnasium, Hameln, Abitur im Juni 1998
■ 1990 – 1991	Schulzentrum Hameln West (Orientierungsstufe), Hameln
■ 1986 – 1989	Klütschule (Grund- und Hauptschule), Hameln

Erklärung zur Dissertation

Hierdurch erkläre ich, dass ich die Dissertation

"The Role of the UL25 Protein of Herpes Simplex Virus 1 During Assembly, Cell Entry and Nuclear Import of the Viral Genome"

selbständig verfasst und keine anderen als die angegebenen Quellen und Hilfsmittel benutzt habe.

Diese Dissertation wurde nicht schon als Diplom- oder ähnliche Prüfungsarbeit verwendet.

Kathrin Rode

Hannover, 8. Oktober 2007